PHENOTYPIC AND GENOTYPIC FEATURES OF MACROPHAGE TROPISM IN HIV-1

Kathryn Twigg Arrildt

A dissertation submitted to the faculty of the University of North Carolina at Chapel Hill in partial fulfillment of the requirements for the degree of Doctor of Philosophy in the Department of Microbiology and Immunology.

Chapel Hill
2016

Approved by:

Ron Swanstrom

Kristina de Paris

Lishan Su

Aravinda de Silva

Nathaniel Moorman

ABSTRACT

Kathryn Twigg Arrildt: Phenotypic and Genotypic Features of Macrophage Tropism in HIV-1.
(Under the direction of Ron Swanstrom.)

HIV-1 preferentially attaches and enters specific cell types by recognizing cell-specific receptors. HIV-1 typically targets memory $CD4^+$ T cells by restricting attachment to cells expressing high CD4 densities and by using the CCR5 coreceptor. HIV-1 can adapt to enter $CD4^+$ nave T cells by evolving to use CXCR4 in addition to CCR5. Alternatively, HIV-1 can adapt infecting macrophages by enhancing the entry using low CD4 densities. Early classification confusion and the lack of a reproducible, high-throughput method to assess cellular tropism has hindered robust identification and characterization of macrophage tropism. We developed cellular tropism assays using a novel cell line to perform both high-throughput identification screens and detailed analyses of receptor and coreceptor interactions.

Clarified definitions of cellular tropism enabled us to probe the mechanism and consequences of evolving macrophage tropism through genotypic and phenotypic characterizations of subject-matched T-tropic and M-tropic *env* genes. M-tropic Env proteins are mostly indistinguishable from T-tropic Env proteins, except for subtle differences in the CD4-binding site (CD4bs) revealed by differences in interactions with CD4, competitive inhibition by soluble CD4, anti-CD4bs antibody sensitivity, and the ability of CD4-binding proximal residues to affect CD4 usage. CD4 usage is highly correlated with entry of monocyte-derived macrophages over a continuous range, making CD4 usage a useful proxy for macrophage tropism.

Other stages of binding and entry are not major factors in the evolution of macrophage tropism and M-tropic Env proteins are not generally sensitive to antibodies. Nor does the antibody environment appear as a major selective pressure on the evolution of macrophage tropism. The genetic determinants are complex; evolving macrophage tropism requires unique

constellations of amino acid substitutions at distal locations in the Env protein. However, substitutions of bulkier, more hydrophobic amino acid residues tend to accumulate in the V5 region of the Env protein. The true genetic determinants of macrophage tropism are still unknown, but we have begun to identify features to help identify new M-tropic viruses, which is an essential part of unraveling the greater mysteries of macrophage tropism.

To my family, bursting with love and support.

To my friends that became family in a strange, new land.

And especially to my eternal editor, cheerleader, fellow-sufferer, and pair-bonded mate:

John Paul Didion, Ph.D.

ACKNOWLEDGMENTS

I am grateful for the mentoring (and patience) and my advisor, Ron Swanstrom. I am also grateful for my second string mentor and fierce collaborator, Sarah Joseph, who was always there when Ron was missing or I needed a second perspective. Elena Dukhovlinova helped me bounce endless ideas and was my go-to coconspirator. Neither myself nor the lab could have done without the tireless devotion of Ean Spielvogel and Zaki Dard, who greased the wheels and kept things moving. Will Ince and Gretja Schnel were my introduction to the Swanstrom lab and I might have been lost without them. Lihua Ping has an exhaustive reference of every protocol ever performed in the Swanstrom lab and never turns down a request for a helping hand. Sook-kyung Lee is the western blot queen and powered through some tricky blotting. My research could not have moved forward without the resources and advice of my constant collaborators Dick Price, David Montefiori, and Celia LaBranche. In addition to helping in a thousand tiny way, Maria Bednar, Laura Kincer, Liz Pollom, and Leslie Arney brought a little sunshine to the lab and made it a better place to live (I mean work). And last, but not least, I am grateful for the various funds and resources provided by the Microbiology and Immunology Department, the School of Medicine, the University of North Carolina and the National Institutes of Health.

TABLE OF CONTENTS

LIST OF TABLES

LIST OF FIGURES

LIST OF ABBREVIATIONS

AIDS	Acquired immunodeficiency syndrome
BBB	Blood-brain barrier
C1-5	Conserved region 1 through 5
CD4bs	CD4-binding site
$CD4^{high}$	Cells expressing high densities of CD4 on the surface
CD4i	CD4-induced (by binding)
$CD4^{low}$	Cells expressing low densities of CD4 on the surface
CSF	Cerebrospinal fluid
CNS	Central nervous system
CVL	Cervicovaginal lavage
EC_{50}	50% effective concentration
Env	HIV-1 Envelope protein
env	HIV-1 *env* gene
HAART	Highly-active anti-retroviral therapy
HAD	HIV-associated dementia
HAND	HIV-associated neurocognitive disorder
HIV-1	Human immunodeficiency virus 1
IC_{50}	50% inhibitory concentration
M-tropic	Macrophage-tropic
MDM	Monocyte-derive macrophage

R5	CCR5-using
SI	Specific Infectivity
SIV	Simian immunodeficiency virus
T-tropic	T cell-tropic
TCA	Tissue culture adapted
V1-5	Variable region 1 through 5
VL	Viral Load
X4	CXCR4-using

CHAPTER 1

INTRODUCTION

1.1 HIV-1 Genome and Replication

1.1.1 Classification and Genome

Retroviridae lentivirus Human immunodeficiency virus type 1 (HIV-1) can be classified into four groups (M, N, O, and P) that represent separate zoonotic transmission events from simians infected with a related lentivirus, simian immunodeficiency virus (SIV). Groups M (main) and N (non-M, non-O) are derived from a chimpanzee strain of SIV (SIV_{cpz}) (2-4). Groups O (outlier) and P (to continue alphabetically (5)) are derived from a gorilla strain of SIV (SIV_{gor}) that was likely derived ultimately from SIV_{cpz} (6-9). The HIV-1 Group most prevalent in human infection is Group M, which is further divided into subtypes (A1, A2, B, C, D, F1, F2, G, H, J and K). Subtype C is the most prevalent world-wide, representing an estimated 50% of all HIV-1 infections, and is predominant in southern Africa and Asia. Subtype B, estimated at 10% of all HIV-1 infections, is the nearly exclusive subtype in North America and Europe and is also frequently found in Asia. Regardless of Group and Subtype, HIV-1 and the closely-related primate lentiviruses are all classified as Group VI viruses (based on genomic replication steps), indicating that the viral genome is positive-sense single-stranded RNA (+ssRNA) that is reverse transcribed into a double-stranded DNA (dsDNA) intermediate, which serves as the template for replication. The HIV-1 genome, which is between 9 kb and 10 kb in length, contains two long terminal repeat (LTR) regions flanking ten genes: *gag*,

pro, *pol*, *env*, *vif*, *vpr*, *vpu*, *nef*, *tat*, and *rev*.

To make the most of only ten genes, each viral gene product has several functions in HIV-1 replication. Gag is structural polyprotein that is cleaved into subunits that make up the matrix, capsid, and nucleocapsid. Env is a structural polyprotein that is cleaved into two subunits, gp120 and gp41, which remain non-covalently associated, and are responsible for attachment and entry into host cells. Pro-Pol is a polyprotein cleaved into several non-structural enzymatic proteins: a protease (PR), which cleaves viral polyprotein precursors into functional subunits (except Env, which is cleaved by cellular protease); a reverse transcription polymerase (RT), which transcribes the viral genomic +ssRNA into dsDNA and includes an RNaseH domain to degrade the +ssRNA template; and an integrase (IN), which incorporates the viral dsDNA into the host cellular genomic DNA. Vif is an accessory protein that antagonizes cellular antiviral APOBEC3G proteins. Vpr is an accessory protein that induces host cell cycle arrest and regulates the pre-integration complex required for nuclear import of the dsDNA viral genome. Vpu is an accessory protein related to Vpr that can down-modulate surface expression of cellular CD4 (which may reduce the probability of super-infection and/or immune activation) and tetherin (an antiviral host protein that prevents virion release). Nef is an accessory protein that down regulates cell surface expression of MHC-I, among other cellular proteins, to avoid immune surveillance. These four accessory proteins are being investigated for additional functions. Tat is a regulatory protein that enhances viral transcription through interaction with host transcription factors. Rev is a regulatory protein that functions inside the cellular nucleus to allow export of unspliced and incompletely spliced viral mRNA.

1.1.2 Replication Cycle

HIV-1 targets host cells by specific associations of the viral Env proteins with cellular receptors. Env (or gp160) is cleaved by cellular protease into two subunits, which remain non-covalently associated: extraviral gp120 and transmembrane gp41. The cleaved gp120-gp41 units trimerize to form a mature, functional spike on the virion surface. Viral attachment

occurs when gp120 binds the cellular CD4 receptor. This binding event induces a structural change in gp120 that forms a binding site for CCR5. When gp120 binds CCR5, structural changes in gp120 reveal the amino-terminal fusion peptide of gp41, which is embedded in the target cellular membrane. Once gp41 has tethered the viral membrane to the cellular membrane, gp41 undergoes a hairpin fold, drawing the two membranes in close proximity to induce fusion, which releases the viral core into the target cell (reviewed in (10)). The viral RNA and polymerase enzymes are then uncoated to start the replication cycle anew.

HIV-1 polymerase initiates replication by reverse transcribing the +ssRNA genome into a complementary DNA strand (cDNA), then destroying the +ssRNA in order to transcribe the second strand of DNA to complete the dsDNA intermediate viral genome. APOBEC3G, a cellular antiviral protein that degrades cytidine on cDNA, can cause errors in transcription of the second strand of DNA, which can cause mutational inactivation of the viral genome, but Vif can antagonize APOBEC3G to protect the viral genome. The dsDNA genome is chaperoned into the nucleus by a pre-integration complex, which is regulated by Vpr and requires cellular proteins as well as viral integrase to traffic the complex and insert the viral genome into the nucleus. Inside the cellular nucleus, integrase inserts the viral genome into the cellular genome by catalyzing strand transfer. After integration, the viral genome can be transcribed into mRNA by cellular machinery, but this process is inefficient until viral Tat is accumulated. Tat binds to a TAR (trans-activation response element), a RNA secondary structure present near the transcriptional start site of nascent RNA transcripts from the integrated viral DNA genome, and recruits host transcription factors to enhance the number and length mRNA transcripts produced. Rev binds the RRE (rev response element) on viral mRNA transcripts and facilitates export of mRNAs that are unspliced or incompletely spliced. Exported mRNAs are translated by host machinery into viral proteins, which will accumulate in the host cell.

Virion assembly begins by association of two copies of full-length, unspliced viral +ssRNA genomes with viral nucleocapsid units of uncleaved Gag polyproteins. These Gag polyproteins traffic and accumulate at the plasma membrane where interactions between Gag

and the +ssRNA genomes recruit and pack a specific number of structural (Gag) and enzymatic (Gag-Pro-Pol) polyproteins required for a mature virion. Env is cleaved by cellular protease into transmembrane and extracellular subunits which remain covalently associated. The transmembrane unit of Env is hypothesized to interact with Gag during assembly, but the nature of this is not yet fully understood. Budding is initiated by subversion of the cellular ESCRT pathway, which allows the immature virions to bud out of the cellular plasma membrane. Vpu antagonizes tetherin, a cellular antiviral protein that prevents virion release, allowing nascent viral particles to find new host cells. Newly released viral particles are still immature non-infectious. Protease (subunit of Pro) cleaves itself from the Gag-Pro-Pol polyprotein and homodimerizes, which frees it to separate the other subunits of the Gag, Pro, and Pol gene products into functional subunits. Nucleocapsid proteins (subunits of Gag), which are still associated with the two +ssRNA genomes compress into an electron-dense core along with the reverse transcriptase and integrase enzymes (subunits of Pol). Capsid proteins (subunits of Gag) form a conical structure surrounding the nucleocapsid-RNA-enzymes complex. Matrix proteins (subunits of Gag) remain associated with the (viral ne cellular) membrane. The fully cleaved and reorganized virus is fully mature and ready to infect a new cell.

1.2 HIV-1 Pathogenesis

1.2.1 Stages of Infection and Disease

HIV-1 is a blood-borne pathogen and can be transmitted by the transfer of bodily fluids from an infected person though contact with mucosal membranes or abrasions of the skin in an uninfected recipient. Infected people do not appear to be able to acquire subsequent infections with newly transmitted viruses. HIV-1 is mostly commonly transmitted through sexual intercourse or intravenous drug use. Most infections were founded by a single virus during transmission and even the most sensitive tests cannot detect HIV-1 infection for at least one to two weeks. The first stage of disease is primary infection, which is clinically asymptomatic. Viral loads are undetectable, probably due to the small seed number, but are

inferred to be rapidly increasing by observations made of subsequent stages.

The second stage of HIV-1 infection is the acute infection, which is when infection becomes detectable. During this stage the viral load (a clinical measure of viruses in the blood) reaches a peak level and the CD4 count (a clinical measure of CD4-expressing cells in the blood, e.g. $CD4^+$ T cells) reaches a nadir level usually within two to four weeks after transmission. Previous guidelines recommended waiting to treat patients until CD4 counts reached certain thresholds in part due to concerns over side-effects from the chemical therapy. However, subsequent research revealed greater benefit from suppressing viral replication as soon as possible and new therapeutic drugs have been discovered with (or engineered for) decreased toxicity shifting the cost-benefit ratio towards increasingly earlier treatment. Current guidelines suggest initiating highly active antiretroviral therapy (HAART) immediately upon detection of infection. Also, because viral loads are high during this stage, the risk of transmitting to others is also increased, which provides an additional benefit to early treatment. During this stage, the immune system is highly activated, which leads (in part) to decreasing viral loads, increasing CD4 counts, and flu-like symptoms in some infected people.

The third stage of HIV-1 infection, called chronic infection or clinical latency, begins when the viral load falls to a set point, where it can remain for months or years without treatment. Falling viral loads are often mirrored by recovering CD4 counts and infected people are usually asymptomatic throughout this phase (even without HAART). Despite lower viral loads and a lack of clinical symptoms, the viral loads in chronic infection are sufficient to transmit HIV-1. HAART can induce a similar clinical latency by suppressing HIV-1 replication, but with several advantages. HAART-induced suppression can extend latency indefinitely and prevents transmission in 100% of cases where viral loads are completely and consistently undetectable. Furthermore, suppression of viral replication reduces chronic immune activation, which has been implicated in some long-term side effects of HIV-1 infection. Without HAART, HIV-induced disease will eventually progress to acquired immune deficiency syndrome (AIDS).

The final stage of HIV-1 infection, or late infection, is AIDS, which is characterized by increasing viral loads (away from the set point maintained through chronic infection) and decreasing CD4 counts (200 cells per μL of blood is used as a clinical threshold). The immune system becomes increasingly dysregulated and ineffective during AIDS, caused in part by depletion of $CD4^+$ T cells (the target cells of HIV-1, discussed in detail below) and years of chronic immune activation. Reduced effectiveness of the immune system increases susceptibility to infection by other pathogens, including opportunistic pathogens, and reactivation of latent viral infections. Several common herpesviruses, which are typically suppressed by a functional immune system, can lead to lymphoma or other diseases when that immune-mediated control is lost. Even at this stage HAART can suppress viral replication and allow recovery of CD4 counts, reverting disease back into a clinical latency.

1.2.2 Neuropathogenesis

Neuro-invasion by viruses is fairly common and spans viruses from several families. The infection of neurons is fundamental to life cycles (e.g. transmission, latency/reactivation) of only a small fraction of these viruses, including several viruses in the herpesviridae (e.g. herpes simplex viruses, varicella zoster virus) and rhabdoviridae (e.g. lyssavirus, vesiculovirus) families, despite being able to enter and infect multiple cell types. These viruses are able to infect neurons and use retrograde neural transport to move from peripheral nerves near the site of infection to the central nervous system (CNS). Although herpes simplex viruses does not require invasion of the CNS, infection of neurons provides a reservoir for episodic reactivation that is protected from immune detection. Because herpes simplex viruses establish latency in neural ganglia using retrograde neural transport, infection can in rare cases penetrate as far as the CNS, which causes severe neurological complications that range from encephalitis and myelitis to behavior alterations if left untreated. Because transmission is primarily through contact, especially at mucosal membranes, anterograde neural transport of viruses during reactivation is necessary to reach peripheral nerves and spread into epithelial

cells to enhance shedding. Lyssavirus has evolved to produce high titers in the salivary glands and is typically transmitted via saliva through punctures of the skin (usually animal bites). In a more extreme example of neural tissue dependency, lyssavirus infection typically reaches the CNS and produces behavioral changes in the host which are thought that enhance viral transmission. Lyssavirus infection in the CNS can cause increased aggression and decreased fear, which is thought to increase interactions with other potential hosts (11). However, even when infections of neurons or other cells in neural tissue are required for the life cycle of a virus, most viruses that infect neural tissue can enter and replicate in a wide range of different cell types and do not have specialized targeting receptors.

The majority of viral infections in the CNS appear accidental in that they occur only rarely and offer no apparent evolutionary advantage (e.g. by enhancing survival or transmission). Even viruses known (and sometimes named) for the disease symptoms caused by infection of the CNS do so in only a small fraction of total infections. Viruses in the togaviridae (e.g. rubella virus and alphaviruses including Eastern, Western, and Venezuelan encephalitis viruses), flaviviridae (e.g. dengue virus, West Nile virus, Japanese encephalitis virus), picornaviridae (e.g. poliovirus, coxsackie A virus), paramyxoviridae (e.g. measles virus, mumps virus, canine distemper virus), bunyaviridae (e.g. La Crosse virus, California encephalitis virus), and other families can all cause viral meningitis resulting in serious or even fatal disease, but typically do so in less than 2% of reported cases. If anything, this number is likely an overestimate, because infections with neuroinvasion are more likely to result in severe symptoms and hospitalization than in cases without neuroinvasion, which can often be mild or even asymptomatic (reducing the rate of reporting). The symptoms of neuroinvasion in these viruses are typically due to inflammation in the CNS rather than direct damage from viral infection and replication, much less targeted antagonism.

Neither neuroinvasion nor macrophage infection are integral to the HIV-1 life cycle. M-tropic viruses are typically only detectable in the CNS and are rarely if ever transmitted (12-20). Latency can be achieved in T cells, providing a reservoir protected from immune de-

tection, without an expansion of host range. The higher frequency of neurological symptoms resulting from neuroinvasion by HIV-1 (estimates range from 25% to more than 50% (21-24)) is likely due to the long-term chronic infection compared to the acute infections of the accidental neuroinvasion viruses. Although HIV-associated neurological symptoms typically occur years after transmission, there is evidence that HIV-1 can penetrate the blood brain barrier and access the CNS very shortly after transmission (25-30). Together these observations suggest that HIV-1 neuroinvasion is of the accidental variety.

On the other hand, the evolution of macrophage tropism in HIV-1 hints that macrophages are a useful target during infection. Latency in peripheral T cells does not exclude the possibility of other models of latency, including sequestration of viral populations in the CNS compartment in general or perivascular macrophages in specific. Macrophages have a long lifespan, which may allow them to serve as viral reservoir with the potential to re-seed and repopulate the lymphatic system. Also, while M-tropic viruses are notable inhabitants of the CNS because M-tropic viruses are rarely found elsewhere, even CNS viruses are more likely to be T-tropic than M-tropic. The CNS as an anatomical compartment may provide conditions for a reservoir in that some anti-HIV therapeutic drugs have poor penetration across the blood-brain barrier (31-38). Thus, there is the potential for T-tropic viruses, which make up the vast majority of HIV-1 in human infection and are the dominant transmitted variant, to form a reservoir in the CNS. However, whether these potential reservoirs actually exist in the CNS and have clinical relevance may remain unsolved until a treatment regimen is designed that can fully eradicate viruses based in the lymphatic system. Regardless of the potential to form a reservoir, HIV-1 replication in the CNS results in the pattern of damage via inflammation observed for the accidental viral infections.

The HIV-associated neuropathogenesis is caused by HIV-1 infiltration of and replication in the CNS. Damage to cells in the CNS can be caused directly by neurotoxic viral proteins gp120, Tat, and Vpr and indirectly through inflammation and immune activation by infected perivascular macrophage and microglia (reviewed in (32, 39)). In combination, direct and

indirect injury results in disruption of the blood-brain barrier (BBB; endothelial barrier responsible for protecting the CNS from infection and injury) through interactions between viral proteins and epithelial cells, disruption of signaling by infection of or viral protein interactions with astrocytes (involved in signal regulation and BBB maintenance) and induction of neuronal apoptosis through release of cytokines and chemokines by activated immune cells. Immune activation of resident CNS immune cells (e.g. perivascular macrophage and microglia) can lead to recruitment of additional immune cells from outside the CNS. Pleocytosis, an influx of lymphocytes, in the CNS can be a cause and/or downstream effect of viral replication in the CNS (40).

Pleocytosis in the CNS may result from the immune recruitment instigated by HIV-1 infection in the CNS and contribute to immune-mediated destruction and bystander killing of CNS cells, which is supported by the observation that initiation of HAART (suppressing infection) can resolve HIV-1 encephalitis and other measures of CNS damage (41-47). However, the lymphocytes recruited to the CNS for any cause may contain $CD4^+$ T cells infected with HIV-1, providing one potential mechanism for HIV-1 infiltration of the CNS. It is also possible that CNS infiltration can be caused by free virus, but it is still unknown whether the small size of viral particles allows penetration of the BBB. The CNS is typically devoid of $CD4^+$ T cells, the primary targets for HIV-1, which may naturally limit HIV-1 replication in the CNS. Once HIV-1 has infiltrated the CNS, pleocytosis can also bring in uninfected $CD4^+$ T cells, proving targets for new infection and maintaining infection in the CNS, which is typically devoid of $CD4^+$ T cells. In most cases viral loads are lower in the CNS compared to the blood, which may result from a combination of barrier protection and limited numbers of permissive target cells.

HIV-1 infection of cells in the brain can cause a range of HIV-associated neurocognitive defects (HAND). The most severe form of HAD is HIV-associated dementia (HAD), which is characterized by severe neurological dysfunction, including impaired cognitive and motor functions, and extensive changes in behavior. The mildest form of HAND is asymptomatic

neurocognitive impairment (ANI), which refers to neurocognitive defects than can be detected clinically, but do not impact the day-to-day life of those diagnosed. Prior to widespread use of HAART, HIV-1 infection resulted in HAD in 20% to 30% of cases (48). The increasing availability of HAART has drastically reduced HAD incidence to 2% of cases (49), but milder forms of HAND are becoming more prevalent with increasing life expectancies after HIV-1 infection. Recent estimates of HAND incidence are as high as 52% (49). Although the ANI subset contributes more than half of HAND diagnoses, cases of ANI are more likely to decline into other forms of HAND compared to cases with no neurocognitive impairment (50), warranting inclusion of ANI in the HAND group and providing a potential target group for high-impact intervention to prevent or delay incidence of symptomatic neurocognitive defects.

1.2.3 Compartmentalization

All HIV-1 infections result in virus present in the CNS as measured by viral loads in the cerebrospinal fluid (CSF) (51, 52), but typically at much lower levels than are observed in the blood. Increased viral loads in the CSF are correlated with cognitive dysfunction (53, 54). Schnell *et al*. characterized a small cohort of subjects with high viral loads in the CSF and revealed that HAND was associated with independent HIV-1 replication in the CNS and that unimpaired neurocognition was not associated with independent HIV-1 replication in the CNS. Independent replication of HIV-1 in the CNS was determined by phylogenetic analysis of viruses isolated from the blood and CSF of each subject. If the blood- and CSF-derived viruses were indistinct and formed a single genetic population, it was determined that there was no independent replication in the CNS and so the viruses will likely overspill from the viruses circulating through the rest of the body. However, if the CSF-derived viruses formed a separate clade that was anatomically separated and genetically distinct from the blood-derived viruses (i.e. compartmentalized), it was determined that a population of HIV-1 was replicating in the CNS independently of the circulating viral population, which allowed this CNS-derived population to diverge (55-61).

Cases of compartmentalized viral populations can be further distinguished into two groups (61). In the first group, the CSF compartmentalized viral populations were clonal amplified or minimally genetically complex, which was associated with pleocytosis (measured by increased levels of white blood cells in the CSF) and viral replication in short-lived cells (measured by a rapid decay of viral load after initiation of HAART) consistent with the half-life of $CD4^+$ T cells (Figure 1.1). Because HAART effectively blocks infection of new cells and because free viruses decay rapidly, viruses present after the initiation of HAART are produced from a cell that was infected prior to the initiation of HAART. When tested for cellular tropism (discussed in greater detail in the next section), viral isolates from the first group were confirmed to be T cell-tropic. In the second group, the CSF compartmentalized viral populations were genetically complex, which was associated with little or no pleocytosis and viral replication in long-lived cells (inferred by slow decay of viral load in the CSF) consistent with perivascular macrophages or microglia. When tested for cellular tropism, viral isolates from the second group were confirmed to be macrophage-tropic. Viral isolates from the blood of all subjects were T cell-tropic.

Invasion of the CNS may occur through the diffusion of free virus across the BBB or through infected cells via pleocytosis. Clonal expansion of an infected cell could produce large numbers of near-identical viruses. In order to replicate, however, pleocytosis must occur to provide host cells capable of sustaining replication. This type of temporary pleocytosis-dependent replication of HIV-1 in the CNS could explain the first group of compartmentalization by T cell-tropic viruses in the CNS, which are often comprised of genetically similar viruses. To maintain long-term replication of HIV-1 in the CNS, there must be either continuous replenishment of memory $CD4^+$ T cells by sustained pleocytosis or the viral population will have to adapt to a cell type that resides permanently in the CNS. Both perivascular macrophages and macrophage-like microglial cells reside permanently in the CNS and can be infected by HIV-1, but only very inefficiently. Adaptation to these cells may provide a mechanism for sustained HIV-1 replication in the CNS and would allow for long-term viral

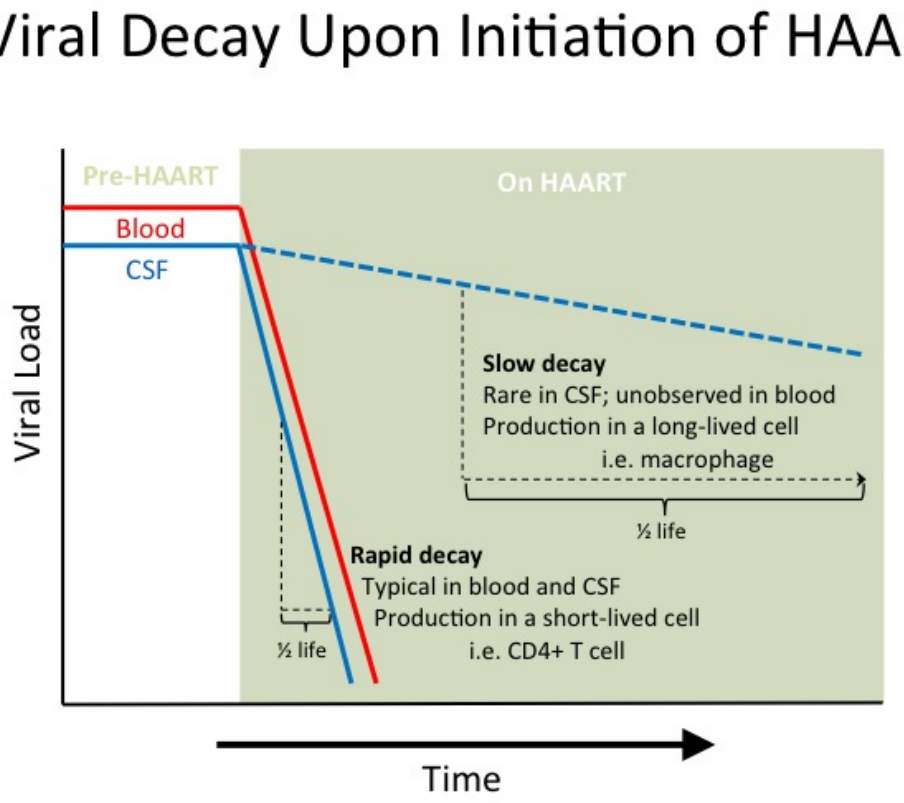

Figure 1.1: **VL decay upon initiation of HAART.** Successful HAART blocks new infection, but does not affect cells already infected with HIV-1. Therefore, the remaining viral production (and viral load) is directly related to the life-span of the cells infected prior to initiating HAART. In essentially all patients infected with HIV-1, viral load (VL) decays rapidly upon initiation of HAART with a half-life of approximately 1 to 2 weeks in the blood (indicated by the solid red line) and cerebrospinal fluid (CSF; solid blue line), which is consistent with virus produced from infected $CD4^+$ T cells in both compartments. In rare cases, patients will have the same rapid decay of VL in the blood, but will have a much slower decay in the CSF (dashed blue line). This indicates that in these patients viruses are being produced in $CD4^+$ T cells in the blood, but are being produced by a longer-lived cell, likely perivascular macrophages or microglia, in the CSF.

evolution, which could explain the genetic complexity in viral populations in the second group of compartmentalization.

Compartmentalization has also been observed for other anatomical locations with the most evidence for compartmentalization in genital secretions (62-80) and breast milk (81-83), kidneys (84), which have significant implications for transmission. Other anatomical compartments have been identified as offering the potential for compartmentalization, including lungs (85-88), liver (89, 90) and gastrointestinal tract (91-95) though some observation are dependent upon very small data sets and will require further investigation. Cellular tropism is only beginning to be explored in these compartments, but a recent study identified cellular tropism variants in the genital tract that differ from the cellular tropism of viral populations in the blood of the same subject (96).

1.3 HIV-1 Cellular Tropism

1.3.1 Env-Specified Target Cells

The pathogenesis of HIV-1 is largely due to the cells targeted for replication. Upon transmission, HIV-1 targets and primarily infects memory $CD4^+$ T cells. A rapid depletion of memory $CD4^+$ T cell unbalances the intricately interwoven immune system and leads to dysregulation and loss of effectivity. However, HIV-1 can bind and enter any cells expressing the CD4 receptor and the CCR5 coreceptor with varying degrees of successful replication. For example, HIV-1 can enter astrocytes, macrophages, and microglia albeit poorly and cause dysregulation in chemical signaling and aberrant immune activation, which can disrupt tissue functions and damage surrounding cells. HIV-1 can evolve to target new cell types in situations where the preferred targets (memory $CD4^+$ T cells) are rare.

HIV-1 targets specific cell types by evolving to interact with a specific combination of receptors, which benefits the virus by avoiding entry into cells that are not ideal for replication. All interactions between HIV-1 and a host cell are mediated by HIV-1 Env, which is the only viral gene product present on the viral surface. This also means that Env is also the only viral

protein exposed to extracellular immune surveillance. Env mitigates immune detection by being heavily glycosylated and host glycosylation patterns are poorly immunogenic. Env also stays one step ahead of detection by being produced from the most highly variable gene in the HIV-1 genome (97). However, sequence variability can be troublesome for maintaining the structures and functions of a protein. The extracellular gp120 portion of Env gets around this problem by having a core structure composed of five conserved regions (C1-C5), in which mutations are deleterious and so are not replicated. These conserved regions are masked by five variable regions (V1-V5), which are more physically and evolutionarily plastic, contain most of the variation in the *env* gene, and are most exposed to potential detection. The variable regions have fewer constraints, so a high mutation rate can keep viruses one step ahead of immune recognition. Because Env also specifies target cells through receptor recognition, the high mutation rate also grants Env the ability to evolve to target new cell types.

1.3.2 Primary Target: Memory $CD4^+$ T Cells

Specificity for a certain cell type is maintained by a viral Env that is specific for a combination of receptors and coreceptors unique to that cell type. For the majority of HIV-1, the Env proteins are only able to attach to cells expressing the CD4 receptor at high densities and, although several immune cell types express CD4, the high densities required are only expressed on the surface of $CD4^+$ T cells making these viruses T cell tropic (T-tropic). Also in this case, the HIV-1 Env can only use CCR5 as a coreceptor making these viruses CCR5-using (R5) and, of $CD4^+$ T cells, CCR5 is only found at efficiently useable levels on the memory subset. Thus, these CCR5-using T cell-tropic (R5 T-tropic) viruses replicate primarily in memory $CD4^+$ T cells. R5 T-tropic HIV-1 describes the vast majority of viruses involved in transmission (or at least in founding the infection), acute infection, and chronic infection (12-14, 16, 20, 98).

R5 T-tropic HIV-1 is evolved to enter and replicate in memory $CD4^+$ T cells, evidenced by adaptation of Env to engage receptors specific for memory $CD4^+$ T cells and adaptation of

accessory proteins to modulate memory $CD4^+$ T cells. However, HIV-1 has been hypothesized to infect several other cell types, including: monocytes, macrophages, dendritic cells. These cells types have the CCR5 coreceptor and the CD4 receptor, though not at densities to allow efficient entry. R5 T-tropic viruses infect monocyte-derive macrophage (MDMs) poorly and DCs undetectably. All of these alternative cell types express CD4 at much lower densities than $CD4^+$ T cells and at levels shown to be inefficient for entry of R5 T-tropic HIV-1 (99).

Consistent with the observation of viral tropism, $CD4^+$ T cells are also the primary source of replicating virus. HAART blocks infection of new cells, but has no effect on cells infected prior to therapy and free virus is only stable for approximately 6 hours or less in blood plasma (100, 101). Thus, when HIV+ subjects initiate HAART, the decay of viral load is related to the lifespan of the cells in which HIV-1 is actively replicating (and producing new viruses). Barring resistance to the drugs used in HAART, the decay of viral load in the blood is invariably short (usually 1-2 days), consistent with the lifespan of an infected $CD4^+$ T cell. Thus, even if viruses are able to enter other cell types, they are not replicating efficiently enough to contribute significantly to the viral population that is replicating efficiently in memory $CD4^+$ T cells.

Another way to evaluate which cell types support replication of HIV-1 is to detect viruses that have succeeded in post-entry steps of replication. Proviral integration is a step required for productive replication that can be easily detected by PCR. Although several candidate cell types were evaluated, integrated HIV-1 proviral genomes are most frequently isolated from $CD4^+$ T cells from subjects both on (14, 102-105) and off (106-108) HAART. HIV-1 may enter off-target cells inefficiently, so likely at some low frequency, but downstream steps can also be cell type-specific.

Viruses must be able to antagonize cell type-specific antiviral mechanisms that attack various stages of HIV-1 replication. HIV-1 has several accessory proteins adapted to hurdles and antiviral mechanisms deployed by $CD4^+$ T cells: Vpr interacts with the pre-integration complex to facilitate nuclear entry of the viral genome (109, 110) and modulates the host cell

cycle to pause in the G2 phase to aid viral replication (111-114). Nef downregulates host MHC-I (115) to evade immune detection and host cell CD4 expression (116, 117), which interferes with Env incorporation and virion budding (118, 119). Vpu can also downregulate CD4 surface expression, but its unique function is to promote the release of budding virus (120) by antagonizing tetherin, which is a human antiviral protein that prevents release of nascent viruses from the surface of the infected cell (121). Vif antagonizes APOBEC, which is a family of cellular antiviral proteins, by targeting them for degradation (122, 123)

Simian immunodeficiency virus (SIV), a lentivirus closely related to HIV-1, uses a viral accessory protein Vpx or Vpr (depending on the strain) to antagonize host antiviral SAMHD1 by marking it for degradation. SAMHD1 is an antiviral protein that reduces the concentration of deoxynucleotides available for use in reverse transcription and is expressed in monocytes, DCs, and resting T cells at levels sufficient to prevent reverse transcription of the HIV-1 genome. SAMHD1 is also expressed in macrophages, but at lower levels. However, HIV-1 does not express Vpx and the Vpr that HIV-1 does express has lost the ability to antagonize SAMHD1. This suggests that not only will HIV-1 fare poorly in DCs without protection from SAMHD1, but that HIV-1 has not evolved to replicate in this cell type, because the selective pressure provided by SAMHD1 would have ensured maintenance of the anti-SAMHD1 function of Vpr.

R5 T-tropic HIV-1 is limited to replication in memory $CD4^+$ T cells through a combination of viral specifications for entry and by defenses employed by other cells types. The loss of anti-SAMHD1 functions in the version of Vpr expressed by HIV-1 suggests that HIV-1 is not consistently replicating in myeloid or resting T cells, because unlike SIV HIV-1 is not evolving to defend against SAMHD1. All evidence suggests that HIV-1 is mostly replicating and evolving in memory $CD4^+$ T cells. However, in some cases, HIV-1 can evolve to infect other cells types.

1.3.3 Alternate Target: Naive CD4$^+$ T Cells

Coreceptor switching is the most common example of HIV-1 that has evolved to infect alternative cell types and occurs during late infection in approximately 50% of HIV+ subjects (124). During chronic infection, HIV-1 can evolve the ability to use CXCR4, another chemokine expressed on the surface of immune cells, as an alternate coreceptor. When this CXCR4-using (X4) variant emerges and rises to high frequency in a viral population, it is called coreceptor switching. These viruses still require a high density of CD4, which limits entry to T cells (T-tropic), but are now able to use CXCR4 (CXCR4-using or X4), which is only expressed at sufficient levels on the naive subset of CD4$^+$ T cells.

Most X4 T-tropic variants retain some ability to use the original CCR5 coreceptor, but it remains unclear whether this is relevant *in vivo*. Animal studies have shown that infection with X4 T-tropic viruses depletes naive CD4$^+$ T cells followed by memory CD4$^+$ T cells, which implies that X4 T-tropic HIV-1 can infect both subsets of T cells, but preferentially targets naive CD4$^+$ T cells. In late infection, the primary target (memory CD4$^+$ T cells) are depleted and so viruses able to target alternate cells types even cell types less efficient for HIV-1 replication become more prevalent (124, 125). In any viral infection, there is selective pressure for HIV-1 to replicate in the best cell type available, i.e. of the cell types accessible to the virus, the one that supports replication most robustly. However, as the target cell population declines, the advantage of efficient replication is balanced against the advantage of being able to find a target cell to replicate in. At some point it may be advantageous to adapt to replicate in an alternative target cell, but retain the ability to replicate in the original target cell. If the population of the original target cells becomes too small to support replication (and evolution), then there is no selective pressure to maintain the ability to infect the original target cell and that ability would become vestigial and eventually lost. Therefore, the observation that some X4 T-tropic viruses maintain the ability to use CCR5 may indicate either ongoing replication in both naive and memory CD4$^+$ T cells; or that the X4 T-tropic population was, at some point, previously R5 T-tropic.

Coreceptor switching is associated with a rapid decline in the health of HIV+ subjects, but the causal link remains unknown. One hypothesis is that HIV-1 replication in and depletion of naive $CD4^+$ T cells directly causes an enhancement in disease progression. However, without HAART, all HIV-1 infections can cause the full spectrum of disease regardless of whether the viral population undergoes coreceptor switching. An alternative hypothesis is that depletion of the memory $CD4^+$ T cells causes immune dysregulation, which results advancing disease, and also produces the selective pressure to increase HIV-1 replication in naive $CD4^+$ T cells. In this case, the appearance of X4 T-tropic viruses would only represent a marker of disease advancement. However, this model does not provide an explanation for why X4 T-tropic variants do not appear in all subjects when the memory $CD4^+$ T cell population is depleted to similar extent, but it is possible that the explanation lies in the different propensities of HIV-1 variants to evolve to use CXCR4 (126).

Different subtypes of HIV-1 group M undergo coreceptor switching at different frequencies. Subtype B infections result in coreceptor switching in 50% of subjects. Subtype D, which is closely related to Subtype B, undergoes coreceptor switching even more frequently. Subtype C, on the other hand, has a reduced incidence of coreceptor switching and SIV undergoes coreceptor switching only rarely. However, all coreceptor switching requires changes in the HIV-1 Env protein specifically in the third variable (V3) region, which is involved in coreceptor binding. The major genetic signatures of coreceptor switching are the emergence of nucleotide substitutions coding for basic amino acids at positions 11, 24, and 25 in the V3 region. This genetic signature has enhanced the ability to identify X4 T-tropic variants by sequence alone without expensive and time consuming functional tests and has provided a tool to tailor treatment. However, the entire V3 regions are more diverse in X4 T-tropic variants, suggesting that the evolutionary requirements are more complex than just those three positions.

1.3.4 Alternate Target: Macrophages

HIV-1 that has adapted to infecting macrophages (or microglial cells, which are macrophage-like cells in the parenchyma of the brain) is detected so rarely (17, 20) that it is difficult to estimate the true frequency of emergence in HIV-1 infection. Most examples of macrophage-tropic (M-tropic) viruses have been identified very late during HIV-1 infection in the CNS of subjects with HIV-associated neurocognitive disorders. It is possible that M-tropic viruses are only detectable in this compartment due to the general lack of T cells in the CNS and that M-tropic viruses are also present in other anatomical compartments, but at frequencies too low to detect over the more abundant R5 T-tropic viruses. However, by the same token, there is more selective pressure to adapt to infect macrophages in a compartment lacking the primary target (memory $CD4^+$ T cells) than in tissues where the primary target is readily available. Either way, when studying M tropism using only M-tropic viruses from the CNS, differences in selective pressures due the different environments provided by different compartments (e.g. differences in the immune responses in the blood vs. those in the brain) must be considered in addition to the selective pressures exerted by the target cell.

Until recently, M-tropic viruses have been identified through infection monocyte-derived macrophages (MDMs). Originally, HIV-1 was cultured and tested in transformed T cell lines that had lost expression of the CCR5 coreceptor, which is required for infection by R5 viruses and only allowed infection by X4 T-tropic viruses. The remaining viruses (the R5 variants) were eventually discovered to infect MDMs and were given the misnomer of macrophage-tropic despite including both R5 M-tropic and R5 T-tropic viruses. When the CCR5 and CXCR4 coreceptors were identified, viruses were divided into X4 variants (which could infect transformed T cell lines) R5 variants (which could infect MDMs) and dual tropic variants (which could use either coreceptor and infect both transformed T cell lines and MDMs). However, viruses infected MDMs to widely varying degrees. Upon identification of T cells as the primary target of HIV-1, it was observed that although R5 T-tropic viruses could infect MDMs, a small fraction of R5 variants infected MDMs far more efficiently by comparison

and so were identified as R5 M-tropic.

Although direct comparisons of infectivity on MDMs have clarified important differences between R5 T-tropic and R5 M-tropic viruses, MDMs are highly variable both between different donors and between different preparations from the same donor over time (99, 132). Viruses are also highly variable in their ability to infect MDMs, including wide variation in a panel of R5 T-tropic viruses sampled from different subjects and used to infect the same preparation of MDMs (99, 132). Because of the (1) low frequency of M-tropic viruses detected, (2) the previous lack of a sensitive and reproducible identification method, and (3) the inherent high variation in the genotypes and phenotypes of HIV-1 isolated from different patients, there are few studies that have characterized verified, true M-tropic viruses and how they differ from typical R5 T-tropic viruses.

In this dissertation, we used M-tropic viruses that were rigorously defined by three criteria (61). First, these M-tropic viruses were isolated from subjects with HIV-associated neurocogntive defects and slow viral load decay rates in the cerebrospinal fluid (CSF) upon initiation of HAART, which indicates that viruses are being produced from long-lived cells, likely macrophages or microglia (compared to the relatively short lived infected memory $CD4^+$ T cells). Second, we analyzed the HIV-1 *env* gene from several viruses from the blood and CSF of each patient, because it is both the viral gene most relevant to the entry phenotype and the most variable gene of the HIV-1 genome, which enhances the ability to differentiate closely related viruses. We used phylogenetic analysis of *env* genes to identify viral populations in the CSF that were compartmentalized from the viral population in the blood of the same subject, which is not typical in HIV-1 infection. Of these CSF compartmentalized viral populations, we excluded those that were comprised of identical or closely related viruses, which suggests a short-term expansion and may be the result of clonal amplification of an infected T cell, and focused on CSF compartmentalized viral populations that were diverse, which suggests a more long-term colonization of this compartment, to identify viral populations that had several generations of adaptation to their new environment. Third, we generated pseudotyped

viruses with *env* genes from the blood or CSF from each of these subjects and the same *env*-deficient HIV-1 genome expression construct with a luciferase reporter gene. We used these *env*-pseudotyped reporter viruses to infect MDMs from several donors, which showed that all *env* genes clones from blood viruses effected poor infection of MDMs and that all *env* genes from CSF viruses that formed compartmentalized, diverse phylogenetic clades effected efficient infection of MDMs. Viruses from the CSF of the same patients that clade with the blood rather than the CSF had results equivalent to blood viruses and it is likely that these blood-like CSF viruses originated in the blood and represent spill-over into the CSF. We used one M-tropic viruses isolated from each of five subjects in Schnell et al. 2011 that conformed to this three-fold definition of M tropism and also one T-tropic virus from each of the same five subjects in order to study matched pairs of M-tropic and T-tropic viruses, which reduces the confounding effects of variation in viruses from different subjects.

For the first phase of this study, we began by clarifying how macrophages differ from memory $CD4^+$ T cells as a target for viral entry. We quantified expression of the CD4 receptor and CCR5 coreceptor on the surface of memory $CD4^+$ T cells and monocytes (later induced to become macrophages, i.e. MDMs) isolated from several donors. We measured the size of these cell types to compare receptor and coreceptor expression densities between cell types. We also measured CD4 and CCR5 density on the Affinofile cell line, which can be experimentally induced to express different levels of CD4 and/or CCR5. To observe how receptor density influences entry, we used M-tropic and paired T-tropic viruses to infect memory $CD4^+$ T cells, MDMs, or Affinofiles that had been induced to different levels of CD4 or CCR5 expression. To evaluate the variation in MDM infectivity, we use a large panel of T-tropic viruses to infect MDMs from four different donors. In this phase, we showed that CD4 densities are approximately 20-fold lower on MDMs compared to memory $CD4^+$ T cells and, using Affinofile cells, we showed the lower CD4 expression found on MDMs presents a large obstacle to infection even when the cell type is unchanged (i.e. Affinofile cells expressing low vs. high CD4 densities). We also showed that infection of Affinofile cells at low vs. high CD4

expression can be used to effectively detect M-tropic viruses and with increased sensitivity and reproducibility compared to MDM infection.

For the second phase of this study, we clarified how M-tropic viruses differ phenotypically from T-tropic viruses using the original five pairs of T-tropic and M-tropic viruses and two additional pairs from two additional subjects. To estimate the magnitude of difference in MDM infection, we used the same panel of seven paired *env*-pseudotyped reporter viruses (fourteen viruses total) to infect MDMs from four different donors (to account for variation between donors). We also used these seven pairs of viruses to infect Affinofile cells expressing CD4 at ten different levels as a more sensitive measure of CD4 usage (i.e. the ability to use low CD4 densities for viral entry into a target cell). To probe for differences in Env conformation by epitope exposure and neutralization sensitivity, we exposed the seven pairs of viruses to a wide panel of antibodies, including poly clonal sera and monoclonal antibodies targeting different epitopes, and also to soluble CD4 (sCD4). To test viral Env stability, we exposed the seven pairs of viruses to different temperatures and assessed for function in entry assays. We compared the relative incorporation of Env into virions by western blotting. Because sensitivity to Env density on target cells proved to differentiate M-tropic viruses from T-tropic viruses, we compared CD4 usage against MDM infectivity for the seven M-tropic and T-tropic virus pairs plus an additional seven viruses of intermediate CD4 sensitivity and seven paired T-tropic viruses (14 pairs or 28 viruses total) and found a strong linear correlation between enhanced CD4 usage and increased infectivity in MDMs. We also observed that, although all T-tropic viruses were relatively resistant to neutralization by sCD4, all M-tropic (enhanced CD4 usage) viruses and viruses with an intermediate CD4 usage phenotype were highly sensitive to neutralization by sCD4. These intermediate CD4 usage viruses may represent an evolutionary intermediate on the path to M-tropism, which if true implies that early stages in the evolutionary process result in increased sensitivity to sCD4, which precedes a gradual enhancement of CD4 usage as viruses evolve to efficiently enter macrophages.

For the third phase of this study, we identified the major genetic determinates of M-tropism

in the original panel of five subject-matched pairs T-tropic and M-tropic viruses. We made chimeric *env* genes that combined regions of the T-tropic and M-tropic viruses from the same subject and evaluating macrophage tropism by relative CD4 usage, which we now understand to be a continuous phenotype (96). By gradually decreasing the regions of Env coded by the M-tropic *env*, we narrowed down the regions that contributed significantly to enhanced CD4 usage. We then used site-directed mutagenesis to identify single amino acid changes or constellations of amino acid changes that were responsible for enhanced CD4 usage both by knock-out mutations in the M-tropic *env* genes and knock-in mutations in the T-tropic *env* genes. Although there was no specific signature that was identical between M-tropic viruses isolated from different subjects, functional amino acid changes did cluster in certain regions. Although substitutions clustered around the CD4 binding site (CD4bs) in some cases, not all of the M-tropic *env* genes required peri-CD4bs substitutions. Only the V5 region was consistently required by all M-tropic primarily isolates tested, implicating the V5 in CD4 interactions with the Env protein. In one case, macrophage tropism required a coding change in the V1/V2 structure, which has recently been solved (133). The roles and functions of V1/V2 are still not fully understood, but this structure is thought to contribute to immune shielding and interactions with adjacent Env subunits within Env trimers. The flexible structure of V1V2 makes it difficult to understand how this cluster of mutations may affect interactions between Env and CD4, but it is clear that it can contribute to using low densities of CD4 for entry. Although the genetic signature of M-tropism is not as clear as the genetic signature of coreceptor switching, we have identified a genetic theme and have begun to clarify how M-tropic viruses have evolved to use lower density CD4 for entry into macrophages.

CHAPTER 2

QUANTIFICATION OF ENTRY PHENOTYPES OF MACROPHAGE-TROPIC HIV-1 ACROSS A WIDE RANGE OF CD4 DENSITIES[1]

2.1 Overview

Defining a macrophage-tropic phenotype for HIV-1 to assess a role in pathogenesis is complicated by the fact that HIV-1 isolates vary continuously in their ability to enter monocyte-derived macrophages (MDMs) *in vitro*, and MDMs vary in their ability to support HIV-1 entry. To overcome these limitations, we identified consistent differences in entry phenotypes between five paired blood-derived, T cell-tropic HIV-1 *env* genes, four of which are CCR5-using (R5) and one of which is CXCR4-using (X4), and cerebrospinal fluid (CSF)-derived, R5 macrophage-tropic *env* genes. We performed entry assays using the CD4- and CCR5-inducible Affinofile cell line, expressing a range of CD4 levels that approximates the range from MDMs to $CD4^+$ T cells. The macrophage-tropic viruses were significantly better at infecting cells expressing low levels of CD4 than the T cell-tropic viruses from the same subjects, with the titration of CD4 providing a distinctive and quantitative phenotype. This difference in CD4 utilization was not due to macrophage-tropic viruses being CD4 independent. Furthermore, macrophage-tropic viruses did not differ from paired T cell-tropic viruses in their ability to use low levels of CCR5 ($t_{\text{paired}} = 1.39$; $P = 0.24$) or their use of an alternative

[1]The work described in this chapter was accomplished in collaboration with Sarah B. Joseph, Adrienne E. Swanstrom, Gretja Schnell, Benhur Lee, James A. Hoxie, and Ronald Swanstrom. The work presented in this chapter was previously published and is reprinted/adapted from Joseph S.B., et al. 2014. Quantification of Entry Phenotypes of Macrophage-Tropic HIV-1 across a Wide Range of CD4 Densities. J Virol 88:1858-69 with permission from American Society for Microbiology.

conformation of CCR5. We also infected MDMs with a panel of viruses and observed that infectivity of each virus differed across four donors and between three preparations from a single donor. We concluded that the evolutionary transition from replication in T cells to that in macrophages involves a phenotypic transition to acquire the ability to infect cells expressing low levels of CD4 and that this phenotype is more reliably measured in Affinofile cells than in macrophages.

2.2 Introduction

The HIV-1 Env protein determines the entry phenotype of the virus, typically using CD4 as the receptor and CCR5 as the coreceptor. The ability of HIV-1 to replicate in a novel cell type likely requires adaptation of the viral envelope protein to efficiently utilize the receptor and coreceptor present on that cell type. The emergence of CXCR4-using virus late in infection has long been thought to represent adaptation to infect a novel host cell (134), most likely $CD4^+$ naive T cells, which are known to express high levels of CXCR4 and very little CCR5 (135). This is consistent with a recent *in vitro* study showing that receptor-mediated entry of $CD4^+$ naive T cells requires use of the CXCR4 coreceptor (136).

Historically, viruses capable of growing in transformed T cell lines were called T cell-tropic viruses. Due to the fact that most T cell lines express CXCR4 but not CCR5, the early isolates capable of growth on these cell lines were predominantly CXCR4-using viruses. In order to distinguish these CXCR4-using T cell-tropic viruses, the remaining CCR5-using (R5) isolates were collectively called macrophage-tropic (M-tropic) viruses, based on the observation that at least some of these isolates could enter and, in some cases, replicate in macrophages. Thus, the early analyses of sexually and vertically transmitted HIV-1 suggested that transmitted/founder viruses are predominantly macrophage tropic (137, 138). These findings were supported by early studies suggesting that macrophages are the initial target cell for sexual transmission (139) and by observations that cervical explants could be infected by the macrophage-tropic virus Ba-L and not by two T cell-tropic strains (140). More recent studies,

however, have contradicted this viewpoint by showing that infectious molecular clones (17, 141, 142) and *env* gene clones (16) generated from transmitted/founder viruses are predominantly CCR5-using viruses and infect monocyte-derived macrophages (MDMs) at levels well below those of prototypic macrophage-tropic viruses.

Uncertainty about the nature of most R5 viruses also comes from the study of macrophage-tropic HIV-1. A virus capable of replicating in MDMs was originally isolated from primary lung cultures taken from an infant who died of AIDS (143). This virus, HIV-$1_{Ba\text{-}L}$, was subsequently passaged on MDMs, where it likely adapted to replication in MDMs in culture. This phenotype has been linked to the ability to infect cells with low levels of CD4 (15, 144-148), and these types of viruses have most often been found in brain tissue of subjects who died with neurologic involvement (146, 148-151). However, there are also reports of these viruses being found in the blood (61, 152). A common observation in studies using MDMs is that they vary in the capacity to support HIV-1 entry, and this variability is usually dealt with by including several donors in a study. The lack of a quantifiable phenotype to measure viruses that enter macrophages with various efficiencies has left the concept of macrophage-tropic viruses vague and inconsistently applied to a wide variety of isolates, thus obscuring the role of these variants in transmission and pathogenesis.

In this study, we addressed this uncertainty by identifying phenotypes that differentiate viruses that have evolved *in vivo* to replicate in macrophages from those that replicate in T cells. We accomplished this by examining the entry phenotypes of well-characterized pairs of macrophage- and T cell-tropic viruses isolated from five subjects, as represented by cloned *env* genes. The macrophage-tropic viruses were all derived from cerebrospinal fluid (CSF), where the virus was previously shown to decay very slowly after initiation of antiretroviral therapy (60), indicating that the virus was being produced by long-lived cells, presumably either perivascular macrophages or microglia (153). In contrast, the T cell-tropic viruses were blood-derived viruses from the same subjects and decayed rapidly after the initiation of therapy, indicating that they were being produced by short-lived cells, presumably $CD4^+$ T

cells. By carefully examining the entry phenotypes of these viruses, we were able to show that the evolutionary transition from replication in $CD4^+$ T cells to replication in macrophages selects for an increased ability to infect cells expressing low levels of CD4 but does not alter the ability to infect cells expressing low levels of CCR5. We observed distinctive macrophage-tropic and T cell-tropic phenotypes by using a CD4 titration curve, which is possible with the CD4- and CCR5-inducible Affinofile cell line (154). We also show that infection of MDMs *in vitro* is an inconsistent assay for defining a macrophage-tropic phenotype. As a result, T cell-tropic viruses may appear to be macrophage tropic when infecting MDMs from some donors/preparations and T cell tropic on others, and some macrophage-tropic viruses may show the reverse. Collectively, these studies provide a more quantitative definition of HIV-1 macrophage tropism, which will allow a more accurate identification of these variants that will lead to an improved understanding of their role in viral pathogenesis.

2.3 Materials and Methods

2.3.1 Study subjects

In this study, we examined the entry phenotypes of previously generated *env* gene clones amplified from the blood and CSF of subjects infected with HIV-1 subtype B (61). These subjects participated in a study of HIV-associated dementia (61) at the University of California at San Francisco. Procedures for sample collection (155), viral decay assays (60), and cloning (61) (see below) have been described previously. All samples were collected with written informed consent, and all protocols were approved by institutional review boards at the collection sites.

Five of these subjects were diagnosed with neurological disease (stages 1 to 3) (Table 2.1) (61), and we consider the viruses in their CSF to be M-tropic based on measurements made both *in vivo* and *in vitro* For four of the subjects (subjects 4013, 4059, 5002, and 7115), the CSF viral load decayed slowly upon initiation of antiretroviral therapy (60), and the *env* clones derived from the CSF mediated the infection of MDMs very efficiently (61), thus indicating

that these clones are replicating in long-lived cells *in vivo* and are well adapted to entry into macrophages (using viruses pseudotyped with these Env proteins). Conversely, the blood viral loads of these subjects declined rapidly after initiation of therapy, indicating production from short-lived cells (60), and blood-derived clones from these subjects mediated the infection of macrophages very poorly, although this varied by the donor source for the MDMs (61). We consider these clones to be T cell-tropic viruses and indicate them as R5 (for four of the subjects) or X4 (for subject 5002) viruses, based on their coreceptor specificity. It is important to note this distinction of R5 T cell-tropic viruses, which are typically not accounted for in the literature; however, for simplicity, we will refer to these five rapid-decay viruses as T cell-tropic without specifying their coreceptor usage. We also included a subject (4051) who had a mixture of T cell-tropic and M-tropic viruses in the CSF, and we observed that the M-tropic lineage in the CSF of this subject increased in abundance relative to the T cell-tropic lineage with the initiation of therapy (unpublished data), consistent with its production from long-lived cells. Thus, we have a well-validated set of five CSF-derived, M-tropic *env* clones and paired blood-derived *env* clones that represent viruses that were growing in T cells and the majority of which are CCR5-using. We used these pairs of clones to develop a quantitative description of CD4 dependence for entry for two types of viruses: M-tropic and T cell-tropic viruses (see below).

We also examined *env* clones from five of these subjects with R5 T cell-tropic HIV-1 subtype B in the blood and CSF (Table 2.2). Their blood and CSF viral loads declined rapidly after the initiation of therapy, and *env* clones isolated from both compartments were unable to efficiently infect macrophages (61). The remaining two subjects were infected with R5 T cell-tropic HIV-1 subtype C. HIV *env* clones generated from the blood of these subjects were unable to infect Affinofile cells expressing low levels of CD4 (20).

2.3.2 Cloning of *env* genes

Two *env* clones Ba-L and JRCSF were obtained from the Division of AIDS, NIAID, through the NIH AIDS Research and Reference Reagent Program, Division of AIDS, NIAID, NIH. The remaining subtype B *env* clones were generated in a previous study (61). Here we briefly review the single-genome amplification (SGA) and cloning procedures. An oligo(dT) primer was used to generate cDNA from HIV-1 RNA isolated from blood plasma or CSF. SGA (156-158) was then used to amplify full-length *env* sequences through the 3 U3 region. After one round of SGA, amplicons were reamplified, gel purified using a QIAquick gel extraction kit (Qiagen), and cloned into the pcDNA 3.1D/V5-His-TOPO expression vector (Invitrogen) by use of a pcDNA 3.1 directional TOPO expression kit (Invitrogen) and Max Efficiency Stbl2 competent cells (Invitrogen). An additional set of *env* clones representing the transmitted virus in the context of heterosexual transmission of subtype C HIV-1 (20) was also included in the study of infection of MDMs.

2.3.3 Cells

293T cells were cultured in Dulbecco's modified Eagle medium (DMEM) with 4.5 g/liter glucose (Cellgro) supplemented with 10% fetal bovine serum (FBS), 50 U/ml of penicillin, and 50 μg/ml streptomycin. Affinofile cells (154) were maintained in DMEM with 4.5 g/liter glucose (Cellgro) supplemented with 10% dialyzed FBS (12 to 14 kDa; Atlanta Biologicals) and 50 mg/ml blasticidin (Invitrogen).

At three time points, monocytes were isolated from healthy donors. Approximately 40 ml of blood was collected from each donor into heparin-treated tubes. Buffy coats were purified using Ficoll-Paque Plus (GE Healthcare) following the manufacturer's directions. We then used negative selection to isolate monocytes (EasySep human monocyte enrichment kit without CD16 depletion; StemCell Technologies). Monocytes were resuspended and cultured in RPMI 1640 supplemented with 10% FBS, 100 mg/ml of penicillin and streptomycin, and 10 ng/ml recombinant human macrophage colony-stimulating factor (M-CSF; Gibco). Mono-

cytes were then plated at a density of 1.1 10^6 cells per 60- by 15-mm dish (6 ml medium per dish) for flow cytometry and at 5 10^4 cells per well of a 48-well plate (0.5 ml medium per well) for infection. After 5 days, a partial medium change was performed. After an additional 2 days (for a total of 7 days), cells were either infected or processed for flow cytometry.

2.3.4 Flow cytometry

CD4 and CCR5 expression levels on Affinofile cells, monocytes, $CD4^+$ T cells, and MDMs were quantified using flow cytometry. In order to avoid disrupting surface receptors, Affinofile cells and MDMs were removed from their culture dishes by nonenzymatic methods. Affinofile cells were removed using cold phosphate-buffered saline (PBS; CellGro), and MDMs were removed using cell dissociation buffer (Gibco). Affinofile cells and MDMs were stained with Fixable Aqua dead cell stain (Invitrogen) and saturating concentrations of either phycoerythrin (PE)-conjugated anti-human CD4 antibody (clone RPA-T4; BD Biosciences) or PE-conjugated mouse anti-human CCR5 antibody (clone 2D7; BD Biosciences). CD4 expression and CCR5 expression on primary cells were quantified by staining peripheral blood mononuclear cells (PBMCs) with Brilliant Violet 421-conjugated anti-human CD3 antibody (clone UCHT1; BD Biosciences), allophycocyanin (APC)-Cy7-conjugated anti-human CD14 antibody (clone MP9; BD Biosciences), and saturating concentrations of either PE-conjugated anti-human CD4 antibody (clone RPA-T4; BD Biosciences) or PE-conjugated mouse anti-human CCR5 antibody (clone 2D7; BD Biosciences). QuantiBRITE beads (BD Biosciences) were then used to translate the mean fluorescence per cell to the number of CD4 or CCR5 antibody binding sites (ABS) per cell. Six bead standards of known size (flow cytometry size calibration kit; Invitrogen) were used to translate measurements of forward scatter into estimates of cell diameter. All flow cytometry assays were performed using a Cyan flow cytometer (Beckman Coulter) and analyzed using FlowJo software (version 9.3.1).

2.3.5 Env-pseudotyped virus stocks

Env-pseudotyped luciferase reporter viruses were generated by cotransfecting 100- by 20-mm dishes of 293T cells with 5 μg of an HIV-1 *env* clone, 5 μg of pNL4-3.LucR-E plasmid (obtained from the Division of AIDS, NIAID, through the NIH AIDS Research and Reference Reagent Program, Division of AIDS, NIAID, NIH), and 30 μL of the FuGENE 6 transfection reagent (Promega). At 5 h posttransfection, the medium was changed and the cells were incubated at 37°C for an additional 43 h. Viral supernatants were then harvested, filtered through a 0.45-μm filter (Millipore), and stored at 80°C. Virus stocks were not subjected to multiple freeze-thaw cycles.

2.3.6 Affinofile cell assays

(159). Affinofile cells were plated at a concentration of 1.8 * 10^4 cells/well in black poly-l-lysine (Sigma)-treated 96-well plates. After 24 h in culture, ponasterone A (Pon A; Invitrogen) and doxycycline (Doxy; Sigma) were added at various concentrations to the medium to induce CD4 and CCR5 expression. Twenty hours later, the medium was replaced with medium lacking Pon A and Doxy, and virus was added to the plates. Cells were spinoculated at 2,000 rpm for 2 h at 37°C and then incubated at 37°C. After 48 h, the cells were washed twice with PBS and lysed with 50 μL of 1 reporter lysis buffer (Promega), and the lysate was stored at 80°C. Virus entry was then assessed by thawing the lysates and quantifying luciferase expression by using a luciferase assay system (Promega).

CD4 usage was examined by infecting Affinofile cells expressing 10 levels of CD4 and a single, high level of CCR5. Affinofile expression of CD4 ranged from uninduced ([Doxy] = 0 ng/ml) to maximally induced ([Doxy] = 6 ng/ml), with eight levels in between (0.07, 0.1, 0.2, 0.3, 0.5, 0.7, 1.0, and 1.5 ng/ml Doxy). CCR5 expression was maximally induced ([Pon A] = 5 μM.

CCR5 usage was examined by infecting maraviroc-treated Affinofile cells expressing a single, high level of CD4 ([Doxy] = 6 ng/ml) and either a high ([Pon A] = 5 μM or low ([Pon

A] = 0 μM level of CCR5. One hour prior to spinoculation, maraviroc was serially diluted and added to cells at 10 concentrations (0, 1.7, 8.2, 41.2, 123.5, 370.4, 1,111.1, 3,333.3, 10,000, and 50,000 nM maraviroc). After spinoculation, the maraviroc-containing medium was removed from each well and replaced with fresh medium.

2.3.7 Titration of virus stocks

Virus stocks were titrated by infecting Affinofile cells expressing the maximum levels of CD4 ([Doxy] = 6 ng/ml) and CCR5 ([Pon A] = 5 μM. We then calculated the volume of each virus stock that generated 800,000 relative light units (RLU) of luciferase expression when infecting maximally induced Affinofile cells. This quantity of virus, which was in the linear range for measuring infectivity, was used in all subsequent experiments infecting either MDMs or Affinofile cells.

2.3.8 Cell-cell fusion assay

A luciferase-based gene reporter assay was used to assess the ability of Env proteins to mediate cell-cell fusion (160, 161). Briefly, quail QT6 cells were transfected with individual HIV-1 *env* expression vectors by using $CaPO_4$ and then infected with a vaccinia virus expressing T7 RNA polymerase for 18 h. A second population of QT6 cells was transfected to transiently express human CCR5 and/or human CD4, or neither; all cells in the second population of QT6 cells were also transfected with the luciferase gene under the control of a T7 promoter and with a green fluorescent protein (GFP)-expressing vector to monitor transfection efficiency. The Env-expressing cells were then mixed with the receptor/coreceptor-expressing cells. Eight hours later, the cells were lysed, and luciferase expression was measured (represented in figures as mean RLU) with a luminometer. In this experimental design, luciferase activity is recorded as a function of the cells expressing the T7 RNA polymerase fusing with the cells expressing the luciferase gene under the control of the T7 RNA polymerase promoter.

2.3.9 Statistical analyses

All statistical analyses were performed using R statistical software (version 2.14.1). Model fitting of infection data was performed using the R statistical package (drc) designed to analyze dose-response models (drm). These analyses fit a four-parameter, log-logistic model to the data.

2.4 Results

2.4.1 Affinofile cells readily distinguish M-tropic and R5 T cell-tropic viruses based on differences in sensitivity to surface CD4 levels

Affinofile cells have been engineered to have inducible and titratable levels of CD4 and CCR5, and they express CXCR4 constitutively. In our previous study, we showed that the ability to maintain a moderate level of infectivity on Affinofile cells with the uninduced level of CD4 on the surface was related to efficient infection of macrophages and the slow decay of viral load in the CSF (61). Here we explored the phenotype of CD4 dependency across the entire range of CD4 concentrations available using Affinofile cells. The sensitivity to CD4 level of viruses pseudotyped with different Env proteins was assessed by measuring their ability to infect Affinofile cells induced to express 10 CD4 levels (ranging from 1,425 to 81,649 CD4 molecules per cell, inferred as antibody binding sites per cell). The shape of the infectivity curve as a function of CD4 density (four-parameter, log-logistic curve) differed for comparing the M-tropic viruses to the R5 (and one X4) T cell-tropic viruses isolated from the same subject (Figure 2.1a; Table 2.1).

There are three features of these titration curves that distinguish the two groups of viruses: (i) the M-tropic viruses retained the ability to infect cells at the lowest level of CD4 expression (1,425 CD4 molecules per cell), at 16 to 24% of their infectivity on high-CD4-expressing cells (81,649 CD4 molecules per cell), while the T cell-tropic viruses infected Affinofile cells with low levels of CD4 at only 0 to 2% of their infectivity on high-CD4-expressing cells (t_{paired}

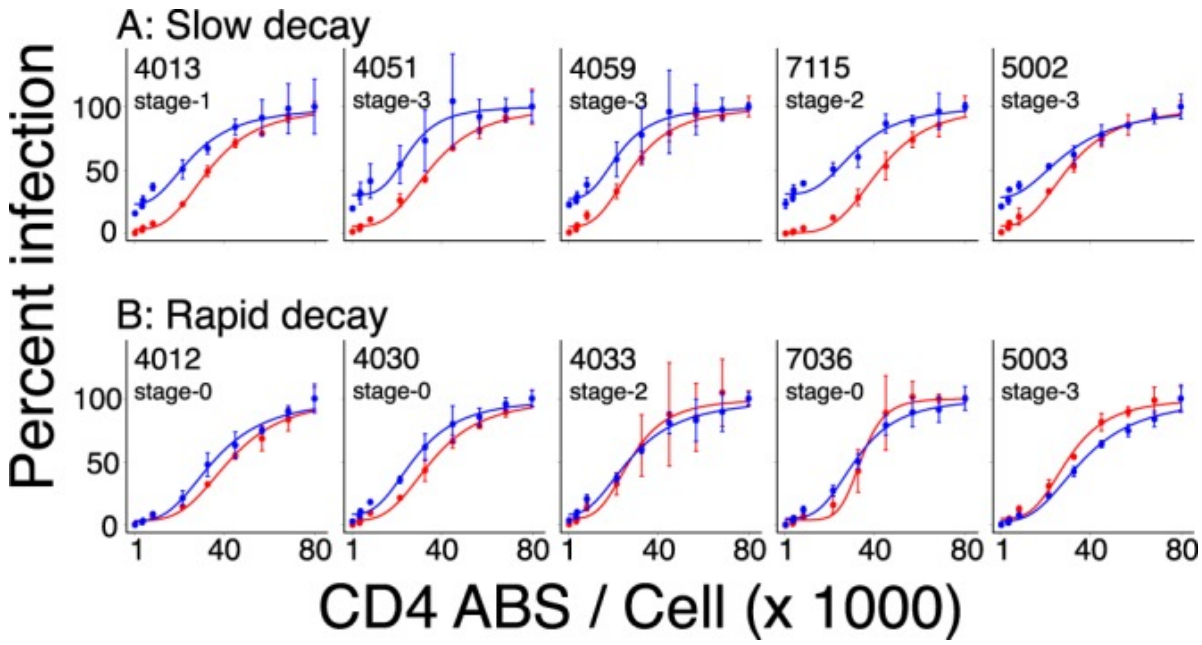

Figure 2.1: **Dose-response curves for infectivity of M-tropic and T cell-tropic viruses to Affinofile cells expressing various densities of CD4.** The sensitivity of pseudotyped viruses to CD4 levels was assessed by measuring their ability to infect Affinofile cells expressing 10 CD4 levels (1,425; 4,590; 4,981; 9,374; 22,667; 33,842; 46,204; 58,153; 69,897; and 81,649 CD4 ABS per cell), with CCR5 fully induced. (A) *env* genes were isolated from viruses in the blood and CSF of subjects who had rapid decay of virus in the blood but slow decay of virus in the CSF with the initiation of anti-HIV-1 therapy (61). These *env* genes were used in a transfection protocol to generate pseudotyped viruses that carried a reporter gene (luciferase). Equal amounts of virus were used at each CD4 level, and the level of infectivity at the highest level of CD4 was taken as 100%. The highest value was within the linear region of the dose-response curve for infectivity for each virus. The lines for each virus were generated by the R statistical package (drc) designed to analyze dose-response models (drm). Red lines represent viruses pseudotyped using *env* genes generated from viruses in the blood. Blue lines represent viruses pseudotyped using *env* genes generated from viruses in the CSF. (B) A similar analysis was done by comparing viruses from the blood and CSF of subjects who had rapid decay of virus in both the blood and CSF after the initiation of therapy (61). The stage designation for each subject refers to AIDS dementia complex staging, where 0 = neurologically asymptomatic, 1 = mild neurological impairment, and 2 and 3 = moderate to severe HIV-associated dementia (HAD) (61).

Table 2.1: CD4 sensitivities and fusogenicities of *env* clones derived from subjects with slow viral decay after initiation of therapy[a]

	CD4 usage curve data											
	% Infectivity at lowest CD4 density			CD4 ED_{50} (ABS/μm^2)			Hill slope			Ability to fuse to cells expressing CD4 and CCR5 (RLU)		
	Plasma	CSF		Plasma	CSF		Plasma	CSF		Plasma	CSF	
Subject	T-tropic	M-tropic	Difference[b]	T-tropic	M-tropic	Difference[b]	T-tropic	M-tropic	Difference[b]	T-tropic	M-tropic	Difference[b]
4013	0.4	15.9	−15.5	19.9	15.7	4.2	3.1	2.6	0.5	83.4	80.9	2.5
4051	1.5	19.7	−18.3	20.9	15.3	5.6	3.3	3.9	−0.6	86.7	234.3	−147.6
4059	0.9	22.8	−22.0	17.0	13.6	3.4	3.1	3.1	0.0	43.1	177.9	−134.8
5002	1.0	21.4	−20.4	18.2	17.9	0.3	2.9	2.3	0.6	24.4	141.9	−117.5
7115	0.1	23.5	−23.4	24.6	18.6	6.0	3.8	3.2	0.6	14.5	188.9	−174.4

[a] See Fig. 1A

[b] Significant difference between paired CSF and plasma clones (paired t test; P <0.02).

= 14.29; degrees of freedom [df] = 4; *P* value = 0.00014); (ii) the CD4 level that increased infectivity by 50% (CD4 ED_{50}) was significantly lower for the M-tropic viruses than for the paired T cell-tropic viruses (t_{paired} = 3.84; df = 4; *P* value = 0.018); and (iii) in most cases, the M-tropic virus approached a plateau level of infectivity at a lower CD4 density than that with the paired T cell-tropic virus. We observed a similar pattern of CD4 utilization for the prototypic M-tropic virus Ba-L (data not shown).

We repeated the above-described assays using T cell-tropic *env* clones isolated from the blood and CSF of five subjects who lacked M-tropic HIV-1 in the CSF (Figure 2.1b; Table 2.2). We observed that pseudotyped viruses generated using these CSF- and blood-derived *env* genes did not differ in their minimal ability to infect Affinofile cells expressing the lowest CD4 level (t_{paired} = 1.25; df = 4; *P* value = 0.28) or in the CD4 level that increased infectivity by 50% (t_{paired} = 0.71; df = 4; *P* value = 0.52). Also, there was no pattern of difference in the approach to a plateau of infectivity at the highest CD4 levels. Thus, the ability to infect cells expressing low levels of CD4 (and the differences in the other parameters) is not specific to CSF-derived clones but rather is specific to the M-tropic clones generated from viruses being produced *in vivo* by long-lived cells. Also, we interpret these results to represent two distinct phenotypes for M-tropic and T cell-tropic viruses and not simply part of a continuum among

isolates in the ability to use differing densities of CD4.

Table 2.2: CD4 sensitivities of env clones derived from subjects with rapid viral decay after initiation of therapy[a]

	% Infectivity at lowest CD4 conc.			CD4 ED_{50} (ABS/μm^2)			Hill slope		
	Plasma	CSF		Plasma	CSF		Plasma	CSF	
Subject	T-tropic	T-tropic	Difference	T-tropic	T-tropic	Difference	T-tropic	T-tropic	Difference
4012	1.0	0.6	0.4	24.9	21.0	3.9	3.5	3.0	0.5
4030	0.5	3.1	−2.6	21.1	16.9	4.2	3.2	2.9	0.3
4033	1.0	2.3	−1.3	16.5	16.8	−0.3	3.6	2.5	1.1
5003	1.0	0.5	0.5	17.8	21.5	−3.7	3.5	2.9	0.6
7036	0.2	0.8	−0.6	19.9	18.8	1.1	6.8	3.5	3.3

[a] See Fig. 1B.

2.4.2 Titration of CD4 density on Affinofile cells mimics the densities of CD4 on $CD4^+$ T cells, macrophages, and monocytes

Given that Affinofile cells provide a clear phenotypic distinction between viruses produced in the central nervous system (CNS) from long-lived cells and viruses present in the blood (Figure 2.1a), we next determined if the density of CD4 on Affinofile cells was similar to the density on the target cells for HIV-1 replication. We used an anti-CD4 antibody to stain $CD4^+$ T cells, monocytes, MDMs, and Affinofile cells either fully induced for CD4 expression or uninduced (Figure 2.2a). The amount of antibody bound to each cell was estimated by creating a standard curve with a control set of fluorescent beads. We also estimated the sizes of the cells by using forward scatter and size standard beads. We found that T cells and macrophages had similar numbers of CD4 molecules on the surface but that $CD4^+$ T cells were significantly smaller than MDMs (Figure 2.2b). Monocytes had a small number of CD4 molecules on the surface and also had a small cell diameter, and the Affinofile cells had a similarly small number of CD4 molecules on the cell surface in the uninduced state and much higher levels in the induced state. We normalized the number of CD4 molecules on the surface by using the

surface area of the cell to obtain the density of CD4 per μm^2 (Figure 2.2c). This showed that the uninduced Affinofile cells had a density of CD4 that was several-fold lower than that on monocytes or MDMs (0.7 versus 3.1 or 3.4 CD4 ABS/μm^2), and these three cell types were approximately 18- to 90-fold lower in CD4 density than the fully induced Affinofile cells (64 CD4 ABS/μm^2). Also, the CD4 density on fully induced Affinofile cells approximated but was still less than the density on $CD4^+$ T cells (78 CD4 ABS/μm^2). Figure 2.2d summarizes the CD4 densities on the different cell types and shows the approximate infectivity patterns for M-tropic and T cell-tropic viruses as a function of CD4 density. These measurements show that the titration of CD4 on Affinofile cells spans the range of CD4 densities found on relevant target cells for HIV-1 infection. Composite CD4 usage curves were generated by fitting a curve to the infectivity data for the five M-tropic clones and fitting a curve to the infectivity data for the paired, T cell-tropic clones.

Infection of MDMs varies between different MDM cultures. Infection of MDMs is one definition of macrophage tropism, and the ability to infect a cell with low levels of CD4 has been used by some investigators as a surrogate marker for macrophage tropism. Infectivity of MDMs can be variable, and typically, infections are repeated with at least two different preparations of MDMs to account for this variability, although how this variability is then reconciled is usually not discussed. In an effort to understand the biological basis for this confounding variability, we infected MDMs with pseudotyped viruses generated from 14 different *env* expression vectors and normalized their infectivity to the infectivity of the M-tropic virus Ba-L (Figure 2.3). We infected a single preparation of MDMs from three donors (Figure 2.3a) and three MDM preparations from one donor (Figure 2.3b). As expected, the normalized infectivity of the prototypic R5 T cell-tropic virus JRCSF was extremely low (0.5 to 2% of that of the M-tropic clone). In contrast, some of the T cell-tropic viruses infected the MDMs quite well. Overall, normalized infectivity of the T cell-tropic viruses was much lower on MDMs from the donors with the lowest CD4 levels (donors 1 and 4) (Table 2.3) than on MDMs from the donor with the highest CD4 levels (donor 3) (Figure 2.3; Table 2.3). Thus, infection of

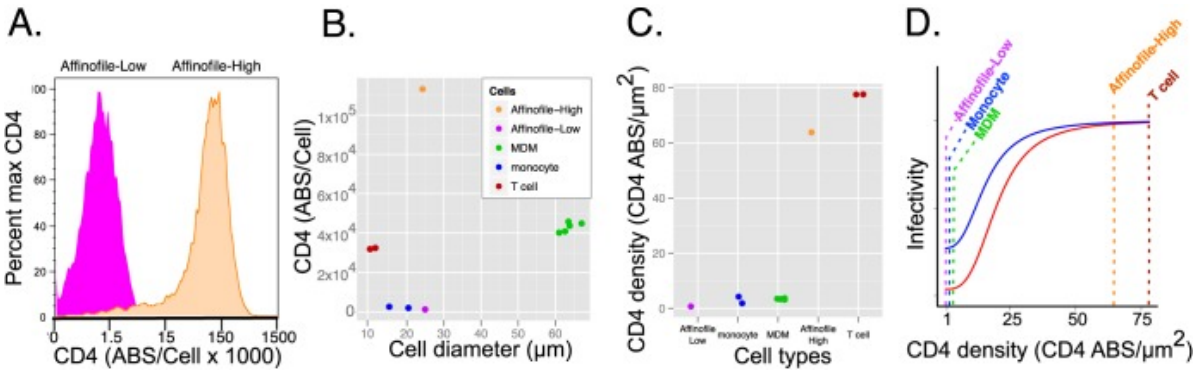

Figure 2.2: **CD4 densities on Affinofile cells approximate the densities of CD4 on CD4$^+$ T cells, MDMs, and monocytes.** (A) Affinofile cells were either uninduced or induced to express the highest level of CD4 on the cell surface. Data shown are flow analysis results for uninduced Affinofile cells and fully induced cells. CD4 was quantified as the number of ABS per cell, based on fluorescence calibration using a fluorescent bead standard curve. Cell size was also estimated based on forward scatter and compared to a bead standard curve. (B) Affinofile cells at the uninduced and induced levels, monocytes, MDMs, and CD4$^+$ T cells were compared by the number of CD4 molecules (ABS) per cell and the cell size, based on diameter. (C) Expression of CD4 as a function of density was plotted for different cell types (uninduced and induced Affinofile cells, CD4$^+$ T cells, monocytes, and MDMs). This analysis shows that uninduced Affinofile cells have a CD4 density that is slightly lower than those of MDMs and monocytes, while fully induced Affinofile cells have a CD4 density that is slightly lower than that of CD4$^+$ T cells. (D) Patterns of entry by M-tropic viruses (blue) and T cell-tropic viruses (red), combined from the data in Figure 2.1 to generate average dose-response curves for infectivity as a function of CD4 density. The CD4 densities of monocytes, MDMs, and CD4$^+$ T cells are indicated, along with the extremes of CD4 densities on uninduced and fully induced Affinofile cells.

MDMs from some donors can give a discrepant entry phenotype compared to the definition obtained using Affinofile cells.

2.4.3 Macrophage-tropic viruses are able to use low levels of CD4 but are not CD4 independent

It is possible that the residual level of infectivity seen at the lowest density of CD4 on Affinofile cells is actually CD4-independent entry. To determine whether the Envs from the CSF-derived viruses were capable of CD4-independent entry, we evaluated the ability of these Envs to mediate fusion with cells expressing CD4 and CCR5 or CCR5 alone. In this assay, one cell type expresses the receptor and coreceptor, while another cell type expresses the viral Env protein. Upon mixing of the cell populations, the Env protein engages the receptor

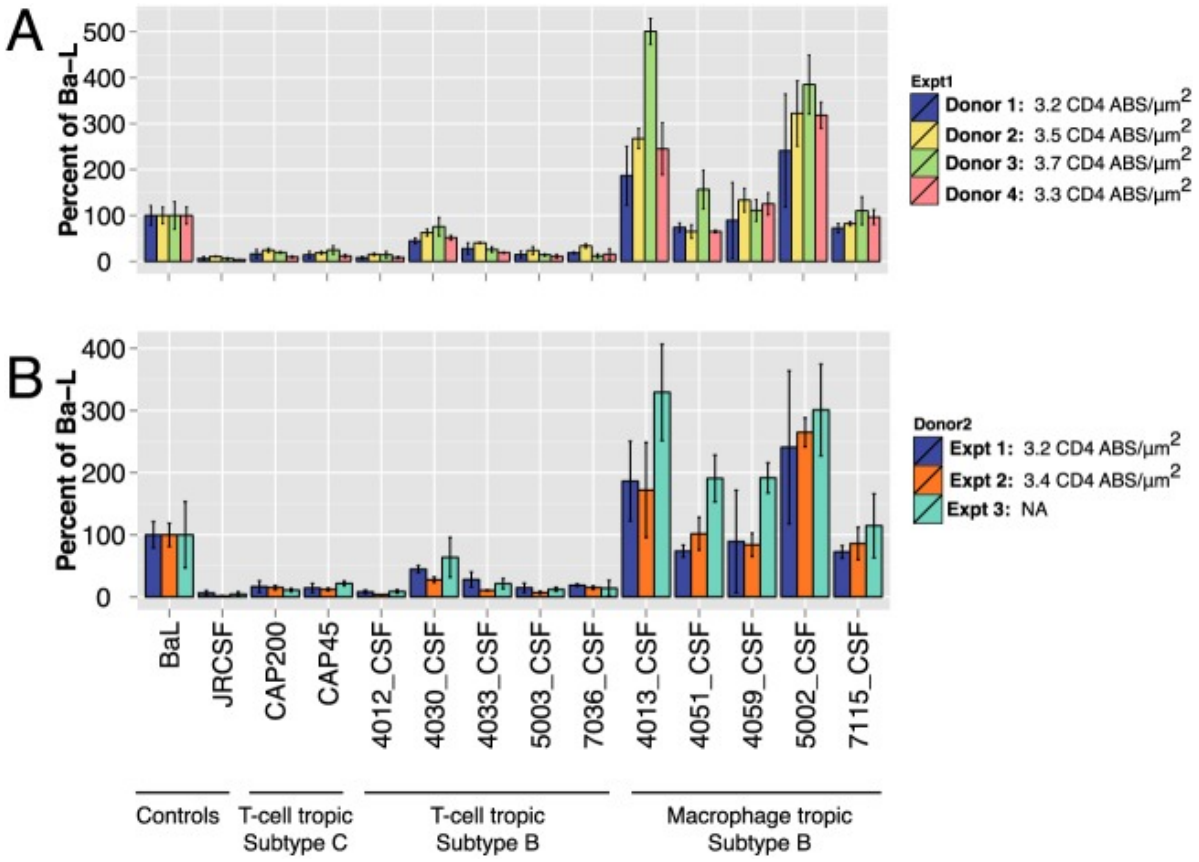

Figure 2.3: **Pseudotyped virus infectivity of MDMs differs across both MDM donors and preparations.** MDMs were infected with a panel of 14 pseudoviruses: a prototypic M-tropic virus (Ba-L), a prototypic R5 T cell-tropic virus (JRCSF), two R5 T cell-tropic viruses derived from the blood of individuals infected with HIV-1 subtype C (20), five R5 T cell-tropic viruses derived from the CSF of individuals infected with subtype B HIV-1 that decayed rapidly after initiation of antiretroviral therapy (61), and five M-tropic viruses derived from the CSF of individuals infected with subtype B HIV-1 that decayed slowly after initiation of antiretroviral therapy (61). These pseudotyped viruses were used to infect preparations of MDMs made from the blood of four different donors, drawn and processed in parallel on the same day (A), and preparations of MDMs prepared from the same donor compared over three different blood donations, each separated by several months (B). The amount of virus used in the infections was standardized to give the same level of infectivity on fully induced Affinofile cells. The level of infectivity with the virus pseudotyped with the Ba-L Env protein was used as 100% infectivity, and infectivities of all other viruses were recorded as percentages of this value.

Table 2.3: Receptor and coreceptor densities on MDMs

	Receptor/coreceptor density (ABS/μm^2)			
	Expt 1		Expt 2	
Donor	CD4	CCR5	CD4	CCR5
1	3.2	1.3	3.4	1.3
2	3.5	1.4		
3	3.7	1.5		
4	3.3	1.8		

and coreceptor, thereby inducing fusion and providing a readout. As a positive control, we used a lab-derived CD4-independent variant of R3A, iR3A, that is capable of mediating CD4-independent fusion with cells expressing only CCR5. As expected, the Env protein from iR3A mediated fusion of cells expressing CCR5 with or without CD4, and the Env proteins from the T cell-tropic viruses isolated from plasma required both CCR5 and CD4 (Figure 2.4). Like the Env proteins from the blood-derived viruses, all of the Env proteins from the CSF-derived M-tropic viruses required both CCR5 and CD4 to mediate fusion (Figure 2.4). Thus, the residual infectivity at low CD4 density of the macrophage-tropic viruses is still CD4 dependent. It is worth noting that most of the Env proteins from the CSF-derived viruses consistently fused cells to a greater extent than their paired blood plasma-derived counterparts (Table 2.1) (t_{paired} = 3.73; df = 4; *P* value = 0.02). In a separate experiment (data not shown), we examined QT6 cells transfected with these constructs and found that they expressed very low CD4 densities (CD4 ABS/μm^2). Thus, the observation that CSF-derived Envs are more active in this fusion assay system is likely due to their ability to utilize low CD4 densities.

In order to confirm that virus entry into Affinofile cells is CD4 dependent, we performed an additional entry assay in the presence of an anti-CD4 antibody (leu3a). We treated Affinofile cells expressing the lowest (uninduced) level of CD4 with the antibody and found that it blocked both the very low levels of entry displayed by T cell-tropic viruses and the higher

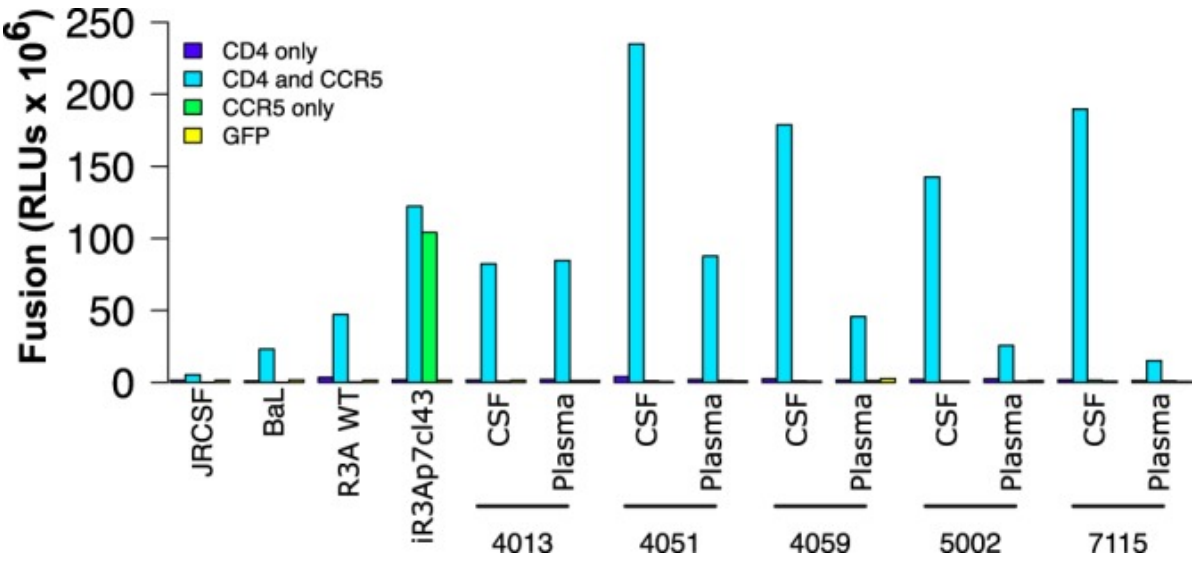

Figure 2.4: **The evolution of macrophage tropism does not select for CD4-independent entry** QT6 cells were transfected with individual HIV-1 *env* expression vectors and infected with a vaccinia virus expressing T7 RNA polymerase. A second population of QT6 cells was transfected with vectors that express CCR5 and/or human CD4, or neither, and with a luciferase expression vector. The two types of cells were then mixed, and 8 h later, the level of luciferase was measured as an indication of cell fusion. Only the lab-derived positive control (iR3Ap7cl43) was able to fuse with cells lacking CD4.

levels of entry displayed by macrophage-tropic viruses (data not shown). Thus, the enhanced ability of macrophage-tropic HIV-1 to enter cells expressing low levels of CD4 is not due to CD4-independent entry. In contrast, the antibody did not reduce entry of vesicular stomatitis virus glycoprotein (VSV-G)-pseudotyped HIV-1 (which does not require CD4 or a coreceptor) and did not completely block entry of a CD4-independent clone (iR3A) (which requires a coreceptor, but not CD4).

2.4.4 M-tropic and R5 T cell-tropic viruses do not differ in the ability to use low levels of CCR5

. In a preliminary study, we examined whether M- and R5 T cell-tropic viruses differ in the ability to infect cells expressing a low level of CCR5. We did this by infecting Affinofile cells expressing high levels of CD4 ([Doxy] = 6 ng/ml; CD4 level = 85,055 ABS per cell) and either high levels of CCR5 ([Pon A] = 5 μM CCR5 level = 30,472 ABS per cell) or low levels of CCR5 ([Pon A] = 0 μM CCR5 level = 2,691 ABS per cell) with our four paired, R5 M-

tropic viruses and R5 T cell-tropic viruses. Reducing CCR5 expression to its uninduced level reduced infectivity by only 0 to 40% and did not reveal any consistent difference between M- and T cell-tropic viruses (Table 2.4) (t_{paired} = 1.1; df = 3; P value = 0.37).

Table 2.4: Parameters describing CCR5 usage when CCR5 levels are low[a]

				Maraviroc sensitivity curve data								
	% Infectivity at lowest CCR5 conc.			Maraviroc IC_{50} (nM)			Hill slope			Maraviroc resistance plateau		
Subject	T-tropic	M-tropic	Difference	T-tropic	M-tropic	Difference	T-tropic	M-tropic	Difference	T-tropic	M-tropic	Difference
4013	86.5	96	−9.5	10.7	6.8	3.9	0.9	0.7	0.1	−1.6	−1.1	−0.5
4051	65.0	58.6	6.4	2.4	1.0	1.4	1.2	0.9	0.2	−0.8	1.2	−2.0
4059	132.3	99.6	32.7	10.7	2.8	7.9	0.9	0.8	0.1	−1.0	−1.5	0.5
5002		79.8			12.0			0.8			−2.4	
7115	66.7	59.7	7.0	52.4	17.5	34.9	1.3	0.9	0.4	0.0	−2.6	2.6

[a] See Fig. 5A.

In order to thoroughly evaluate the sensitivity to CCR5 expression levels, we chose to treat $CD4^{high}$ $CCR5^{low}$ Affinofile cells with the CCR5 antagonist maraviroc to titrate the available CCR5 coreceptor molecules and then infect the cells with M- and T cell-tropic pseudotyped viruses representing blood- and CSF-derived viruses from our five experimental subjects (Figure 2.5a). We compared the maraviroc sensitivities of the four R5 T cell-tropic viruses to those of their paired M-tropic viruses (Table 2.4). Subject 5002 was excluded from this analysis because the T cell-tropic clone was previously shown to be a CXCR4-using virus (61). We observed that the remaining four pairs of M- and R5 T cell-tropic viruses did not differ in the 50% inhibitory concentrations (IC_{50}) of maraviroc (t_{paired} = 1.55; df = 3; P value = 0.22) or the slopes of their maraviroc resistance curves (t_{paired} = 3.13; df = 3; P value = 0.052).

We also examined whether the evolution of macrophage tropism selects for viruses capable of using a conformation of CCR5 that is insensitive to maraviroc (Figure 2.5b-c). Use of this alternative conformation can be observed as partial resistance to maraviroc when CCR5 expression levels are high but not when they are low (20). This type of resistance cannot be explained by use of an alternative coreceptor (e.g., CXCR4) but rather is due to use of an alternative CCR5 conformation that is generated when CCR5 is expressed at high levels.

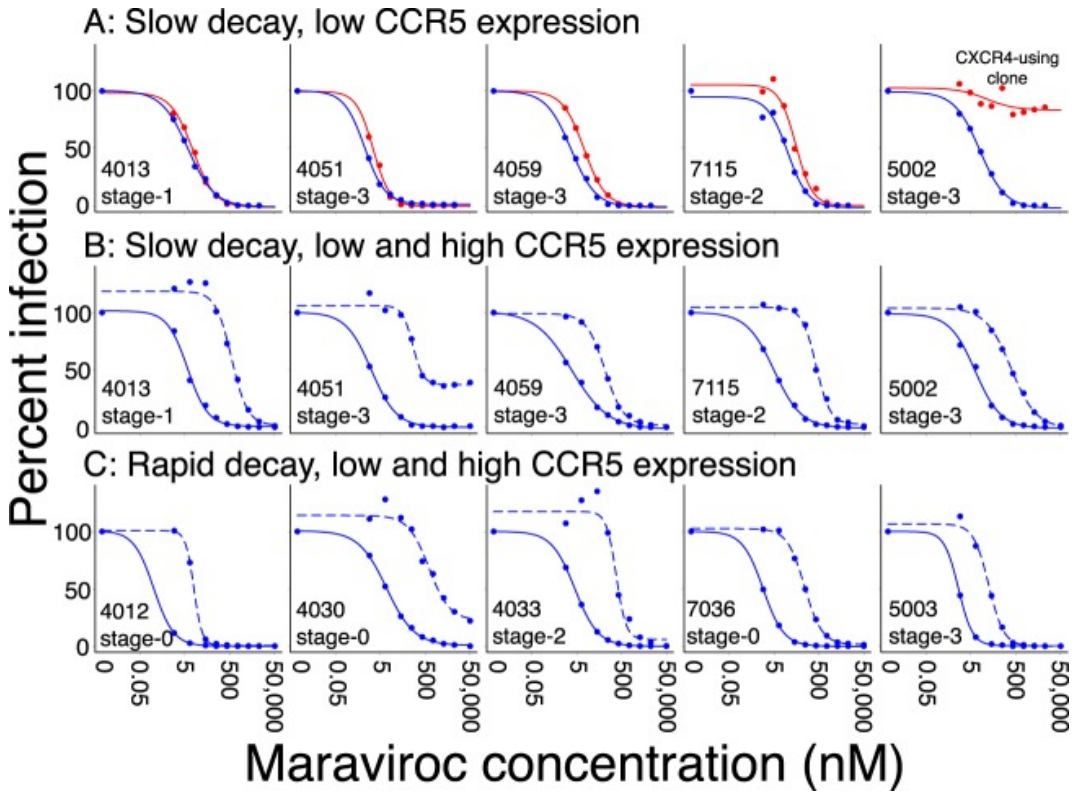

Figure 2.5: **The evolution of macrophage tropism does not select for an increased ability to infect cells expressing low levels of CCR5 or the ability to use an alternative CCR5 conformation.** (A) Affinofile cells expressing high CD4 and low/uninduced CCR5 were treated with 10 different concentrations of the CCR5 antagonist maraviroc (193, 194) and then infected with viruses pseudotyped using the five CSF-derived, M-tropic *env* clones (blue) and the paired blood-derived, T cell-tropic *env* clones (red) from subjects with slow decay of virus in the CSF with the initiation of therapy (as described in the legend to Figure 2.1). Differences in sensitivity to maraviroc were observed only between the blood-derived, CXCR4-using virus from subject 5002 and the paired CSF-derived, CCR5-using virus. The lack of difference in maraviroc sensitivity between the M- and T cell-tropic viruses shows that the evolution to infect macrophages does not select for the ability to use lower levels of CCR5. (B and C) The same five R5 M-tropic pseudotyped viruses described for panel A (B) and five R5 T cell-tropic CSF-derived clones (C) were used to infect Affinofile cells expressing high CD4 and either low CCR5 (4,048 ABS per cell; solid blue lines) or high CCR5 (39,162 ABS per cell; dashed blue lines) in the presence of 10 different levels of maraviroc. We previously observed that expression of CCR5 at high levels on Affinofile cells results in a population of CCR5 molecules that can mediate entry for a subset of viruses even in the presence of maraviroc, giving rise to a residual plateau of infectivity in the presence of the inhibitor (20) and describing an alternative entry phenotype for these viruses. When we compared M-tropic (B) and R5 T cell-tropic (C) pseudotyped viruses with respect to the ability to use the alternative conformation of CCR5 for entry in the presence of maraviroc, we found no consistent difference among the two groups of viruses, as indicated by a plateau of resistance in only one M-tropic virus (4051) and one R5 T cell-tropic virus (4030).

We identified two clones with this type of resistance. These clones were partially resistant to maraviroc when infecting $CD4^{high}$ $CCR5^{high}$ Affinofile cells (CD4 level = 141,450 ABS per cell; CCR5 level = 39,162 ABS per cell) but were sensitive to maraviroc when infecting $CD4^{high}$ $CCR5^{low}$ Affinofile cells (CD4 level = 141,450 ABS per cell; CCR5 level = 4,048 ABS per cell). One resistant clone was M-tropic (CSF clone from subject 4051), and one was R5 T cell tropic (CSF clone from subject 4030). Thus, there is no consistent pattern that distinguishes R5 T cell-tropic viruses from M-tropic viruses in their ability to use this alternative form of CCR5.

2.5 Discussion

Assessing the cellular tropism of HIV-1 is complicated by the fact that isolates are highly variable in their ability to infect target cells and target cells vary in their susceptibility to infection. Thus, most tropism assays do not yield easily interpretable, binary results. This is well illustrated by studies of macrophage tropism, which have revealed that viruses can vary up to 1,000-fold in the ability to infect MDMs (15), with most being capable of some level of infection (Figure 2.3). In addition, our study and other studies have shown that MDMs are highly variable in their susceptibility to HIV-1 (Figure 2.3) (162, 163). These sources of variation mean that assays that assess infection of MDMs do not yield unequivocal results that clearly separate HIV-1 variants adapted to growing in $CD4^+$ T cells, with their high levels of CD4, from viruses that have evolved the ability to grow in cells with low levels of CD4, such as macrophages. We have attempted to provide a more rigorous definition of both an entry assay that can identify the evolutionary step that allows entry using low levels of CD4 and examples of viruses that have undergone that evolutionary step to validate the assay.

MDMs themselves are only a representation of the heterogeneous populations of cells that collectively represent macrophage-like cells in the body. The vast majority of macrophages are found in tissue, where they differentiate either from progenitor cells that migrated into the tissue during embryonic development or from blood-derived monocytes (164). In the central

nervous system, for example, microglia are the predominant macrophage-like cells in the brain parenchyma (165) and are derived from precursors that colonize the brain during embryonic development (166, 167). Their location allows microglia to survey the brain for pathogens and to promote brain development and homeostasis by performing tasks such as synaptic pruning (168) and phagocytosis of apoptotic neurons (169). In contrast, perivascular macrophages are located in the perivascular (Virchow-Robin) spaces of blood vessels that traverse the central nervous system and are derived from monocytes that migrate from the blood (170). Their position ensures that they are often the first immune cells that pathogens encounter after breaching the blood-brain barrier. As a result, they are exposed to more pathogens than cells elsewhere in the brain and may be more likely to be infected by HIV-1. Consistent with this possibility, a study of simian immunodeficiency virus (SIV)-infected brains found that perivascular macrophages are infected more often than microglia (171). Similarly, the liver has macrophage-like resident cells, i.e., Kupffer cells, that migrate into the liver during embryonic development (167, 172) and can have an influx of macrophages as the result of inflammation. These observations point out that ontogeny and anatomical location influence macrophage function and, potentially, relevance to infection by HIV-1.

Macrophage function is further affected by the activation state, which can change rapidly in response to changes in the signaling environment (173, 174). Macrophages have been classified as either M1 or M2, with activated M1 macrophages having proinflammatory, antimicrobial phenotypes and M2 macrophages having anti-inflammatory, wound-healing phenotypes (175). It is now appreciated that even this dichotomy does not capture the full continuum of macrophage phenotypes (176) and that additional macrophage diversity is generated from the complex signaling environment (176) and from inherent differences, such as basal gene expression (177), that alter how cells respond to signals. Together, cellular ontogeny, signaling environment, activation state, and basal gene expression generate diverse macrophage populations capable of performing a variety of functions.

The major function of CD4 is to act as a coreceptor with the T cell receptor in interac-

tions with antigen-presenting major histocompatibility complex (MHC) class II complexes. Since macrophages are antigen-presenting cells, the low levels of CD4 that are expressed on macrophages cannot function in this role. Thus, it is not clear that the CD4 that is found on macrophages is biologically significant (for the macrophages), although it has been proposed (178) that CD4 in this context could serve an alternative function, as a coreceptor to and enhancer of signaling of Fc receptors. However, CD4 is not detected on macrophages of mice (179), suggesting that its presence is dispensable. There is no information concerning whether the different types of macrophages and macrophage-like cells in the body, or their different activation states, vary in the level of surface CD4 expression. Thus, the use of monocytes that are induced to differentiate in cell culture to measure viral entry phenotypes overly simplifies what is likely to be a much more complex interaction between HIV-1 and macrophages in vivo. In our own attempts to examine the levels of CD4 on macrophages, we have found that they can vary between donors (Figure 2.3a; Table 2.3) and in the same donor at different collection times (Figure 2.3b; Table 2.3). This makes it difficult to ascribe an entry phenotype consistent with macrophage tropism. Difficulty in assigning a clear macrophage-tropic phenotype has also been reviewed by Duncan and Sattentau (180).

How does the range of CD4 densities spanned in our tropism assay compare to CD4 densities expressed on MDMs and other potential target cells, at least as represented as primary cells in culture? A common misconception about macrophages is that they express fewer CD4 molecules per cell than do T cells, when in fact they express similar numbers of receptors per cell but express CD4 at much lower densities (CD4/$\mu\mathrm{mol}^2$). In this study, we confirmed (Figure 2.2b) the earlier observation that when exposed to M-CSF, monocytes can differentiate into macrophages that express numbers of CD4 molecules similar to those expressed on T cells (132), but we observed that their large size causes MDMs to have CD4 densities that are approximately 20-fold lower than those of T cells (Figure 2.2c). Furthermore, we showed that at their uninduced level, Affinofile cells express CD4 densities that are somewhat lower than those of monocytes and MDMs, while at their maximum induction level they express CD4

densities that are almost as high as that of T cells (Figure 2.2c). Thus, our assay roughly spans the range of CD4 densities present on macrophages and T cells and reveals differences between viruses adapted to replication in cells that express very different CD4 densities (Figure 2.2d).

While manipulating CD4 densities on Affinofile cells serves as a tractable system for testing entry phenotypes, accurately assessing those phenotypes also requires defining how true macrophage-tropic viruses perform within that system. Studies using other systems have shown that some brain-derived viruses are capable of replicating in macrophages and have an increased ability to enter (148, 149, 181) and/or fuse with (147, 181) cells expressing low levels of CD4. The ability to use low levels of CD4 for entry (148) has also been observed for a small number of prototypical macrophage-tropic viruses previously generated by coculturing lung tissue (BaL) (87), brain tissue (JR-FL) (150), or PBMCs (Ada) (182) with primary cells or by cloning viruses directly from brain tissue (YU-2) (183). It is worth considering, however, whether coculturing with MDMs or PBMCs allowed some of these viruses to evolve additional phenotypes that do not represent M-tropic viruses in vivo. We recently observed this for Ba-L, which has a neutralization-sensitive phenotype (K. T. Arrildt, unpublished data) that would likely be selected against *in vivo* A common feature of most of these M-tropic clones is that they were not generated using endpoint dilution PCR to avoid PCR-mediated recombination of the viral genomes that can obscure their original sequence organization in vivo.

We previously generated a panel of env genes from viruses that were validated as being derived from macrophage-tropic variants by multiple in vivo and in vitro measures, including coming from a compartmentalized viral population in the CSF/CNS, being produced from long-lived cells, and being able to infect macrophages and cells with low levels of CD4 (60, 61). In addition, the env genes were generated by endpoint dilution to avoid PCR-mediated recombination, and in each case the CSF/CNS-derived viruses were paired with blood-derived viruses from the same subject. We believe that these viruses are well-validated examples of

variants that can evolve within the CNS in late-stage infection. We found that these viruses largely fell into two distinct groups: T-tropic viruses with very low infectivities (2%) when CD4 levels were low and M-tropic viruses that retained moderately high infectivities (15%) even with low levels of CD4 (Figure 2.1a; Table 2.1).

Differences in infectivity remained pronounced for viruses infecting cells expressing all but the highest levels of CD4, as seen by the M-tropic viruses having significantly lower CD4 ED50 values (Table 1). Thus, our assay is a reliable and quantitative method for distinguishing M- and T-tropic viruses based on their capacity to infect cells expressing low CD4 densities. Using these types of assay parameters, we have been able to show that most isolates of HIV-1, including the transmitted virus (20), require high levels of CD4 for entry, indicating that most of the time HIV-1 is replicating in $CD4^+$ T cells, with their high densities of surface CD4, and that the virus does not have the entry properties of viruses that have evolved to infect macrophages. We have been able to identify rare examples of viruses with intermediate entry phenotypes (29), although we do not know if this represents phenotypic variation or evolutionary intermediates. Other investigators have also used Affinofile cells to identify a low-CD4-density entry phenotype (184).

We argue that the ability to enter cells with a low density of CD4 must be the first phenotypic change for a lineage of macrophage-tropic virus, because this mediates the initial step in the viral life cycle, i.e., entry. There may be other phenotypic adaptations to replication in macrophages, but these will appear linked on genomes that encode an Env protein that can enter cells with a low density of surface CD4. This reasoning leads to the conclusion that an entry phenotype using a low density of CD4 is a necessary feature of macrophage tropism, although it is not clear if this is the only viral function that must evolve to allow efficient replication in macrophages in vivo. Since macrophage-tropic lineages appear to evolve infrequently, at least with respect to the bulk of viral replication in $CD4^+$ T cells, the normal viral gene products are not selected for function in macrophages but rather for function in T cells. Conversely, the use of VSV-G pseudotypes to enhance entry into macrophages (or other cell

types) to assess viral protein function obscures the fact that the protein being tested likely has not been selected for function in that cell type.

Do macrophage-tropic viruses ever appear in the blood? We failed to find macrophage-tropic variants in the blood of 62 subjects with intermediate levels of $CD4^+$ T cells (20). However, in macaques that were depleted of $CD4^+$ T cells at the time of infection, macrophages were easily detected as being infected, and these animals had relatively high viral loads (185). In macaques with end-stage disease that were infected with the X4 virus D12, there was clear evidence of infection of macrophages in the lymph nodes (186). In a study by Gray et al. (152), viruses isolated from the blood of patients late in infection (late R5 viruses) were found to infect macrophages better than viruses isolated early in infection (early R5 viruses). These late R5 viruses were found to have phenotypes similar to those of a prototypical macrophage-tropic virus (Ada) and were thus inferred to be macrophage tropic. However, as noted above, the use of MDMs can result in viruses being identified as macrophage tropic despite being poorly adapted to infecting macrophages in vivo. Thus, the extent to which macrophage-tropic viruses evolve outside the CNS and reach a significant fraction of the systemic viral load remains an important question about HIV-1 pathogenesis.

Do R5 T cell-tropic viruses ever infect macrophages? The fact that most HIV-1 lineages (in both the CNS and blood) are R5 T-cell tropic suggests that these lineages do not replicate predominantly in macrophages. However, this does not indicate that these viruses exclusively infect T cells. While macrophage-tropic HIV-1 is better overall at entering MDMs in vitro (Figure 2.3), T cell-tropic viruses can enter MDMs at reduced levels. The effect that intermittent infection of macrophages by T cell-tropic viruses, if it occurs, may have on pathogenesis or latency is unknown.

We also examined several other entry-associated features of low-CD4-density entry. Using a cell-cell fusion assay, we were able to show that both M- and T cell-tropic clones still require CD4 and a coreceptor (CCR5 in this assay) for entry (Figure 2.4), indicating that the entry activity of M-tropic viruses at low levels of CD4 does not represent CD4-independent entry.

We also found that M-tropic and T cell-tropic viruses do not differ in the ability to infect cells expressing low levels of CCR5, their overall sensitivity to CCR5 density (Figure 2.5a; Table 2.4), or their ability to utilize an alternative conformation of CCR5 (Figure 2.5b-c). These findings are consistent with previous studies showing that macrophage tropism is not related to sensitivity to the CCR5 antagonist TAK-779 (147, 148, 187).

Having a more quantitative assay to define macrophage-tropic viruses will help to bring clarity to two other relevant issues. First, viruses with the ability to infect cells with low levels of CD4 create independently replicating populations and potentially establish alternative types of latently infected cells. The observation that initiating therapy causes these $CD4^{low}$ viruses to slowly decay within the CSF of most subjects (152) indicates that they are produced from long-lived, but not immortal, cells within the CNS. However, it is not known if these cells (macrophages and/or microglia) can have latent infections that stochastically release virus over time. If this were a significant reservoir, either in subjects currently on therapy or after the introduction of purging strategies for latently infected $CD4^+$ T cells, then the rebound virus should be able to enter cells with low levels of CD4. Second, there are reports of infection of cells that have no detectable CD4, such as astrocytes (188) and renal tubular cells (84, 189). It is not clear if low-level infectivity of these cell types (or other cell types) occurs with M- or T-tropic HIV-1, although it has been reported that up to 10 to 20% of astrocytes are infected in vivo (188), despite there being no evidence that HIV can replicate in these cells (188, 190, 191). It is important to examine the entry phenotype of viruses reported to be in these cell types to be able to conceptualize a pathway that could account for viral entry in the absence of CD4. In this regard, a report that monocytes in the blood (with their low densities of CD4) were infected with a virus that was unable to infect T cells (192) also deserves careful examination, as this type of infection is the basis for the Trojan horse model for introduction of virus into the CNS.

The use of Affinofile cells to profile the dependence of viruses on CD4 density to define the entry phenotype will allow for a more rigorous identification of viral variants that have

undergone the evolutionary step to be able to use low levels of CD4 in viral replication. Clarifying when and where such viruses evolve will allow them to be placed more accurately in the context of HIV-1 pathogenesis and latency. In addition, identifying the cell type in which a virus is replicating will also allow an appropriate link to be made between selection for a viral gene product function in the context of host cell interaction.

CHAPTER 3

PHENOTYPIC CORRELATES OF HIV-1 MACROPHAGE TROPISM[1]

3.1 Overview

HIV-1 is typically CCR5-using (R5) and T cell-tropic (T-tropic), targeting memory $CD4^+$ T cells throughout acute and chronic infection. However, viruses can expand into alternative cells types. Macrophage-tropic (M-tropic) HIV-1 variants have evolved to infect macrophages, which have only low levels of surface CD4. Most M-tropic variants have been isolated from the central nervous system during late-stage chronic infection. We used the HIV-1 *env* genes of well-defined, subject-matched M-tropic and T-tropic viruses to characterize phenotypic features of the M-tropic Env protein. We found that, compared to T-tropic viruses, M-tropic viruses infect monocyte-derived macrophages (MDMs) on average 28-fold more efficiently, use low-density CD4 more efficiently, have increased sensitivity to soluble CD4 (sCD4), and show trends toward sensitivity to some CD4 binding site antibodies, but no difference in sensitivity to antibodies targeting the CD4-bound conformation. M-tropic viruses also displayed a trend toward resistance to neutralization by monoclonal antibodies targeting the V1/V2 region of Env, suggesting subtle changes in Env protein conformation. The paired M- and T-tropic viruses did not differ in autologous serum neutralization, temperature sensitivity, entry kinet-

[1]The work described in this chapter was accomplished in collaboration with Celia C. LaBranche, Sarah B. Joseph, Elena N. Dukhovlinova, William D. Graham, Li-Hua Ping, Gretja Schnell, Christa B. Sturdevant, Laura P. Kincer, Macpherson Mallewa, Robert S. Heyderman, Annelies Van Rie, Myron S. Cohen, Serena Spudich, Richard W. Price, David C. Montefiori, and Ronald Swanstrom. The work presented in this chapter was previously published and is reprinted/adapted from Arrildt K.T., et al. 2015. Phenotypic Correlates of HIV-1 Macrophage Tropism. J Virol 89:11294-311 with permission from American Society for Microbiology.

ics, intrinsic infectivity, or Env protein incorporation. We also examined viruses with modestly increased CD4 usage. These variants have significant sensitivity to sCD4 and may represent evolutionary intermediates. CD4 usage is strongly correlated with infectivity of MDMs over a wide range of CD4 entry phenotypes. These data suggest that emergence of M-tropic HIV-1 includes multiple steps in which a phenotype of increased sensitivity to sCD4 and enhanced CD4 usage accompany subtle changes in Env conformation.

3.2 Introduction

HIV-1 host cell entry is determined solely by the Env virion surface protein. The Env protein precursor, gp160, is cleaved into two proteins: the external gp120 protein and the membrane spanning gp41 protein, which remain associated as a heterodimer and form trimers of these heterodimers. Attachment of gp120 to the host CD4 receptor induces conformational changes in gp120 that allows a secondary interaction with the host CCR5 coreceptor. CCR5 binding induces conformational changes in gp41, which promotes fusion of the viral and cellular membranes. Because the Env protein is the sole determinant of target cell entry specificity, any change in the cell types targeted must reflect a change in the properties of this protein.

The vast majority of HIV-1 isolates sampled during acute and chronic infection are CCR5-using T cell-tropic (R5 T-tropic) viruses, which are adapted to (16, 20, 98), and replicating in (12-14) $CD4^+$ memory T cells. R5 T-tropic viruses require the high densities of the CD4 receptor found on $CD4^+$ T cells for efficient entry, and use the CCR5 coreceptor, which is most abundant on the memory subset of $CD4^+$ T cells. In approximately half of late-stage HIV-1 infections, a viral population evolves the ability to use CXCR4 as a coreceptor (124, 126, 195). These CXCR4-using T cell-tropic (X4 T-tropic) viruses use CXCR4 to target $CD4^+$ nave T cells (196, 197), which express lower densities of CCR5 and higher densities of CXCR4 compared to $CD4^+$ memory T cells (132, 198). Alternatively viral populations can evolve to use lower densities of the CD4 receptor enabling more efficient entry of macrophages, which

express CD4 at densities 20-fold less than is found on $CD4^+$ memory T cells, but express similar levels of the CCR5 coreceptor (99). Other studies have also observed that macrophages express lower levels of CD4 than $CD4^+$ T cells (132, 199). Most M-tropic variants use the CCR5 coreceptor (R5 M-tropic), but X4 M-tropic viruses have been reported (200). Because M-tropic variants are detected so rarely (17, 20), the true frequency and characteristics of M-tropic viruses are only beginning to be explored.

Historically, M-tropic variants have been identified by detecting infection of monocyte-derived macrophages (MDMs) in cell culture. However, different preparations of MDMs can vary widely in their capacity to be infected varying both between different donors and from the same donor at different times (99, 132). Because MDMs have a lower surface density of CD4 than $CD4^+$ T cells, which is a significant impediment to entry by T-tropic viruses (18, 99, 147), it has been possible to use entry efficiency as a function of CD4 density to identify viruses that have adapted to entering macrophages. Initially this was done using cells engineered to have either high or low levels of CD4 (201). The dependence on receptor level for viral entry can now be demonstrated most convincingly using the Affinofile cell line in which the surface density of CD4 and/or CCR5 can be experimentally manipulated (154). Using this approach, it has been possible to identify M-tropic viruses, most often isolated from the CSF of subjects late in disease, by their ability to efficiently enter cells with low CD4 densities ($CD4^{low}$ cells) as a surrogate marker for macrophage tropism (61, 99).

Although it is possible to observe differences in entry phenotype using MDMs, it is difficult to account for the inherent variability among both the viruses and the cells in unequivocally assigning cellular tropism. Differences in how macrophage tropism is defined can lead to substantially different observations about M-tropic viruses. Although it is widely observed that M-tropic viruses are able to enter more efficiently at low CD4 densities (15, 61, 99, 145-147, 202) and are more sensitive to neutralization by soluble CD4 (sCD4) (130, 203, 204) compared to T-tropic viruses, few other characteristics are widely agreed upon. Similarly, several amino acid changes in the HIV-1 Env protein have been associated with macrophage

tropism (145, 181, 202, 203, 205-213), but the changes are not consistent across different subjects when macrophage tropism is defined as a distinct set of evolutionary variants within that subject (134). Furthermore, viruses isolated from the brain are sometimes referred to as neurotropic but without a clear definition of what this means phenotypically other than being located in the central nervous system (CNS) at the time of isolation.

In this study, we sought to gain insight into the mechanisms and consequences of evolving macrophage tropism by investigating characteristics that are unique to M-tropic and T-tropic viruses. We generated pseudotyped viruses using HIV-1 *env* clones from rigorously defined M-tropic viruses and subject-matched R5 (and in one case X4) T-tropic viruses, which reduced the effect of natural variation observed in viruses between subjects and allowed us to evaluate the phenotypic consequences specific to the evolution of macrophage tropism. We first sought to clarify the magnitude of improved entry efficiency of M-tropic variants for MDMs by pooling data from a panel of MDM donors infected by our virus pairs. Next we carried out neutralization assays using reagents that target the CD4 binding site (CD4bs) to evaluate the accessibility of epitopes within the CD4bs after the evolution of macrophage tropism. To evaluate the hypothesis that M-tropic Envs adopt an open conformation (similar to viruses adapted to tissue culture) to enhance the interaction with CD4, we examined the overall stability of the Env protein at different temperatures and the ability of neutralizing antibodies to access epitopes that are normally hidden on primary isolates. We also tested Env proteins for neutralization by autologous sera to reveal differential contributions of the antibody-mediated immune pressure to the evolution of macrophage tropism in the CNS compared to T cell tropism in the blood. We assessed the relative incorporation of Env into the virus particle as a potential mechanism for increasing interactions with target cell CD4 molecules. Finally, we used a large panel of subject-matched pairs of Env-pseudotyped viruses with a range of CD4-usage phenotypes to evaluate CD4 usage as a predictor of MDM infection. By comparing CD4-usage and MDM infectivity, we identified a subset of viruses with an intermediate entry phenotype that have increased sensitivity to sCD4 and may represent an evolutionary

intermediate on the way to evolving the full macrophage tropism phenotype. Collectively, this work provides new information about the nature of HIV-1 Env proteins that have evolved to become macrophage-tropic.

3.3 Materials and Methods

3.3.1 Cells

293T cells and TZM-bl cells (214) were maintained in Dulbeccos modified Eagle medium (DMEM) with 4.5 g/L glucose (Cellgro) supplemented with 10% fetal bovine serum (FBS), 100 U/ml penicillin, and 100 μg/ml streptomycin (Sigma). Affinofile cells (154) were maintained in DMEM with 4.5 g/L glucose (Cellgro) supplemented with 50 mg/ml blasticidin (Invitrogen). Affinofile cells can be induced to express a range of CD4 densities on the cell surface, which at maximum induction is similar to CD4 densities on TZM-bl cells (E. N. Dukhovlinova and K. T. Arrildt, unpublished data) and approaches but is still lower than that on $CD4^+$ T cells (99).

Monocyte-derived macrophages (MDM) were prepared as previously described (99). Briefly, blood was collected from four healthy donors. Buffy coats were prepared from whole blood by centrifugation into a Ficoll gradient (Ficoll-Paque Plus, GE Healthcare). Monocytes were isolated from the buffy coats by negative selection (EasySep human enrichment kit without CD16 depletion, StemCell Technologies). Purified monocytes were maintained in RPMI 1640 medium (Cellgro) supplemented with 10% FBS, 100 U/ml penicillin, 100 μg/ml streptomycin (Sigma), and 10 ng/ml recombinant human macrophage colony-stimulating factor (M-CSF, Gibco).

Study subjects and sources of *env* gene clones. We examined *env* gene clones generated in several studies including previously described clones generated from the blood and CSF of five adult subjects infected with HIV-1 subtype B and diagnosed with HIV-associated neurological disease (61), and from four pediatric subjects infected with HIV-1 subtype C and diagnosed with delays in neurological development (29). We also examined new *env* clones that were

generated from the blood and subject-matched CSF, semen, or cervicovaginal fluid (CVF) of five subjects infected with HIV-1 subtype B or C (Table 3.1). In all cases, *env* gene amplicons were generated from virion RNA by synthesizing cDNA and using end-point dilution PCR. Selected amplicons were cloned into an expression vector (pcDNA3.1), and the *env* clones were used in a transfection procedure to generate pseudotyped viruses.

3.3.2 Generation of pseudotyped viruses

293T cells were plated at a density of 2.5 x 10^6 cells in a 100-mm dish and incubated at 37°C. After 18 - 20 hours, the 293T cells were transfected with 2 μg of an *env* expression vector, 5 μg of pNL4-3.LucR-E- plasmid (obtained through the NIH AIDS Research and Reference Reagent Program, Division of AIDS, NIAID, NIH), and 30 μL FuGENE 6 (Promega) in serum-free DMEM. After 5 hours, the medium was fully changed. After 48 hours, the supernatant was collected, filtered through a 0.45 μm syringe filter (Millipore), and stored at -80°C in small, single-use aliquots. Virus stocks were not subjected to multiple freeze-thaw cycles.

Virus stocks were titered on Affinofile cells induced to maximum expression of CD4 and CCR5. Infectivity was measured using a Luciferase Assay System kit (Promega) and a luminometer (Veritas), which measures in relative light units (RLU). Titration curves within the linear range of a virus dilution series were used to calculate the volume of viral stock resulting in 800,000 RLU , which is near the upper limit of the linear range, for each individual virus. This virus-specific titration volume was used for infection of MDMs and Affinofile cells. Alternatively, the volume of viral stock resulting in 150,000 RLU was used for infection of TZM-bl cells in neutralization assays (215). The p24-Gag concentration of viral stocks was determined using the p24 AlphaLISA assay (PerkinElmer).

Table 3.1: Source material and characteristics of HIV-1 *env* genes

Designation	Subject	env Clone	Tissue[1]	Tropism[2]	Age Class	Reference
4013T	4013	P9	Blood	R5 T	Adult	[Schnell 2011]
4013M	4013	C7	CSF	R5 M	Adult	[Schnell 2011]
4051T	4051	P25	Blood	R5 T	Adult	[Schnell 2011]
4051M	4051	C3	CSF	R5 M	Adult	[Schnell 2011]
4059T	4059	P26	Blood	R5 T	Adult	[Schnell 2011]
4059M	4059	C19	CSF	R5 M	Adult	[Schnell 2011]
5002T	5002	P10	Blood	X4 T	Adult	[Schnell 2011]
5002M	5002	C1	CSF	R5 M	Adult	[Schnell 2011]
7115T	7115	P6	Blood	R5 T	Adult	[Schnell 2011]
7115M	7115	C21	CSF	R5 M	Adult	[Schnell 2011]
27569T	27569	P-B10	Blood	R5 T	Adult	(Joseph and Kincer)[3]
27569M	27569	C-A11	CSF	R5 M	Adult	(Joseph and Kincer)[3]
30005T	30005	P-F10	Blood	R5 T	Adult	(Joseph and Kincer)[3]
30005M	30005	C-C12	CSF	R5 M	Adult	(Joseph and Kincer)[3]
S4007T	4007	P13	Blood	R5 T	Pediatric	[Sturdevant 2012]
S4007Int.	4007	C02	CSF	R5 Int.	Pediatric	[Sturdevant 2012]
S4013T	4013	P14	Blood	R5 T	Pediatric	[Sturdevant 2012]
S4013Int.	4013	C14	CSF	R5 Int.	Pediatric	[Sturdevant 2012]
S4049T	4049	P23	Blood	R5 T	Pediatric	[Sturdevant 2012]
S4049Int.	4049	C03	CSF	R5 Int.	Pediatric	[Sturdevant 2012]
S4058T	4058	P05	Blood	R5 T	Pediatric	[Sturdevant 2012]
S4058Int.	4058	C12	CSF	R5 Int.	Pediatric	[Sturdevant 2012]
D929T	929	PD11	Blood	R5 T	Adult	(Dukhovlinova)[4]
D929Int.	929	VB7	CVF	R5 Int.	Adult	(Dukhovlinova)[4]
D1361T	1361	P6G1	Blood	R5 T	Adult	(Dukhovlinova)[4]
D1361Int.	1361	VE9	CVF	R5 Int.	Adult	(Dukhovlinova)[4]
PC018T	C018	PG11	Blood	R5 T	Adult	(Ping)[5]
PC018Int.	C018	S1B2	Semen	R5 Int.	Adult	(Ping)[5]

[a] CSF, cerebrospinal fluid; CVF, cervicovaginal fluid.

[b] R5, CCR5 using; X4, CXCR4 using; T, T cell-tropic; M, macrophage-tropic; Int., intermediate.

[c] Unpublished sources: B. Joseph and L. P. Kincer, unpublished data; E. N. Dukhovlinova, unpublished data; L. Ping, unpublished data.

3.3.3 MDM assay

Monocyte-derived macrophages (MDMs) were plated at a density of 5.0 x 10^4 cells per well of a 48-well plate. Five days after plating, a 50% medium change was made. After an additional two days, viruses were added to the well and the plates were centrifuged at 2000 rpm for 2 h at 37°C. The plates were washed once with phosphate buffered saline (PBS), washed once with medium, then a full medium change was done to remove unbound virus. After 48 h, the cells were washed twice with PBS and lysed with 50 µL of Reporter lysis buffer (Promega), and the lysate was stored at -80°C. Virus entry was then assessed by thawing the lysates and quantifying luciferase expression by using a luciferase assay system (Promega).

3.3.4 Affinofile cell assay

Assays were performed as described previously (159). Briefly, Affinofile cells were plated at a density of 2.0 x 10^4 cells per well of a 96-well black plate (Costar) that had been pre-treated with poly-L-lysine (75 µL of 0.1 g/L poly-L-lysine in PBS was added to each well, plates were incubated at 37C, then the solution was removed before adding the cells). After 18 - 20 h, ponasterone A (Invitrogen) was added to the medium at a final concentration of 5 nM to induce maximum expression of CCR5, and doxycycline (Sigma) was added to the medium at a ten different final concentrations ranging from no drug (minimal induction) to 5 ng/ml (maximum induction) to induce different levels of CD4 expression. After 20 additional hours, the medium with the chemical inducers was replaced with normal medium (i.e. lacking ponasterone A and doxycycline) and virus was added to the cells. The plates were centrifuged at 2000 rpm for 2 h at 37°C, then incubated at 37°C. After 48 hours, the medium was removed and the cells were washed once with PBS then lysed with 50 µL of Reporter lysis buffer (Promega). The lysate was stored at -80°C. Virus entry was then assessed by thawing the lysates and quantifying luciferase expression by using a luciferase assay system for firefly luciferase (Promega).

3.3.5 Flow cytometry

Monocyte-derived macrophages (MDM) were plated at a density of 1.1 x 10^6 cells in a 60-mm dish. Affinofile cells were plated at a density of 1.8 x 10^5 cells in a well of a 24-well plate. Cells were harvested for flow cytometry simultaneously with the infection of identically treated cells for experiments that incorporate both measurements. Cells were removed from culture dishes using non-enzymatic methods to avoid disruption of surface molecules. MDMs were removed using Cell Dissociation Buffer (Gibco) and Affinofile cells were removed using chilled PBS (CellGro). All cells were stained with Fixable Aqua dead cell stain (Invitrogen) and saturating concentrations of phycoerythrin (PE)-conjugated anti-human CD4 antibody (clone RPA-T4; BD Biosciences). We used QuantiBRITE beads (BD Biosciences), which are conjugated with PE, as a standard to translate mean fluorescence per cell to the number of CD4 antibody binding sites (ABS) per cell. Flow cytometry was performed using a Cyan flow cytometer (Beckman Coulter) and analyzed using FlowJo software (version 9.3.1).

3.3.6 Neutralization assays

Neutralization assays using TZM-bl cells have been previously described (215). Briefly, a neutralizing antibody, polyclonal serum, soluble CD4 (sCD4), or T20 was serially diluted across a 96-well black plate (Costar). Virus was added at a single concentration (approximately 150,000 RLU) and incubated with the antibody, heat-inactivated serum, or sCD4 for 60 min at 37°C. TZM-bl cells were added to a density of 1.0 x 10^4 cells per well and incubated for 48 h at 37°C. For the T20 time course, a single inhibitory concentration (50 μg/ml) of T20 was added at different times post infection. The cells were lysed with BriteLite (PerkinElmer) and luciferase activity was assessed by measuring luminescence (Victor-Wallac luminometer). Alternatively, the cells were washed once with PBS and lysed with 50 μL of Reporter Lysis Buffer (Promega) for firefly luciferase reporter viruses or *Renilla* Luciferase Assay Lysis Buffer for *Renilla* luciferase reporter viruses, and the lysate was stored at -80°C. Virus entry was then assessed by thawing the lysates and quantifying luciferase expression by using

the Luciferase Assay System (Promega) for firefly luciferase reporter viruses or the *Renilla* Luciferase Assay System (Promega) for *Renilla* luciferase reporter viruses.

To assay the stability of infectivity at different temperatures, virus was incubated at -80, 0, 25, 37, 49, or 60°C for 1 h before adding TZM-bl cells and infecting as described above. To test the rate of temperature inactivation as a function of time, viruses were incubated at 49°C for up to 60 min or were incubated at 0°C for up to 53 h before adding TZM-bl cells and infecting as described above.

3.3.7 Western Blotting

To evaluate the relative quantities of Env on the surface of a virion, viruses were made as described above, except that they were never frozen. After filtering, 8.0 ml of the cell medium was centrifuged at 20,500 x g for 90 min at 4°C to pellet the virus. The supernatant was removed and the pellet was resuspended in PBS at 1/50 of the original volume. To denature and inactivate the resuspended virus, 5X Laemmli buffer (312.5 mM Tris-Cl pH 6.8, 10% SDS, 25% 2-mercaptoethanol, 0.01% bromophenol blue, 50% glycerol) was added to a final concentration of 1X and incubated at 95°Cfor 10 min.

The denatured virus was diluted 1:5 to detect Env and 1:50 to detect p24. Using a 4 - 20% polyacrylamide tris-glycine gel (Invitrogen), the denatured virus was loaded at seven different volumes from 1 ul to 10 µL to create a titration curve. The gels were electrophoresed at 100 V for 2 h and then transferred to polyvinylidene difluoride (PVDF) membranes by electrophoresing at 150 mA per gel for 2 h. The PVDF membrane was blocked in 5% non-fat dry milk (Bio-Rad) in tris-buffered saline (TBS) for 1 h at ambient temperature. The blocking solution was decanted and fresh blocking solution was added. The primary antibody, either a purified rabbit anti-gp140 IgG (generously provided by Dr. Nancy Haigwood, Oregon National Primate Research Center, OHSU) or a purified rabbit anti-p24 antibody (NIH AIDS Research and Reference Reagent Program), was added to the blocking solution at a final dilution of 1:10,000 and incubated 16 h at 4°C. The primary antibody and blocking solution

were decanted. The PVDF was washed three times for 10 minutes with 0.03% Tween 20 in TBS. Fresh blocking solution with the secondary antibody, horseradish peroxidase (HRP)-conjugated goat anti-rabbit IgG (Bio-Rad), at a final dilution of 1:10,000 was added to the PVDF and incubated at ambient temperature for 1.5 h. The PVDF was washed six times for 10 minutes with 0.03% Tween 20 in TBS. The HRP was detected using the ECL Prime kit (GE Healthcare) and recorded by exposure to film (GE Healthcare) for 10 s, 20 s, 30 s, 60 s, or 5 min. After the film was developed, it was analyzed using ImageQuant TL (GE Healthcare). Titration curves were made for each exposure time and the inference of relative amount was made within the dynamic range of exposures for subsequent analyses.

3.3.8 Statistical analyses

All statistical analyses were calculated using Prism GraphPad software. A four parameter logistic equation (4PL; also called a sigmoidal dose-response with variable slope) was used for all non-linear regression analysis, except for cold sensitivity, which followed an exponential decay. Log-transformed MDM infectivity values were analyzed by paired t-test. Antibody and heat sensitivity IC_{50} values and cold sensitivity half-life values were analyzed by Wilcoxon signed-rank test and values outside of the limit of detection of each assay were reported at the limit of detection for the purposes of non-parametric comparison. CD4 usage descriptive statistics and log-transformed IC_{50} values for sCD4 were analyzed by paired t-test, except when comparing non-subject-matched intermediate viruses to M-tropic viruses where the unpaired t-test was used.

3.4 Results

3.4.1 Identification of Macrophage-tropic and paired T cell-tropic HIV-1 *env* isolates

We used *env* gene expression vectors derived from one macrophage-tropic (M-tropic) and one T cell-tropic (T-tropic) virus isolated from each of seven subjects (Table 3.1). Five of these subject-matched pairs (from subjects 4013, 4051, 4059, 5002, and 7115) were previously de-

scribed with the M-tropic viruses being classified using the following 3-fold definition (60, 61). First, the viruses were isolated from the cerebrospinal fluid (CSF) of subjects who had slow viral load (VL) decay after initiation of antiretroviral therapy (ART), which implies that the viruses were being produced from long-lived infected cells (e.g. macrophages/microglia) that continued to produce viruses longer after new infections were blocked by ART, compared to the rapid VL decay seen in the blood, consistent with virus produced from infected T cells. Second, phylogenetic analysis of the *env* genes showed that these CSF viruses were genetically diverse and distinct from the T-tropic viruses found in the blood of the same subjects (i.e. compartmentalized), implying that the CSF viruses were replicating actively and independently from the viruses found in the blood. Third, reporter viruses pseudotyped with these CSF-derived Env proteins were able to infect Affinofile cells expressing the minimum density of CD4 ($CD4^{low}$ Affinofile cells) more efficiently than reporter viruses with the subject-matched blood-derived T-tropic Env proteins, indicative of viral evolution to infect cells with a low surface density of CD4 such as macrophages within the central nervous system (CNS) compartment. We have shown that infectivity in $CD4^{low}$ Affinofile cells is an assay that can reliably identify M-tropic HIV-1 (61, 99) and provides a method amenable to high-throughput screening. Post-therapy initiation samples were not available for the remaining two subjects (27569 and 30005), thus their tropism was assessed by phylogenetic analyses (compartmentalization) and infection of $CD4^{low}$ cells.

Although Env proteins derived from these subjects were previously assessed in separate studies (61, 99), we reanalyzed Env-pseudotyped viruses for entry phenotypes over a wide range of cell surface CD4 densities, which are shown in Figure 3.1a using a semi-log plot to display the data. Consistent with previous studies, the Env proteins from the M-tropic clones were significantly better at mediating infection of cells expressing the lowest densities of CD4 (P value = 0.006). In addition, there are differences over the entire CD4 usage curves, which also clearly distinguish the CSF-derived M-tropic viruses from the blood plasma-derived T-tropic viruses. We found a 1.8-fold change in average Hill slope (Pvalue <0.0001) and a 2.7-

fold change in the average CD4 EC_{50} (*P* value = 0.02), which indicates that the M-tropic Envs are able to mediate entry with significantly fewer CD4 molecules than their paired T-tropic Envs and confirms that CD4 receptor density is a potent restriction factor in Env-mediated entry.

Because most of the variation in CD4 usage between viruses is represented by the ability to enter using the minimum CD4 levels expressed on Affinofile cells, we can use a simplified $CD4^{low}$ usage assay in which virus infection of $CD4^{low}$ Affinofiles is normalized to infection of $CD4^{high}$ Affinofiles (14, 22) to enable screening larger panels of viruses for CD4 usage. To assess the variation in pseudotyped virus preparations and evaluate the effects of the *env*-deficient genome reporter construct, we pseudotyped five subject-matched pairs of *env* expression plasmids in triplicate with either a *env*-deficient Subtype B HIV-1 genome expression plasmid encoding a firefly luciferase reporter (transfections 1-3) or an *env*-deficient Subtype C HIV-1 genome expression plasmid encoding a *Renilla* luciferase reporter (transfections 4-6) and performed a $CD4^{low}$ usage assay (Figure 3.1b). Overall, the results between transfections and with the different reporter constructs were similar with some detectable variation in $CD4^{low}$ usage when the same *env* gene was pseudotyped with the different reporter constructs (i.e. 4013M and 4051M had somewhat higher $CD4^{low}$ usage values with the subtype C reporter construct), which could be due to differences in the interactions between the Env proteins and the structural proteins in the pseudoviruses or to variation in the Affinofile cells between experiments (i.e. infection using the subtype B or subtype C reporter construct). For each reporter construct, there was very little variation in $CD4^{low}$ usage between transfections of the same *env* plasmid. This assay emphasizes the substantial difference in the ability of M-tropic viruses to use low density CD4 compared with T-tropic viruses and reveals the high fidelity of the CD4 usage assays.

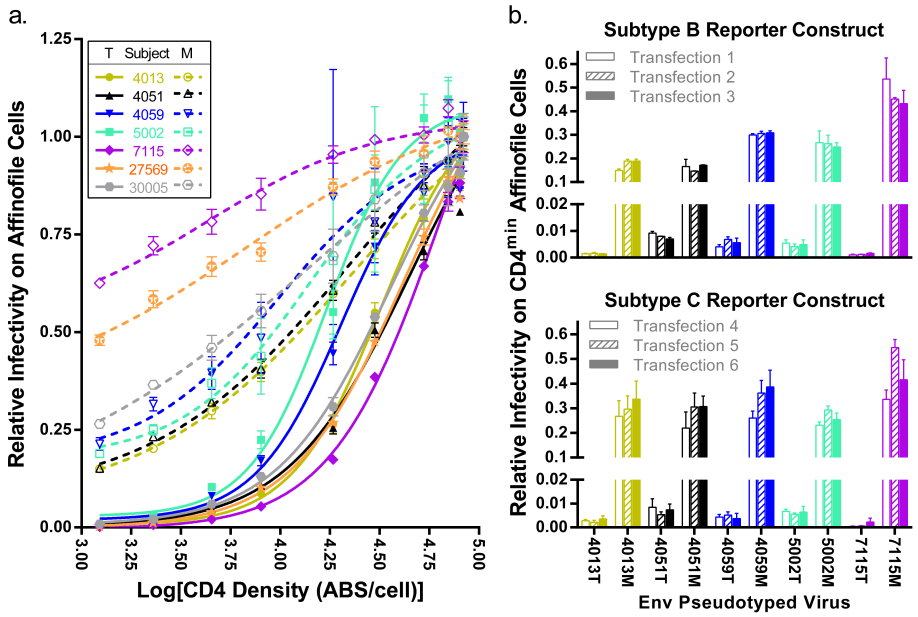

Figure 3.1: **Increased CD4 usage differentiates M-tropic viruses from T-tropic viruses** (a) Paired T-tropic and M-tropic *env* genes were used to pseudotype luciferase reporter viruses. These paired viruses were then used to infect Affinofile cells expressing various levels of CD4 and infectivity was measured by the relative light units (RLU) produced by luciferase. CD4 densities were measured by flow cytometry and reported as the $\log_{10}$ value of antibody binding sites (ABS) per cell. Infectivity is normalized to infectivity at the maximum induction of CD4 and fitted to a dose-response curve, which represents the CD4 usage of each virus and can be described using the Hill slope and EC_{50} values. Viruses expressing T-tropic Env proteins (T) are represented with closed symbols and solid lines. Viruses expressing M-tropic Env proteins (M) are represented with open symbols and broken lines. Unique color and shape combinations (as specified in the legend within the figure) identify the subjects from which the *env* genes were isolated and these identifiers are maintained across all of the figures. M-tropic Env proteins effected a 62-fold increase in average entry at the lowest density of CD4 over subject-matched T-tropic Env proteins (t_{paired} = 4.2, df = 6, P value = 0.006). M-tropic Env proteins also had enhanced CD4 usage over the entire range of CD4 densities as described by a 2.7-fold lower EC_{50} value (t_{paired} = 3.1, df = 6, P value = 0.02) and a 1.8-fold lower Hill slope value (t_{paired} = 10., df = 6, P value <0.0001) compared to subject-matched T-tropic Env proteins. (b) Five pairs of T-tropic and M-tropic *env* genes were pseudotyped in triplicate with either a Subtype B (top, transfections 1-3) or Subtype C (bottom, transfections 4-6) *env*-deficient HIV-1 genome containing a firefly (Subtype B) or *Renilla* (Subtype C) luciferase reporter gene. The resulting sixty pseudoviruses (10 *env* vectors x 2 reporter vectors x 3 replicates) were used to infect $CD4^{low}$ Affinofiles and infectivity was reported as a fraction on infectivity on $CD4^{high}$ Affinofiles (infected concurrently). The average standard deviation across transfections for viruses pseudotyped with the Subtype B construct is 1.1% (a range of 0.012% to 5.5%) and with the Subtype C construct is 2.9% (a range of 0.061% to 11%). There were minor differences in the relative infectivity of viruses produced with the Subtype B reporter versus those produced with the Subtype C reporter (SD of differences = 5.4%), but these differences were not statistically significant (t_{paired} = 1.4, df = 9, P value = 0.21).

3.4.2 Macrophage-tropic Env proteins increase infectivity of monocyte-derived macrophages 28-fold over T cell-tropic Env proteins

To evaluate the extent to which infectivity of monocyte-derived macrophages (MDMs) can distinguish M-tropic viruses from T-tropic viruses, we used this panel of seven paired pseudotyped viruses to infect MDMs derived from four donors. Similar to previous reports (99), we found that virus infectivity varied up to 5-fold across MDM donors (data not shown). However, by pooling data from multiple donors we were able to estimate the magnitude of the differential infectivity on MDMs for these two groups of viruses. When the relative infectivity data was averaged across the four MDM donors and the seven virus pairs, we observed that the ability of M-tropic viruses to infect MDMs was 28-fold higher than that of T-tropic viruses (P value = 0.0004; Figure 3.2).

3.4.3 Macrophage-tropic Envs are potently inhibited by soluble CD4 and show a trend toward enhanced sensitivity to CD4 binding site antibodies, but are not differentially inhibited by a small molecule drug targeting the CD4 binding site

In order to better understand how the M-tropic Envs are able to mediate entry using lower densities of CD4, we performed a competitive inhibition assay by incubating sCD4 with the pseudotyped viruses prior to infection, then measured the relative infectivity (normalized to the Envs incubated without sCD4) on TZM-bl cells (Figure 3.3a). The viruses pseudotyped with M-tropic Envs were, on average, 27-fold more sensitive to sCD4 than those pseudotyped with the paired T-tropic Envs (P value = 0.002), confirming that there is a statistically significant difference in how M-tropic Env proteins interact with CD4 compared to T-tropic Env proteins. We then compared the values for our panel of 14 pseudotyped viruses (7 subject-matched pairs of M- and T-tropic Env proteins) with our previously published data on a large panel of acute and chronic subtype C Envs (20). The subtype B T-tropic Envs did not differ significantly in their sensitivity to sCD4 relative to the acute or chronic subtype C Envs, suggesting that the T-tropic viruses display sensitivity to sCD4 that is typical of plasma-derived

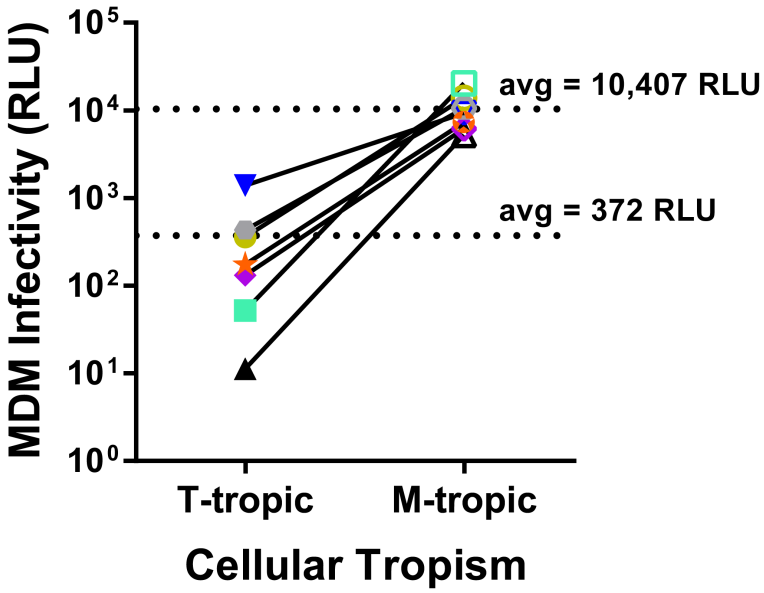

Figure 3.2: **M-tropic viruses are better adapted to infection of MDMs compared to T-tropic viruses** Paired T-tropic and M-tropic pseudotyped reporter viruses were used to infect monocyte-derived macrophages (MDMs) isolated from four donors. Infectivity on MDMs was normalized to infectivity on Affinofile cells expressing maximum CD4 levels. Normalized infectivity values were averaged across donors for each virus and plotted. Closed symbols represent T-tropic Env proteins (T) and open symbols represent M-tropic Env proteins (M) with links between subject-matched pairs. Colors and symbol shapes identify the originating subject as detailed in Figure 3.1. Comparing the mean infectivity of T-tropic and M-tropic viruses revealed that M-tropic Env proteins confer a 28-fold increase in the average MDM infectivity over subject-matched T-tropic Env proteins. Mean values are listed and marked with broken lines. The log normalized values were compared between T-tropic and M-tropic infectivity by paired t-test ($t_{\text{paired}} = 7.0$, df = 6, P value = 0.0004).

viruses.

The enhanced interaction between M-tropic Envs and CD4 could be due to having a more exposed CD4 binding site (CD4bs), an increased affinity for CD4, or to prematurely shifting into the CD4-induced (CD4i) state (a conformational shift that occurs following CD4 binding and results in the conformation that can bind the CCR5 coreceptor). If sensitivity to sCD4 is due to a more exposed CD4bs, then sensitivity to sCD4 would predict sensitivity to neutralizing antibodies targeting the CD4bs. To evaluate exposure of the CD4bs, we performed infectivity assays in the presence of antibodies targeting the CD4bs, specifically b12 (216), VRCO1 (217), and CH31 (218) (Figure 3.3b-d). We found that four of the seven M-tropic

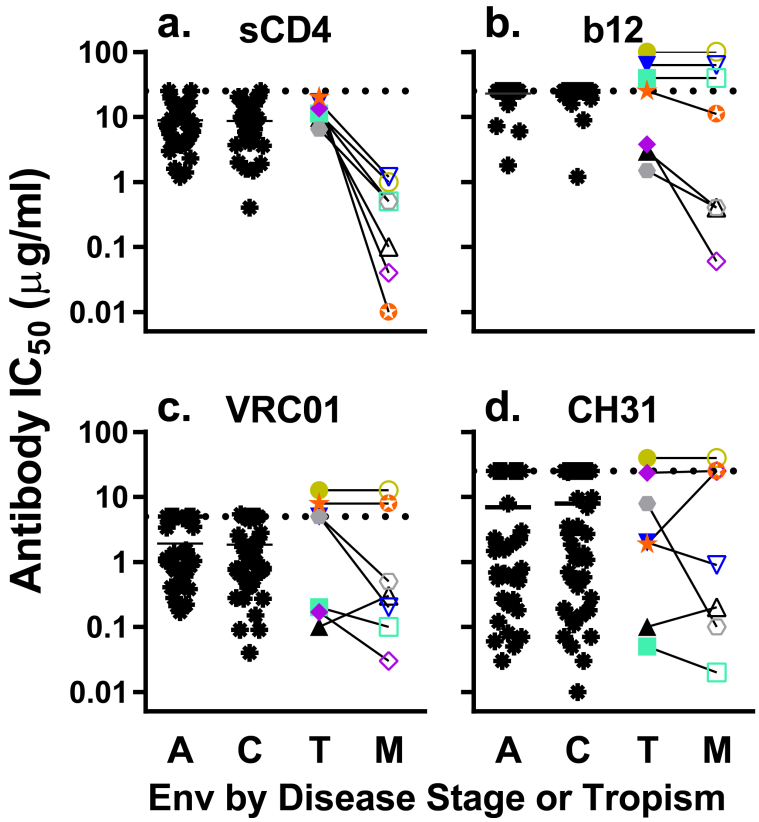

Figure 3.3: **M-tropic viruses are significantly more sensitive to neutralization by sCD4 and show trends toward increased sensitivity to some CD4bs-targeting antibodies compared to paired T-tropic viruses** Pseudotyped reporter viruses were exposed to various concentrations of (a) sCD4, or an antibody with an epitope overlapping the CD4 binding site (CD4bs) (b) b12, (c) VRCO1, or (d) CH31 in a TZM-bl neutralization assay. IC_{50} values were calculated from dose-response curves and plotted. Dashed lines represent the limits of detection. IC_{50} values above the limit of detection (LOD) were plotted at the LOD, except for pairs where both viruses had IC_{50} values that exceeded the LOD, in which case the symbols were stacked above the LOD line. The same Env-pseudotyped viruses were used in each panel: a control group of T-tropic acute (A) and chronic (C) viruses (black asterisks), and our panel of matched T-tropic viruses (closed symbols) and M-tropic viruses (open symbols) from seven subjects. The data for the acute and chronic subtype C viruses are reproduced from Ping et al. (20) to allow a comparison to a large data set of typical viral Env proteins. Viruses expressing M-tropic Env proteins had a statistically significant 27-fold increase in sensitivity to neutralization by sCD4 over subject-matched T-tropic Env (statistical analysis performed on log-normalized EC_{50} values; t_{paired} = 5.5, df = 6, P value = 0.002). M-tropic Env proteins showed trends toward sensitivity to neutralization by b12 (W_{paired} = 10, P value = 0.1) and VRC01 (W_{paired} = 10, P value = 0.3) over subject-matched T-tropic Env proteins that did not reach statistical significance using a Wilcoxon matched pairs test. No difference in sensitivity to neutralization by CH31 was observed (W_{paired} = -3, P value = 0.8).

clones were more sensitive to neutralization by b12 than the paired T-tropic clones, but the remaining three pairs were completely resistant making the overall difference between M-tropic and T-tropic neutralization not statistically different. Similarly, four of seven M-tropic clones were more sensitive than the paired T-tropic clones to VRC01 (though one pair was reversed), but again the overall differences in neutralization were not significant. There was no detectable difference in CH31 neutralization between the two groups. Two additional CD4bs antibodies, F105 and CH103, were tested on a smaller panel of ten pseudotyped viruses (five pairs: 4013, 4051, 4059, 5002, and 7115), but none of the viruses showed any neutralization at the maximum level of F105 tested (14 μg/ml) and all but one pair of viruses (4051) had IC_{50} values above the 10 μg/ml limit of detection for CH103 (data not shown). The paired viruses that were susceptible to neutralization by CH103 had similar IC_{50} values (4051T, 0.14 μg/ml; 4051M, 0.16 μg/ml). Taken together, there is a trend toward increased sensitivity to neutralization by some anti-CD4bs antibodies, but this conclusion is limited by sample size, which is due to the limited number of independent M-tropic viruses isolated. Larger panels of paired Env proteins will be needed to definitively determine whether there are changes in the CD4bs that can be probed by antibody neutralization.

We also probed the CD4bsof these viruses using the inhibitor BMS-626529 (Table 3.2), which is thought to interact with a target overlapping the CD4bs, though there are conflicting reports about whether BMS-626529 competes with CD4 for binding to the CD4bs or whether it binds outside of the CD4bs and prevents assumption of the CD4i Env conformation (219, 220). In general, the IC_{50} values were indistinguishable between paired M-tropic and T-tropic viruses and ranged from 0.34 nM to 4.2 nM, which is typical for primary isolates. Two exceptions were the 5002T Env protein, which was highly resistant (IC_{50} = 310 nM) and contained the known resistance mutation S375M (220), and the 4013T Env protein, which was moderately resistant (IC_{50} = 42.0 nM) with no known resistance mutations. A tight range of IC_{50} values across Env proteins suggests that the BMS-626529 inhibitor is able to access and interact similarly with its target in the CD4bs on both M-tropic and T-tropic Env proteins.

Table 3.2: Env sensitivity to BMS-626529

	IC_{50} for BMS–626529 (nM)	
Subject ID	T-tropic	M-tropic
4013	42.0	2.0
4051	0.87	0.5
4059	0.34	0.45
5002	310.0	1.3
7115	1.4	4.2

3.4.4 Macrophage-tropic Envs do not have enhanced sensitivity to HIV-1 neutralizing antibodies

To evaluate whether macrophage tropism is associated with changes in Env protein conformation in regions outside of the CD4bs, we tested the neutralization sensitivity of our well-defined panel of fourteen pseudotyped viruses against a large panel of neutralizing HIV-1 antibodies. We used five polyclonal sera and HIV-Ig to detect gross changes in Env conformation (Figure 3.4a-b), and six monoclonal antibodies (mAb) to examine changes in specific epitopes in the V1/V2 region (Figure 3.4c-e), the N-linked glycosylation coat (Figure 3.4f), or the membrane proximal external region of gp41 (MPER; Figure 3.4g-h). There were no significant differences in sensitivity between the M-tropic and T-tropic Envs to any of the polyclonal antibodies (Figure 3.4a-b), implying that there are no significant changes in neutralization sensitivity as a whole. However, analysis of the sensitivity to monoclonal antibodies again suggested possible differences.

The epitopes of the PG9 and PG16 antibodies (221) are in the V1/V2 region of HIV-1 Env and require interactions with the N-linked glycosylation sites at amino acids 156 and 160 (133). Loss of glycosylation at either of these sites confers resistance to neutralization by PG9 and PG16. Within our panel of seven paired Env proteins, only one (4013M) has a known resistance mutation (N160Y) and this Env protein was resistant to all three V1/V2-antibodies

tested. The remaining six M-tropic viruses were almost uniformly resistant to neutralization by both PG9 and PG16 (Figure 3.4c-d), which is in contrast to the paired T-tropic viruses that showed the wide variation in neutralization sensitivity that was also observed in the larger panel of acute and chronic Env proteins. This pattern of neutralization resistance in M-tropic viruses and variable neutralization in T-tropic viruses was continued in analysis of V1/V2 antibody CH01 (Figure 3.4e), which has a more complex and conformation-dependent epitope (222). However, due to the high variation in the control groups and the small sample size, we were unable to show a statistically significant difference in neutralization between M-tropic and T-tropic viruses. These data suggest that the conformation of Env that defines the surface epitopes, perhaps through the orientation of the carbohydrate side chains, may be altered as part of the evolution to be able to enter cells with a low density of CD4.

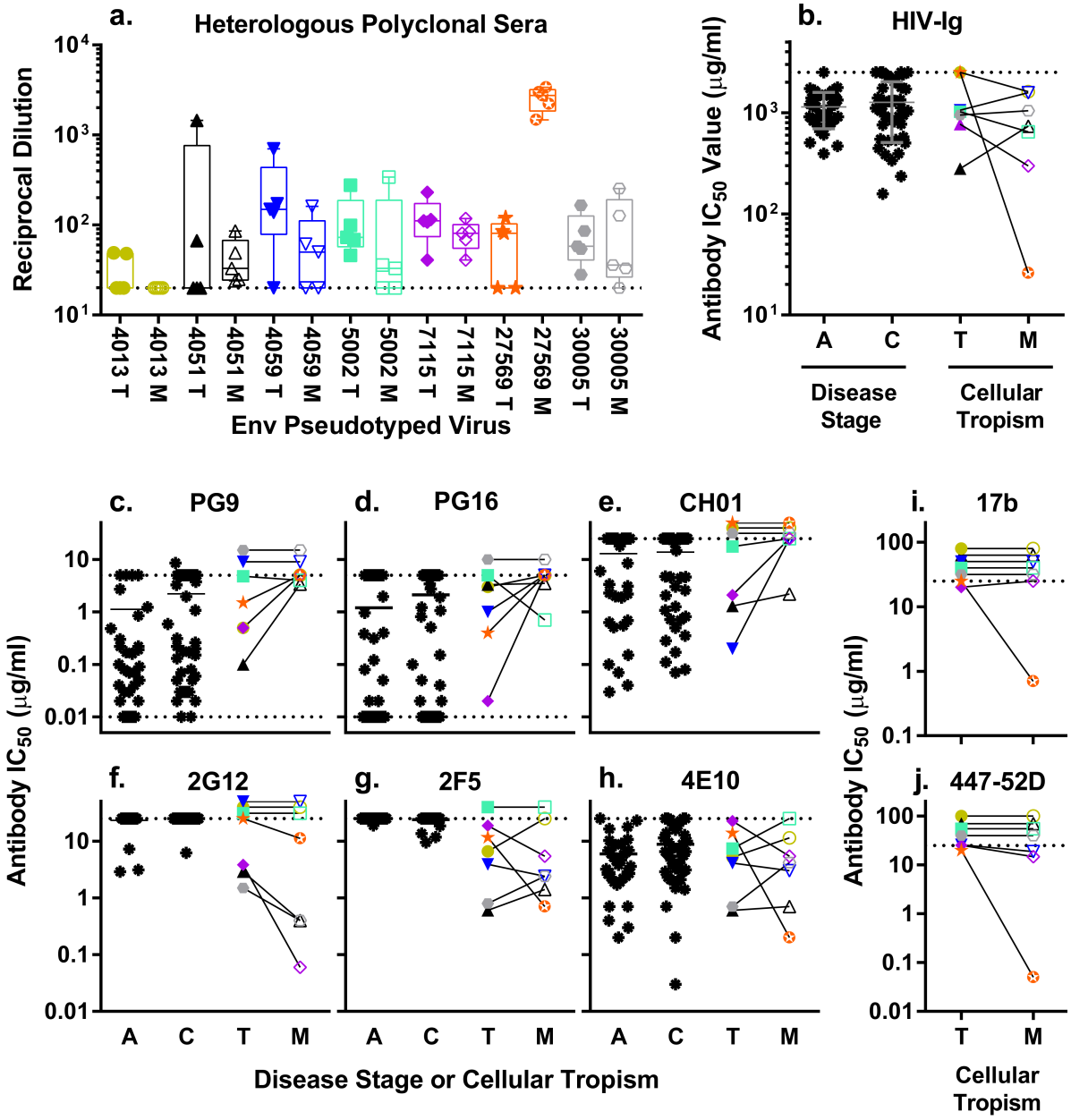
a.
Heterologous Polyclonal Sera
Reciprocal Dilution
10^4
10^3
10^2
10^1
4013 T
4013 M
4051 T
4051 M
4059 T
4059 M
5002 T
5002 M
7115 T
7115 M
27569 T
27569 M
30005 T
30005 M
Env Pseudotyped Virus
b.
HIV-Ig
Antibody IC_{50} Value (μg/ml)
10^3
10^2
10^1
A
C
T
M
Disease Stage
Cellular Tropism
c.
PG9
d.
PG16
e.
CH01
i.
17b
f.
2G12
g.
2F5
h.
4E10
j.
447-52D
Antibody IC_{50} (μg/ml)
10
1
0.1
0.01
100
A
C
T
M
Disease Stage or Cellular Tropism
Cellular Tropism

Figure 3.4 *(previous page)*: **Similar to T-tropic viruses, M-tropic viruses are generally resistant to neutralization by non-CD4bs-targeting antibodies with subtle trends toward increased resistance to V1/V2-targeting antibodies and decreased resistance to a glycan-targeting antibody** Pseudotyped reporter viruses were exposed to various concentrations of (a) polyclonal sera from five HIV-infected subjects; (b) purified polyclonal HIV-Ig; and monoclonal antibodies: anti-V1/V2 (c) PG9, (d) PG16, and (e) CH01; anti-glycosylation (f) 2G12; and anti-MPER (g) 2F5 and (h) 4E10 in a TZM-bl neutralization assay. The data for the acute and chronic subtype C viruses are reproduced from Ping et al. (20) to allow a comparison to a large data set of typical viral Env proteins. IC_{50} values were calculated from dose-response curves and plotted. Dashed lines represent the limits of detection. IC_{50} values above the limit of detection (LOD) were plotted at the LOD, except for pairs where both viruses had IC_{50} values that exceeded the LOD, in which case the symbols were stacked above the LOD line. Data for the same Env-pseudotyped viruses were used in each panel: T-tropic acute (A) and chronic (C) viruses (black asterisks; panels b-h only), T-tropic viruses (closed symbols), and M-tropic viruses (open symbols). Subject-matched viruses are linked and the IC_{50} values of T-tropic and M-tropic viruses were compared using a Wilcoxon matched pairs test. M-tropic and subject-matched T-tropic Env proteins were not significantly different in neutralization by polyclonal sera (a; $F_{ANOVA} = 0.8$, $r^2 = 0.1$, P value = 0.6) or HIV-Ig (b; $W_{paired} = 12$, P value = 0.5); nor by monoclonal MPER-targeting antibodies 2F5 (g; $W_{paired} = 1$, P value = 1) and 4E10 (h; $W_{paired} = -2$, P value = 0.9). M-tropic Env proteins trended toward increased resistance to neutralization by monoclonal V1/V2-targeting antibodies PG9 (c; $W_{paired} = -13$, P value = 0.1), PG16 (d; $W_{paired} = -13$, P value = 0.2), and CH01 (e; $W_{paired} = -10$, P value = 0.1) and increased sensitivity to neutralization by monoclonal glycosylation-targeting antibody 2G12 (h; $W_{paired} = 10$, P value = 0.1) compared to subject-matched T-tropic Env proteins. Thirteen of the fourteen viruses were resistant to neutralization by monoclonal antibodies 17b (i) and 447-52D (j), which target epitopes typically only present in the CD4-bound conformation of the viral Env protein from primary isolates (17b, $W_{paired} = 1$, P value = 1; 447-52D $W_{paired} = 6$, P value = 0.3).

The epitope of 2G12 is dependent on glycans at amino acid positions 295, 332, and 392 with some interactions with glycans at 386 and 448 (223). In our panel of seven pairs, four of the seven pairs (eight viruses) were resistant to neutralization by 2G12 (Figure 3.4f), which is partially explained by loss of glycosylation sites in seven out of eight viruses. The remaining three pairs showed a pattern of increased sensitivity in the M-tropic viruses compared to the paired T-tropic viruses. However, the small sample size compounded by resistance mutations that obscured comparisons of four of seven pairs again limited our ability to assign statistical significance to this observation. In contrast, antibodies targeting the MPER showed no difference in neutralization between M-tropic and T-tropic viruses either in directionality

or variability (Figure 3.4g-h). The sensitivity of M-tropic and T-tropic viruses to 2F5 and 4E10 (224) covered similar ranges and contained similar variance that does not seem to be correlated by subject or cellular tropism.

Primary isolates from the blood are typically resistant to antibodies targeting the CD4-induced epitopes on the Env protein. However, most M-tropic viruses were isolated from the relatively immune privileged CNS, which may release these viruses from the selective pressure that is thought to restrict exposure of CD4i epitopes. In an effort to probe exposure of CD4i epitopes, we used two additional monoclonal antibodies directed at regions of the Env protein that interact with the coreceptor and are exposed after CD4 binding. Specifically, we examined monoclonal antibodies 17b (225), which has an epitope overlapping the CCR5 binding domain, and 447-52D (226), which targets the Env protein V3 loop (Figure 3.4i-j). Viruses pseudotyped with either the M-tropic or T-tropic Env proteins were highly resistant to both 17b and 447-52D. All viruses tested had IC_{50} values above the detection threshold (¿ 20 μg/ml) for mAb 17b. Only two viruses had detectable neutralization (below a detection threshold of 25 μg/ml) by mAb 447-52D (5002T IC_{50} = 18.7 μg/ml and 7115M IC_{50} = 14.8 μg/ml), but both viruses were still relatively resistant.

Resistance to CD4i antibodies could reflect that M-tropic viruses, like most primary isolates, do not expose CD4i epitopes or it could reflect an absence of the specific antibody epitopes used to probe these conformations, which could mask any potential exposure of CD4i epitopes. To determine whether these Env proteins contain epitopes recognizable by the b12, 17b and 447-52D antibodies, we have carried out a preliminary analysis by inserting single point mutations to encode alanine at positions 155 or 177 in the V1/V2 loop, which is physically distal from the targeted epitopes; these mutations individually induce an open conformation in the Env protein of the JR-CSF isolate as measured by increased sensitivity to b12, 17b and 447-52D (W. D. Graham and K. T. Arrildt, unpublished data). Neutralizations assays with the b12, 17b and 447-52D antibodies were repeated with viruses pseudotyped with the mutant Env proteins that maintained viability. We observed that at least one of the

Env proteins for four of the five pairs of Env proteins showed increased sensitivity to either one or two of the antibodies, indicative of the presence of the epitope. Because high neutralization sensitivity to antibodies directed at CD4i epitopes is typically associated with tissue culture adapted (TCA) strains where the Env protein has adopted an overall open conformation (17, 98, 227, 228), the lack of sensitivity to these antibodies is consistent with M-tropic Env proteins that, despite high sensitivity to sCD4, are not in an open conformation.

3.4.5 Macrophage-tropic Envs do not have enhanced sensitivity to autologous serum antibodies

Most viruses currently identified as being M-tropic were isolated from the relatively immune-privileged CNS, which may have protected these viral populations from antibody-mediated selective pressure. The CNS typically maintains IgG at concentrations far lower than the plasma (approximately 400X) (229), though levels may increase in subjects with HIV-associated neurocognitive disease (230-232). To better understand the antibody environment in which M-tropic viral populations evolve, we tested the sensitivity of five pairs of viruses to neutralization by autologous serum (Figure 3.5) that was contemporaneous with when the viruses were collected. The neutralization of paired T-tropic and M-tropic Env-pseudotyped viruses by autologous serum were nearly identical in each case with no distinguishable differences in the IC_{50} values (*P*value = 1.0). Furthermore, the IC_{50} values for all viruses fell within the normal range of sensitivity for primary isolates from chronic infection with an average IC_{50} of 1:100. (serum dilution) and a range of 1:48 to 1:200. (233-243). These observations suggest that differences in antibody-mediated immune pressure between anatomical compartments are not a major factor in the evolution of macrophage tropism.

3.4.6 There are no gross stability differences between M-tropic Envs and paired T-tropic Envs

Antibodies can access only the outer surface of the Env spike and cannot reveal changes in the core structure or stability of the protein. To assess whether there were differences in the stability of the Env proteins, we incubated a smaller panel of 10 (representative) pseudotyped

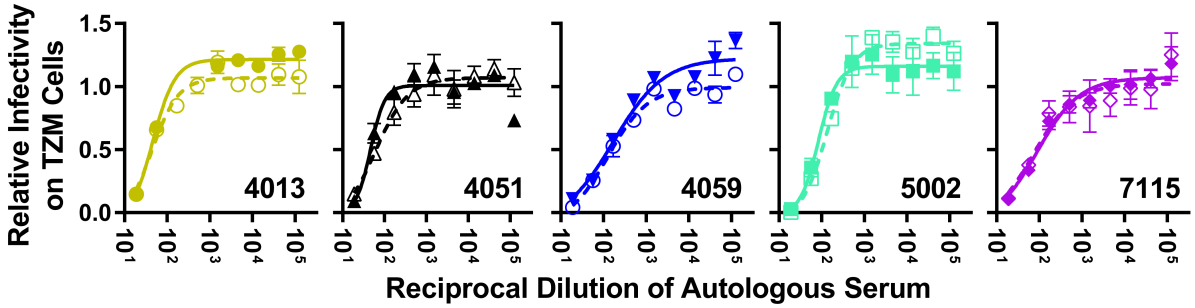

Figure 3.5: **M-tropic viruses have not evolved an increased sensitivity to autologous serum** Five paired T-tropic (closed symbols, solid lines) and M-tropic (open symbols, broken lines) pseudoviruses were exposed to heat-inactivated autologous serum (from the same subject and sampling time as the viruses isolated) in a TZM-bl neutralization assay. The relative infectivity was analyzed as a function of the reciprocal dilution of the autologous serum. No detectable differences in sensitivity to autologous serum were detected between paired T-tropic and M-tropic viruses (W_{paired} = -1.0, P value = 1.0). The average IC_{50} across subjects and tropism is 1:100. with a range from 1:48 to 1:200 (SD = 1:50, SEM = 1:16).

viruses (5 pairs) at different temperatures to assess the stability of the Env trimers as measured by the loss of infectivity. We first incubated each of the viruses for 60 min at six different temperatures (-80°C, 0°C, 25°C, 37°C, 49°C, and 68°C) prior to infection of TZM-bl cells and normalized the data to infectivity after incubation at 25°C (Figure 3.6a). Overall, the pseudotyped viruses were most stable at either 25°C or 37°C and were fully inactivated at 68°C. Although different temperatures produced variable levels of inactivation for individual viruses, neither sensitivity nor resistance to any temperature was consistently associated with either M-tropic or T-tropic viruses. Our second assay measured the loss of infectivity over time at 49°C, which has been previously shown to result in a moderate rate of virus inactivation (244), to provide a more quantitative assessment of the level of heat sensitivity for each Env protein (Figure 3.6b). Four out of the five pairs showed similar viral decay curves when comparing the T-tropic and M-tropic viruses. One pair showed a significant difference in temperature sensitivity over time, with the M-tropic virus being the most sensitive virus tested (subject 7115). However, this difference was not recapitulated for other M- and T-tropic clones generated from the same subject (data not shown). Finally, we measured the decay of infectivity of the panel of pseudotyped viruses at 0°C over the course of 53 hours (Figure

3.6c). Sensitivity to cold was highly variable between viruses, but neither sensitivity nor resistance to cold was consistent with cellular tropism. Taken together, these results show that the ability of M-tropic viruses to enter cells using a low density of CD4 and the enhanced sensitivity to sCD4 are not the result of a less stable Env protein.

3.4.7 Env-mediated fusion rates do not differ between macrophage-tropic and T cell-tropic Envs

We next considered the possibility that enhanced entry could be due to an enhancement in viral fusion with the cellular membrane, which may compensate for low attachment by making each attachment event more likely to result in entry (245). T20 is a fusion inhibitor that mimics the C-terminal heptad repeat (CHR) region of gp41, which normally binds to the N-terminal heptad repeat (NHR) to form a six-helix bundle that induces virus-host membrane fusion. However, when T20 binds the NHR it stabilizes gp41 in a pre-fusion conformation and blocks binding by the CHR, effectively blocking fusion. To determine whether there were any significant differences in sensitivity to T20 between the five pairs of viruses, we titrated T20 to find the concentration required to inhibit fusion with TZM-bl cells for each of the ten pseudotyped viruses (Figure 3.7a). We did not detect any consistent differences in T20 sensitivity between the T-tropic and M-tropic Envs. We then used a fully inhibitory T20 concentration (50 μg/ml) to compare the kinetics of fusion between the two groups of viruses as they became resistant to T20, i.e. the time to formation of the six-helix bundle and fusion with the target cell (Figure 3.7b). There was no difference in the rate of fusion between any of the pairs, suggesting that the rate of fusion is not a factor in macrophage tropism.

3.4.8 Increased Env incorporation does not explain increased CD4 usage by macrophage-tropic Envs

A simple way for a virus particle to increase the probability of interacting with CD4 would be to increase the number of Env trimers on the surface of the virion. To evaluate whether the

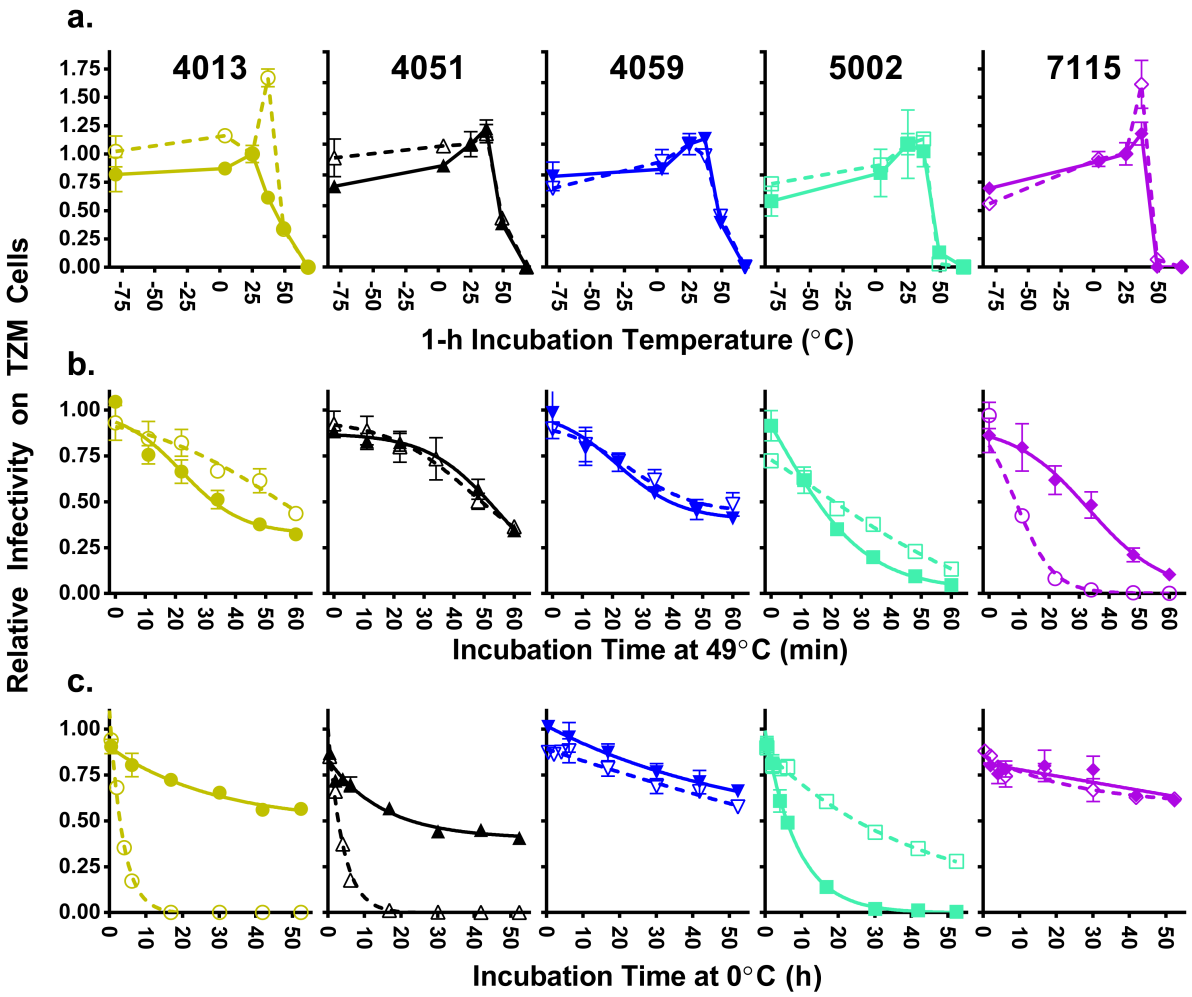

Figure 3.6: **M-tropic viruses do not differ from T-tropic viruses in sensitivity to temperature** The effect of temperature on infectivity was assessed for five pairs of subject-matched T-tropic (closed symbols, solid lines) and M-tropic (open symbols, broken lines) Env-pseudotyped reporter viruses. (a) Viruses were incubated at various temperatures for one hour prior to infecting TZM-bl cells and the remaining infectivity was normalized to infectivity after incubation at 25°C. Viruses with M-tropic Env proteins were compared with subject-matched T-tropic Env proteins proteins at five temperatures (-80°C, 4°C, 37°C, 49°C, and 68°C), but revealed no significant differences between tropism groups (-80°C, W_{paired} = -3, P value = 0.8; 4°C, W_{paired} = -5, P value = 0.6; 37°C, W_{paired} = -7, P value = 0.4; 49°C, W_{paired} = -1, P value = 1; 68°C, W_{paired} = -1, P value = 1). Viruses were incubated at (b) 49°C or (c) 0°C for various lengths of time prior to infecting TZM-bl cells. Remaining infectivity was normalized to an untreated aliquot of each virus. M-tropic Env proteins differed in some cases from paired T-tropic Env proteins, but these differences were not correlated with tropism (b, W_{paired} = 7, P value = 0.4; c, W_{paired} = 3, P value = 0.8).

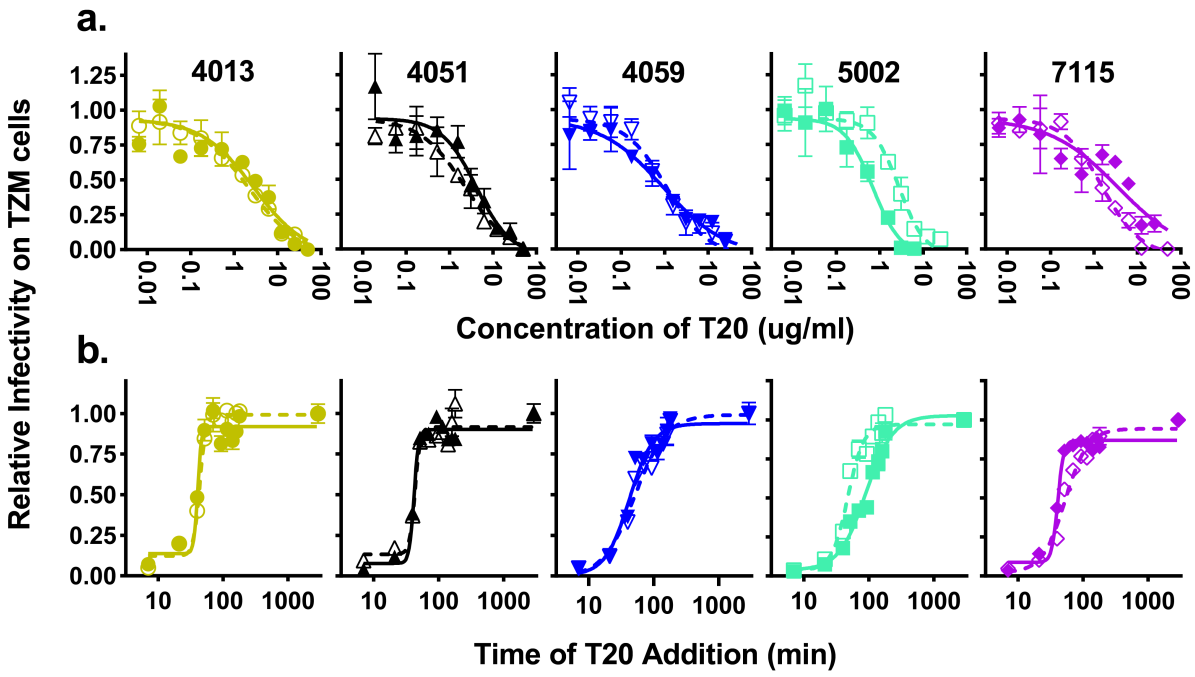

Figure 3.7: **M-tropic viruses have similar fusion kinetics to T-tropic viruses** Inhibition assays with T20 were performed on five pairs of subject-matched T-tropic (closed symbols, solid lines) and M-tropic (open symbols, broken lines) Env-pseudotyped reporter viruses. (a) Viruses were exposed to different concentrations of T20 prior to infecting TZM-bl cells and remaining infectivity was normalized to untreated virus. T20 dose-response curves did not differ detectably between matched-pairs (W_{paired} = 9, P value = 0.3) and were similar across subjects. (b) A saturating concentration (50 μg/ml) of T20 was added to viruses at various times after the addition of cells. Resistance to T20 over time was plotted as a normalized value of remaining infectivity. The resulting measures of fusion kinetics did not differ detectably between matched-pairs (W_{paired} = -5, P value = 0.6) and were similar across subjects.

M-tropic Envs had increased expression on the surface of the virion, we used western blotting to quantify the ratio of gp120 (to represent Env) to p24 (to represent the number of virions). We then calculated the relative ratio of M-tropic Env per virion as a fold-change over the paired T-tropic gp120 per virion (Figure 3.8a). For these experiments, the estimation of the amount of each protein was conducted using a dilution series to work within the dynamic (although nonlinear) range of western blot analysis (data not shown). The fold-change values did not significantly differ from 1. Based on these results, we conclude that differential Env incorporation does not explain the enhanced CD4 usage observed for the M-tropic pseudotyped viruses.

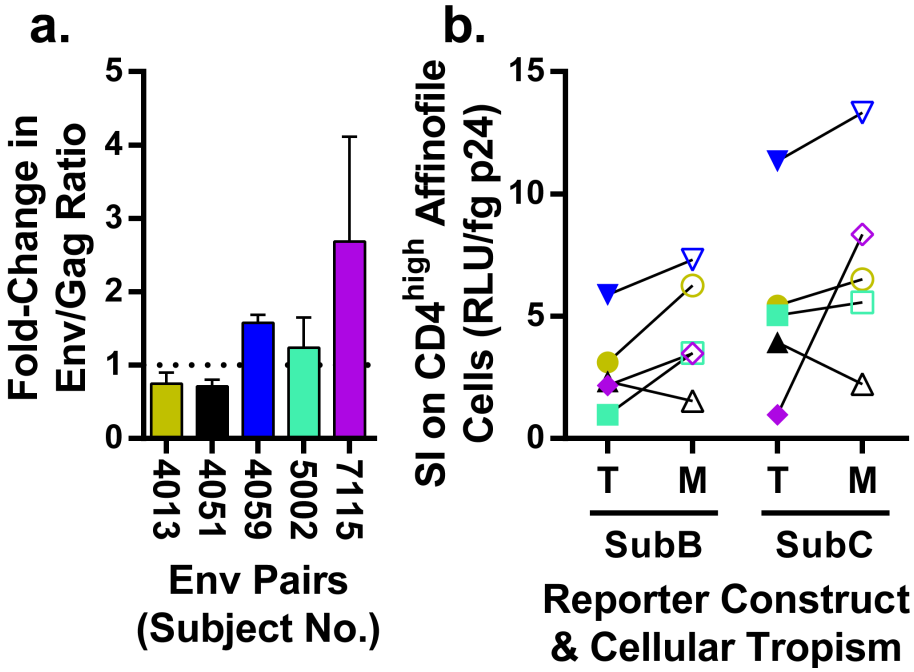

Figure 3.8: **M-tropic Env proteins are incorporated at levels similar to T-tropic Env proteins** (a) Western blot analysis was used to evaluate the relative incorporation of Env proteins into virions using five pairs of T-tropic and M-tropic Env-pseudotyped viruses. For each virus, the abundance of Env was detected by Western blot normalized to the abundance of Gag. The normalized values of Env proteins in M-tropic viruses were compared to those of subject-matched T-tropic viruses and reported as the fold-change value of M-tropic over T-tropic Env incorporation. The fold-change values (mean = 1.4, SD = 0.8) were not found to deviate significantly from a hypothetical mean of 1 (t_{paired} = 1, df = 4, P value = 0.3, which represents the null hypothesis of an equal abundance of Env proteins on the surface of viruses expressing T-tropic and M-tropic Env proteins. (b) Five paired T-tropic (T, closed symbols) and M-tropic (M, open symbols) *env* genes were pseudotyped with an *env*-deficient HIV-1 genome that was either Subtype B with a firefly luciferase reporter gene (SubB) or Subtype C with a *Renilla* luciferase reporter gene (SubC). Virion density was represented by p24 concentration and infectivity was titered on $CD4^{high}$ Affinofile cells. The specific infectivity (SI) values reported are the linear relationship of infectivity (RLU) per virion as represented by a structural protein product, p24-Gag (fg). Although the Subtype C construct gives overall higher SI values, the effect of HIV-1 Subtype cannot be directly compared, because different reporters are used. Despite a small apparent trend of increased SI of M-tropic viruses in both reporter constructs, any differences in SI between paired T-tropic and M-tropic viruses are not significant when taken together (W_{paired} = 13, P value = 0.13) or separated by reporter construct (SubB: W_{paired} = 13, P value = 0.13; SubC: W_{paired} = 9, P value = 0.31). Also, because the CD4 density on $CD4^{high}$ Affinofiles is saturating for M-tropic viruses and not saturating for T-tropic viruses, the SI values for T-tropic viruses are likely an underestimate, which may account for a slight reduction in observed SI compared to M-tropic viruses.

Env protein incorporation can be affected by interactions been Env and structural proteins (reviewed in(246). We examined whether such interactions alter specific infectivity (SI) in our experimental system where SI is defined as the infectivity per viral particle (Figure 3.8b). SI was assessed by measuring the infectivity of pseudoviruses produced from the same ten pairs of *env* clones carrying either the structural proteins encoded by the *env*-deficient HIV-1 Subtype B reporter genome or Subtype C reporter genome and using p24 concentration to infer the per virion relative infectivity. There were similar trends within each reporter construct in that there was an approximately 10-fold range of SI values when comparing a single reporter construct (Subtype B or C) across the different Env proteins. Also, there was a trend toward a small increase in infectivity of the M-tropic viruses; however, CD4 densities on $CD4^{high}$ Affinofile cells are not saturating for infection by T-tropic viruses making it possible that their SI values are underestimated. Also, while the Subtype C reporter virus appears to confer a slight enhancement in SI overall, the two reporter constructs cannot be directly compared because the different luciferase reporter enzymes (firefly versus *Renilla*) may exhibit different amounts of luminescence resulting from the same number of infection events. Thus, although we see variation between Env proteins, the variation between different subjects is greater than between the paired M- and T-tropic Env proteins indicating that macrophage tropism, defined by the Env protein, is not achieved by increasing the per particle infectivity.

3.4.9 CD4 usage is predictive of MDM infectivity and, along with sensitivity to sCD4, reveals viruses with intermediate phenotypes

Using well-characterized, subject-matched M-topic and T-tropic *env* genes, we have demonstrated that MDM infectivity (averaged over multiple donors), low CD4 usage, and sensitivity to sCD4 are clear phenotypes that can be used to distinguish M-tropic viruses from paired T-tropic viruses. Based on these defined characteristics, we identified seven additional HIV-1 *env* genes cloned from compartmentalized virus in the CSF early after HIV-1 infection of infants (29), or in the genital tract of adults (E. N. Dukhovlinova and L. Ping unpublished

data) that showed a modest enhancement of entry on $CD4^{low}$ Affinofile cells (i.e. intermediate between values of T-tropic and M-tropic viruses) and seven subject-matched T-tropic Env proteins isolated from the blood. Viruses with intermediate CD4 usage phenotypes are rare and may provide information about the evolution of macrophage tropism. We analyzed the viral entry phenotypes of these additional seven intermediate pairs using Affinofile cells expressing CD4 across the full range of densities. We found that viruses with an intermediate entry phenotype on $CD4^{low}$ cells also showed differences in entry phenotype compared to both M-tropic and T-tropic viruses over the entire range of CD4 densities (Figure 3.9a). When we used our entire fourteen-pair panel of twenty-eight viruses (fourteen T-tropic, seven M-tropic, and seven intermediate) to infect MDMs, we found that differences in the ability to use CD4 (as captured by the Hill slope of the CD4 titration curve) was predictive for infectivity on MDMs ($r^2 = 0.57$; Figure 3.9b). This result demonstrates that a substantial fraction of MDM infectivity can be accounted for by the ability of the Env protein to use low CD4 densities for entry.

Given that the CD4 entry phenotype appears to be continuous within the dynamic range that was tested, we asked whether this was also the case for sCD4 sensitivity. As shown above, M-tropic Envs are significantly more sensitive to sCD4 than the paired T cell-tropic Envs. Using this same approach, we were also able to show that intermediate Env proteins are significantly more sensitive to sCD4 than subject-matched T-tropic Env proteins (Figure 3.9c; P value = 0.0005). Furthermore, the sCD4 IC_{50} values of the intermediate viruses were similar to those of the well-characterized M-tropic viruses. Taken together, this suggests that evolution of the M-tropic entry phenotype may be a multi-step process marked by increased sensitivity to sCD4 and enhanced entry at low CD4 densities.

3.5 Discussion

HIV-1 evolution to enter and replicate in macrophages results in Env proteins that can more efficiently utilize the low densities of CD4 found on macrophages for viral entry. This

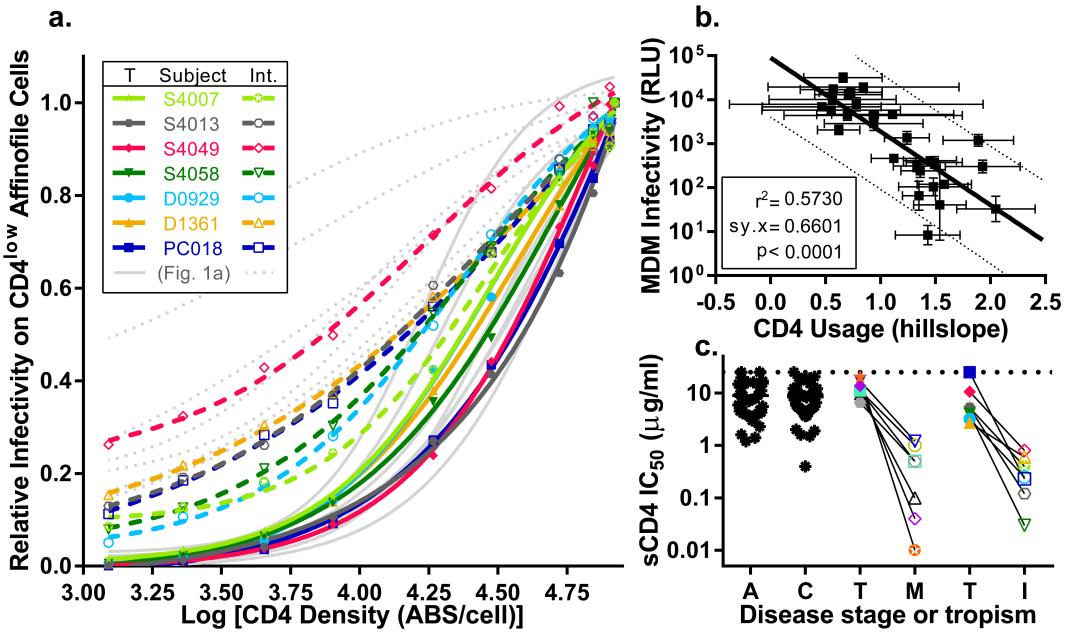

Figure 3.9: **Viruses of intermediate CD4 usage reveal a correlation between CD4 usage and MDM infectivity** Seven pairs of subject-matched Env-pseudotyped viruses in which one virus had a modest enhancement in entry of $CD4^{low}$ Affinofile cells (intermediate, Int.) and the other virus was T-tropic (T) were analyzed and plotted overlapping the data for the original seven pairs of M-tropic (M) and T-tropic (T) viruses shown previously in Figure 3.1. (a) CD4 usage of intermediate (open symbols, broken lines) and T-tropic (closed symbols, solid lines) viruses was evaluated by the Affinofile cell assay as previously described and plotted against previously shown data for subject-matched T-tropic (solid light gray lines) and M-tropic (dotted light gray lines) viruses from Figure 3.1. Unique colors are used to identify each subject as specified in the figure legend (the overlap in symbols with those from Figure 3.1 is not meaningful). The intermediate viruses differ from paired T-tropic viruses in Hill slope (t_{paired} = 2.9, df = 6, *P* value = 0.03), but not in EC_{50} (t_{paired} = 1.0, df = 6, *P* value = 0.34). Similarly, intermediate viruses also differ from unpaired M-tropic viruses, but only in EC_{50} (t_{paired} = 2.5, df = 12, *P* value = 0.03) and not Hill slope (t_{paired} = 0.09, df = 12, *P* value = 0.93). (b) CD4 usage was represented by Hill slope values for each virus, which was plotted against log normalized values of infectivity on MDMs. We evaluated the correlation of CD4 usage and MDM infection and plotted the linear regression (solid line) with the 95% confidence band (broken lines). Variation in CD4 usage could explain 57% of the variation in MDM infectivity (r^2 = 0.57, Sy.x = 0.66, *P* value <0.0001). (c) Neutralization sensitivity to sCD4 was evaluated in a TZM-bl neutralization assay as previously described and reported as IC_{50} values. Subject-matched pairs of intermediate (Int., open symbols) and T-tropic (T, closed symbols) viruses were plotted against data from Figures 3.3a for subject-matched pairs of T-tropic (T, close symbols) and M-tropic (M, open symbols) viruses and the panel of viruses from acute (A) and chronic (C) infection (black asterisks). The colors and symbols are the same as those identified in Figure 3.1a and 3.9a. Subject-matched viruses are linked. Similar to M-tropic Env proteins, Int. Env proteins are 23-fold more sensitive to neutralization by sCD4 compared to subject-matched T-tropic Env proteins (c; t_{paired} = 6.8, df = 6, *P* value = 0.0005).

ability to use a low density of CD4 is a key feature that distinguishes M-tropic viruses from the more typical R5 T-tropic viruses, which require high densities of CD4 for entry into target T cells. We found that low density CD4 usage and sensitivity to soluble CD4 (sCD4) are distinct criteria for macrophage tropism. Furthermore, CD4 entry phenotypes are more reproducible than the relative infection of monocyte-derived macrophages (MDMs). We also found suggestive evidence that the evolution of macrophage tropism includes multiple stages. Although we observed that the enhanced CD4 usage of all the M-tropic viruses was accompanied by an increased sensitivity to sCD4, we also observed multiple intermediate viral lineages that had significantly increased sensitivity to sCD4 but, in some cases, had only a slight increase in the ability to use low CD4 densities. Based on these results, we hypothesize that macrophage tropism evolves through multiple stages that can be marked by an increase in sCD4 sensitivity, enhancement of CD4 usage, and other subtle changes in the Env protein conformation.

In order to make a more accurate assessment of the phenotypic changes that emerge during the evolution of macrophage tropism, we designed our analysis to contain three vital attributes. First, we examined pairs of M-tropic and T-tropic *env* genes isolated from the same subjects without *ex vivo* passaging of their virus. This minimizes the effect of strain-to-strain variation and focuses our analyses on the evolutionary event(s) that took place within each subject. Also, because we used a single pair of *env* genes from each subject, each comparison was an independent observation. Second, we analyzed the phenotypes of Env proteins expressed from *env* genes that had been generated by end-point dilution PCR, which avoids artificial recombinants during amplification. Third, we made phenotypic comparisons across a group of *env* gene pairs from different subjects to identify generalizable differences between T-tropic and M-tropic viruses. These key features allowed us to further define the properties of Env proteins that result in low density CD4 usage and an M-tropic phenotype.

Infection of MDMs *ex vivo* has long been used as a measure of macrophage tropism (15, 17, 146, 148, 151, 157, 247). However, different preparations of MDMs vary in their ability to be infected in ways that have not been controlled experimentally (99, 132, 148). The typical

approach to this substantial experimental problem has been to compare several donors and infer a result. An additional complication of this approach is that R5 T-tropic viruses also vary widely in their ability to infect MDMs (99). This two-dimensional variability (virus and cells) makes it difficult to unequivocally assign cellular tropism in isolation. However, by pooling MDM infection data from four donors and multiple subject-matched M-tropic and T-tropic pairs of viruses, we found a 28-fold increase in average MDM infection by M-tropic over T-tropic viruses (Figure 3.2). These data provide a quantitative estimate of the typical gain in efficiency of MDM infectivity achieved in transitioning to macrophage tropism.

The difference in CD4 density on the surface of macrophages and $CD4^+$ T cells inspired use of cell lines with either high or low levels of CD4 as a method to assess the relationship between efficiency of CD4 usage and macrophage tropism (146, 148, 248, 249). The efficiency of CD4 usage as a surrogate phenotype for macrophage tropism is most easily seen using Affinofile cells, in which CD4 expression can be varied (154) over a wide range and can approximate the surface densities of CD4 on T cells and on MDMs (99). This more sensitive measure of CD4 usage allowed us to identify HIV-1 variants that are characterized by both an intermediate entry phenotype on $CD4^{low}$ cells and an intermediate entry phenotype on MDMs (Figure 3.9b). Based on this analysis, we were able to demonstrate that HIV-1 infection efficiency on $CD4^{low}$ cells predicts macrophage tropism and also predicts intermediate entry phenotypes.

We have focused our study on the role of HIV-1 Env in mediating cell entry and so have not considered other potential viral proteins or sequences that may evolve as part of the adaptation to macrophages. We have ruled out that the differences observed between M-tropic and T-tropic viruses result from differences in the specific infectivity (SI) as conferred by their Env proteins (Figure 3.8b). We also evaluated whether increased Env incorporation, which is mediated by interactions between Env and Gag proteins, could contribute to enhanced CD4 usage, but found comparable levels of Env proteins per viral particle between subject-matched T-tropic and M-tropic virions (Figure 3.8a). Thus the M- and T-tropic viruses are equivalent

in how they contribute to particle formation and conferring infectivity in the presence of high levels of CD4, with the differences being much greater in viruses isolated between subjects than between the M- and T-tropic viruses within a subject.

The enhanced ability of M-tropic viruses to use low CD4 densities for entry suggests an altered interaction between Env and CD4. This suggestion is supported by the observation that the Hill slope determined by CD4 titration is significantly different between these two groups of viruses (Figure 3.1a). Previous studies have reported that M-tropic variants are also more sensitive to sCD4 than T-tropic variants (130, 203, 204). We confirmed this observation by showing that M-tropic variants were on average 27-fold more sensitive to sCD4 compared to their T-tropic counterparts (Figure 3.3a). However, we found no difference in the ability of M-tropic or T-tropic viruses to interact with the CD4 binding site (CD4bs) small molecule agonist BMS-529626 (Table 3.2). A previous report found differences in sensitivity to BMS-663068 (the prodrug form of BMS-626529) when comparing M-tropic and T-tropic viruses (187), however that study included multiple and unequal numbers of clones from each compartment of several subjects, which complicates the statistical analysis that assumes independence of observations. When we probed with a series of CD4bs antibodies, we found suggestive patterns in two of the three CD4bs antibodies tested that hinted at an increased sensitivity of M-tropic viruses in the pairs of viruses that were not completely resistant (Figure 3.3b-d). Two additional CD4bs antibodies, F105 and CH103, were also tested, but the viruses were almost uniformly resistant to neutralization (data not shown), which has been suggested to result from the steric restriction related to the angle of access between the antibodies and the Env trimer (250-252), suggesting that the angle of CD4 access is not dramatically changed in the M-tropic viruses. The variability in antibody sensitivity between Env proteins to these antibodies limits the statistical power of these analyses, given the limited number of subject-matched M-tropic and T-tropic Env pairs available. However, the patterns of increased sensitivity to the relatively bulky CD4bs antibodies, when coupled with the significant increases in sensitivity to sCD4 suggest that conformational differences around the CD4 binding site may

exist in Env proteins from M-tropic viruses.

We also examined whether conformational differences around the CD4 binding site create a more open conformation. Early observations revealed that tissue culture-adapted viruses, in the absence of antibody selection, result in the premature exposure of CD4-induced epitopes (253-256), indicating that the Env protein for these viruses is in a more open conformation that exposes the coreceptor binding site. Furthermore, studies have shown that tissue culture-adapted viruses evolved to use low CD4 for entry (257, 258), were more sensitive to sCD4 (259-261), and had greater sensitivity to antibody neutralization than typical primary isolates (227, 254, 257, 262). Together, these observations raised the possibility that these phenotypes co-vary and are generated by the same mechanism. To determine whether selection to use low CD4 densities for cell entry results in an open Env conformation, we examined Env sensitivity to polyclonal sera and monoclonal antibodies directed against the V3 and CD4i epitopes as a general probe for these two conformational states. We found that there was no difference in antibody sensitivity to polyclonal sera or to most monoclonal antibodies when comparing the M-tropic and T-tropic viruses (Figure 3.4), indicating that M-tropic viruses have not assumed the open conformation of tissue culture-adapted viruses. Furthermore, there was no difference in T-tropic and M-tropic viruses in sensitivity to autologous, contemporaneous serum (Figure 3.5) and the IC_{50} values from all viruses tested were similar to those typically reported for chronic infection (233-243). However, M-tropic viruses appeared to be more resistant to the V1/V2-targeted antibody PG9 (Figure 3.4c), suggesting that M-tropic viruses may differ in the Env conformation of the V1/V2 region, which is now understood to be highly ordered (133, 263) and is thought to contribute to the structure and function of the Env trimer (264-268). Although our ability to assign significance to V1/V2 antibody resistance as a feature of M tropism is limited by sample size (N = 7) and the inherent variability to the neutralization of primary isolates, this observation is consistent with that obtained using a larger panel of unpaired T-tropic and M-tropic viruses (130). Overall, the neutralizing antibody sensitivity properties of M-tropic Env proteins reveals them to be more like R5 T-tropic Env proteins

than tissue culture-adapted variants, but with intriguing differences in the CD4bs and perhaps the V1/V2 loop region.

Dissociation of attached virions prior to successful entry is common (245) and is likely to be a more substantial problem when CD4 is at a low density. Increased efficiency of post-attachment entry steps may be able to compensate when attachment conditions are poor, which led us to examine properties of fusion (the final step) and properties that may affect the conformational changes that occur between attachment and fusion. Differences in Env protein stability affect the conformational changes required for entry (269) and differences in stability can be probed by sensitivity to inactivation at different temperatures. Env proteins display variation in sensitivity to heat (244, 269, 270) and cold (270-272). Heat lability is a feature of the open conformation of tissue culture-adapted viruses, but not of comparatively stable primary isolates (244, 269). Although there was some variation in heat sensitivity between Env proteins from different subjects, the subject-matched M-tropic and T-tropic virus pairs were generally indistinguishable (Figure 3.6b). There were significant differences in cold sensitivity within pairs, but sensitivity was inconsistent across T-tropic or M-tropic Env protein pairs (Figure 3.6c). Therefore, thermal sensitivity is also unlikely to be a co-evolving feature of HIV-1 cellular tropism or CD4 usage. By contrast, fusion was consistent within a subject-pair, despite some variation between viruses from different subjects (Figure 3.7). Overall, we found no evidence that fusion efficiency or Env protein instability is linked to cellular tropism or CD4 usage. From these observations, features of M tropism appear to be limited to the Env-CD4 interaction.

The evolutionary path to HIV-1 macrophage tropism remains poorly understood. A number of Env substitutions have been suggested to contribute to macrophage tropism (145, 181, 202, 203, 205-213), but none of these suggested mutations can distinguish the paired M-tropic and T-tropic viruses used in our study. By including additional HIV-1 variants identified by intermediate CD4 usage, we observed that both MDM infection and low CD4 usage vary across a wide range. This suggests sequential adaptation to infecting macrophages that may

require the accumulation of several mutations. Direct comparison revealed that variation in CD4 usage could explain more than half of the observed variation in MDM infection (Figure 3.9b). We do not know if other factors also impact entry into macrophages or if the remaining variation is due to experimental variation.

We previously showed that T-tropic and M-tropic viruses differ in CD4 usage but not in CCR5 usage, as measured by maraviroc sensitivity (99). We also observed that M-tropic and intermediate variants have similar increases in sensitivity to sCD4 when compared to T cell-topic variants (Figure 3.9c). Other groups have also identified viruses from the CNS that, like our intermediate viruses, are sensitive to sCD4 but unable to efficiently infect MDMs (e.g. Dunfee 2009, Gonzalez-Perez 2012). The lack of a positive relationship between sensitivity to sCD4 and the ability to infect MDMs made it difficult for previous studies to assign tropism for these viruses. The increased sensitivity of our CD4 usage assay allowed us to detect a group of viruses with intermediate enhancement of CD4 usage, sensitivity to sCD4, and an intermediate ability to infect MDM *in vivo* Together, these findings imply that sCD4 sensitivity is a phenotype that can be detected early in the enhancements in low CD4 usage. Also, the general resistance to neutralizing antibodies combined with a pattern of sensitivity to sCD4 indicate that M-tropic Env proteins exist in a state that is distinct from both R5 T cell-tropic (which are resistant to sCD4) and tissue culture-adapted Env proteins (which are globally sensitive to neutralization).

Because our viruses represent a cross-section of viral populations rather than a longitudinal study of evolving populations, it is difficult to determine whether a continuous range of values (e.g. CD4 usage or MDM infectivity) represents a continuous phenotype or large variation around a bimodal phenotype. However, if CD4 usage and MDM infectivity are on a multi-step evolutionary path to macrophage tropism (as suggested by our detection of intermediates), then defining the mutations on this pathway and understanding the nature of the change in the interaction between the viral Env protein and host CD4 receptor remain as important questions to inform our understanding of the evolution of macrophage tropism.

CHAPTER 4

MAJOR GENETIC DETERMINANTS OF MACROPHAGE TROPISM OCCUR IN THE V5 REGION OF ENV[1]

4.1 Overview

Although HIV-1 is normally CCR5 using and T cell-tropic (T-tropic), viral populations can evolve to become CCR5-using and macrophage-tropic (M-tropic). Identifying the genetic determinants of macrophage tropism has been stymied by high variation in the HIV-1 *env* gene and lack of a sensitive, reproducible, and high-throughput assay for detecting macrophage tropism. By comparing subject-matched pairs of T-tropic and M-tropic *env* genes, we reduced variation occurring naturally between subjects. Development of the $CD4^{low}$ Affinofile assay as a sensitive proxy for macrophage tropism expanded the number of *env* genes evaluated per assay and reduced assay-to-assay variation. In this way, we were able to identify variable region 5 (V5) of the HIV *env* gene as a major determinant of macrophage tropism. Although other contributors were identified near CD4 binding sites and in the V1/V2, only V5 involvement was consistent across all subjects tested, suggesting a role for V5 in CD4 interactions. We then created M-tropic *env* genes from each T-tropic *env* gene using site-directed mutagenesis to induce between two and seven amino acid substitutions. Testing whether these manually generated M-tropic *env* genes recapitulate the soluble CD4 sensitivity and enhanced infection of MDMs *in vitro* will evaluate the $CD4^{low}$ Affinofile assay results and provide detailed in-

[1]The work described in this chapter was accomplished in collaboration with Ean Spielvogel, Zaki Dard, Paige McClear, and Ron Swanstrom.

formation about the relationship between CD4 usage, sCD4 sensitivity, and MDM infection as phenotypic correlates of macrophage tropism. Identification of genetic determinants may eventually enable genetic screening for M-tropic HIV-1 to assist in both therapeutic evaluation and understanding macrophage tropism frequency and evolution *in vivo*.

4.2 Introduction

HIV-1 is mostly CCR5-using (R5) and T cell tropic (T-tropic), which preferentially targets memory $CD4^+$ T cells (12-14) by requiring CCR5 as the coreceptor and high cell surface densities of the CD4 receptor. However, HIV-1 can evolve variants with different entry requirements to expand into different cell types. The most frequent example is the emergence of CXCR4-using (X4) T-tropic variants in which the virus is adapted to use CXCR4 as an alternate coreceptor to CCR5 (16, 18, 124, 126, 136, 195), but still requires high CD4 densities. X4 T-tropic viruses have an expanded host range and preferentially infect nave $CD4^+$ T cells (196, 197, 273), which have higher CXCR4 expression than memory $CD4^+$ T cells and little to no CCR5 expression (132, 198). Promiscuity in coreceptor usage has also been observed to increase over the course of infection (274), allowing the viral population to sample a wider range of potential host cells. Emergence of X4 variants or variants with promiscuous coreceptor usage has been correlated with later stages of infection (126, 195), when the original target cells (memory $CD4^+$ T cells) are substantially reduced (134). Because these variants are rarely seen early in infection, it seems likely that viruses losing their optimal host are under selective pressure to adapt to host cells that are more abundant despite, perhaps, being less than ideal for replication.

HIV can also evolve changes in receptor usage. Macrophage-tropic (M-tropic) viruses have adapted to use lower cell surface levels of the CD4 receptor (99, 187) to allow expansion into macrophages or microglia (153), which have 20-fold lower expression of CD4 on the cell surface compared to $CD4^+$ T cells (15, 99, 145-148, 202). Changes in coreceptor use are not correlated with M-tropism and most M-tropic variants are R5 M-tropic (99), though

there are infrequent exceptions (205, 275). M-tropic variants are rare (17, 20, 141, 142) and are most often detected in the central nervous system (CNS) of subjects with advanced HIV-1 infection (146, 148-151). However, more recent studies have been able to identify HIV-1 variants with intermediate cellular tropism phenotypes between that of T-tropic and M-tropic viruses very early after infection and during chronic infection (29, 30, 96), which may represent evolutionary intermediates on the path to macrophage tropism.

To adapt to target a new host cell, HIV-1 must first adapt to efficiently bind and enter that cell type. Receptor specificity and entry are determined by a single viral gene: HIV-1 env. The Env gene product is cleaved into two subunits, an external gp120 protein and a transmembrane gp41 protein, which remain non-covalently associated and form trimers on the viral surface made up of three gp120-gp41 pairs. The gp120 protein contains the epitope for the CD4 receptor and, after conformational changes induced by binding CD4, the epitope for the CCR5 coreceptor. The gp41 protein contains the fusion mechanism, which is triggered by CCR5 binding-induced conformational changes in gp120 and results in a major structural rearrangement in gp41 that brings the viral and cellular membranes in close proximity to induce fusion.

Several genetic mutations have been reported as important determinants for macrophage tropism (Table 1). Several reported determinants involve substitutions near the CD4 binding residues, e.g. the loss of a potential N-linked glycosylation site (PNGS) at Env position 386, which could reducing steric hindrance at the CD4 binding site (CD4bs) (187), or T283N, which has the potential to enhance the interaction between gp120 and CD4 by creating an additional hydrogen bond between the substituted asparagine and CD4 (15, 202). However, determinants have been reported across the env gene from V1/V2 to the V5. More recently, several substitutions in the V1/V2 region have been implicated in macrophage tropism, including E153G, which been suggested to be a marker for 50% of M-tropic strains (203), and N*197S (where * denotes a potentially N-linked glycosylated site; PNGS). These V1/V2 mutations do not seem to directly interact with CD4, but may be functioning as part of the

conformational switch region which can now be interpreted based on the recently published sheet scaffold structure of the V1/V2 domain (133). Despite the number of studies identifying potential genetic determinants of macrophage tropism, few of these determinants overlap between subjects and none of those identified so far could fully distinguish our highly validated subject-matched pairs of M-tropic and T-tropic env gene sequences.

Table 4.1: Amino Acid Residues Reported as Associated with Macrophage Tropism

Reference	(203)	(203)	(271, 280)	(280)	(205)	(205)	(15, 145, 207)	(213)	(181)	(154, 213)	(205)	(212)	(212)	(212)	(206)	(202, 206)	(206, 208)	(203)	(213)	(213)	(213)
T-tropic[a]	E	D	N	V	P	T	T	S	H/T	F	M	N	X	X	R	N	T	N*	A	D	G
M-tropic[a]	G	N	S,X	T	S/K/R	K/E	N	T	P	L	I	X	P	S	K	D	X	X	V	N	R
Position	153	167	197	200	238	240	283	303	308	317	326	362	363	364	373	386	388	396	430	460	462
Consensus[b]	E	D	N*	V	P	T	T	T	H	F	I	N*	Q	S	M	N*	T	N*	V	N	N*
4013T	E	D	N*	I	L	R	T	T	P	F	I	E	P	S	M	N*	T	N*	V	R	N*
4051T	E	D	N*	V	P	T	T	T	P	F	I	N*	Q	S	T	N*	T	N*	V	R	N*
4059T	E	N	N*	V	E	K	T	T	N	W	I	E	Q	V	M	N*	S	S	V	G	Δ
5002T	D	D	N*	V	P	T	I	T	H	F	T	N*	Q	S	M	N*	T	N*	V	H	N
7115T	E	D	N*	V	P	K	T	T	H	F	I	K	Q	S	M	N*	S	N	V	N	N
SJC-T	E	D	N*	I	P	T	T	T	H	F	I	T	H	S	M	N*	T	N	V	N	N*
SJR-T	G	E	N*	V	P	K	I	T	H	F	I	N*	Q	S	M	N*	S	N*	V	N	S
4013M	E	D	N*	I	P	T	T	T	H	I	I	T	N	S	M	N*	T	N*	V	Y	I
4051M	E	D	N*	V	L	K	T	T	P	F	I	N*	Q	S	T	T	T	N*	V	N	N*
4059M	E	N	N*	V	E	K	T	T	S	W	I	E	Q	V	M	N*	S	N*	V	S	N*
5002M	E	D	N*	V	P	T	T	T	H	F	I	N*	Q	S	M	N*	T	N*	V	Y	S
7115M	E	D	S	V	P	K	T	T	H	F	I	K	Q	S	M	N*	S	N*	V	N	N*
SJC-M	E	D	N*	V	P	T	I	T	H	F	I	T	H	S	M	N*	S	N	V	K	N*
SJR-M	G	E	N*	V	P	K	I	T	R	F	I	N*	Q	S	M	N*	S	T	V	I	N*

[a] Amino acid residues reported to be associated with tropism

[b] Consensus amino acid residues derived from the Los Alamos National Laboratory "HIV Sequence Compendium" published October 6, 2015. (http://www.hiv.lanl.gov/content/sequence/HIV/COMPENDIUM/compendium.html)

* potential N-linked glycosylation site (PNGS)

Discovery of a consistent genetic signature in X4 variants has allowed deep and rapid screening through next generation sequencing techniques, even though the full determinants of CXCR4 usage may be far more complex. Unfortunately, a genetic signature has been more difficult to uncover in macrophage tropism. Detecting M-tropic variants currently requires phenotypic assays, which until recently has relied on infecting monocyte-derived macrophages, which are available only in small batches and vary widely between batches. Therefore, few M-tropic viruses are detected, and the true prevalence of M-tropic viral populations remains unclear. Discovery of the genetic determinants of macrophage tropism could

provide clues for the mechanism of enhanced CD4 usage and may also reveal a genetic signature for macrophage tropic viruses. Deep screening for such a genetic signature could detect the early appearance of M-tropic virus in the CSF (or the blood) as a minor variant in asymptomatic subjects not yet on therapy. Enhanced detection of M-tropic virus could also help clarify the role of macrophage tropism in neurocognitive disease and its potential as a reservoir.

To identify the genetic determinants of M-tropism, we used HIV-1 env genes cloned from rigorously defined M-tropic viruses and subject-matched T-tropic viruses to make reciprocal swaps between subject-matched env genes. We generated pseudotyped viruses expressing each of the recombinant env genes and tested the CD4 usage (which is a phenotypic correlate of macrophage tropism (96, 99)) of these viruses compared to the parental M-tropic and T-tropic viruses. We used several reciprocal swaps from each pair of subject-matched M-tropic and T-tropic viruses to identify small regions responsible for enhanced CD4 usage. To identify individual amino acid determinants of CD4 usage enhancement, we made individual mutations in both the M-tropic (for loss of function) and the T-tropic (for gain of function) and again tested CD4 usage. When we identified the several amino acid changes responsible for enhanced CD4 usage in each M-tropic Env protein, we made those mutations in the subject-matched T-tropic Env protein and tested both CD4 usage and infectivity on monocyte-derived macrophages. Previous work suggested changes in the CD4bs and the V1/V2 region, but the data were inconclusive. Therefore, we tested these T-turned-M-tropic Env proteins for neutralization sensitivity to antibodies targeting the CD4bs and the V1/V2 regions to clarify whether these regions change during evolution to macrophage tropism. Collectively, this work identifies regions of the HIV-1 env gene involved in evolving macrophage tropism and provides a foundation for future mechanistic studies.

4.3 Materials and Methods

4.3.1 Parental *env* gene clones

We examined *env* gene clones generated in previous study from the blood and CSF of five subjects infected with HIV-1 subtype B and diagnosed with HIV-associated neurological disease (61; Table 4.2). Amplicons of viral *env* genes were generated from virion RNA using end-point dilution PCR and cloned into an expression vector (pcDNA3.1). The resulting *env* vectors have been evaluated for cellular tropism and for phenotypic characteristics using Env-pseudotyped viruses (61, 99, 276).

Table 4.2: Source material of parental *env* genes

Subject	Tropism[1,2]	Tissue[3,4]	Clone	Reference
4013	R5 T	Blood	P9	(61)
4013	R5 M	CSF	C7	(61)
4051	R5 T	Blood	P25	(61)
4051	R5 M	CSF	C3	(61)
4059	R5 T	Blood	P26	(61)
4059	R5 M	CSF	C19	(61)
5002	X4 T	Blood	P10	(61)
5002	R5 M	CSF	C1	(61)
7115	R5 T	Blood	P6	(61)
7115	R5 M	CSF	C21	(61)

[1] R5 T, CCR5-using T cell tropic

[2] R5 M, CCR5-using macrophage tropic

[3] X4 T, CXCR4-using T cell tropic

[4] CSF, cerebrospinal fluid

4.3.2 Recombinant *env* genes

We combined regions from one M-tropic and one subject-matched T-tropic *env* vector to make recombinant *env* genes for each of five subjects using several methods: restriction digest, overlap-extension PCR, or site-directed mutagenesis. Recombinant *env* vectors were only made with pairs of subject-matched *env* genes.

For restriction digest recombination, we digested M-tropic and T-tropic *env* vectors with restriction enzymes that excised the same region from both vectors, then the excised regions were swapped and ligated into the other vector (e.g. we excised a BamHI-EcoRI fragment from the M-tropic *env* vector from subject 4013 and inserted that fragment into a BamHI- and EcoRI-digested T-tropic *env* vector from subject 4013 and vice versa).

To insert large regions for which there were no convenient restriction sites, we used a modified overlap extension PCR (OE-PCR) protocol. OE-PCR required a 30 - 40 bp region on both ends of the region of interest that was homologous (95% identical) between the M-tropic and subject-matched T-tropic *env* gene. To generate the insert, we PCR amplified or synthesized dsDNA that corresponded to the region of interest in one *env* gene (e.g. from the M-tropic *env* gene) and the homologous regions on either end. This fragment was used to prime PCR on the subject-matched *env* gene expression vector (e.g. on the T-tropic *env* expression vector; see Appendix A for the protocol and cycling conditions) to generate a recombinant *env* expression vector.

To make coding changes individually, we used site-directed mutagenesis PCR (SDM-PCR) to mutate a codon from one *env* vector to the corresponding codon in the subject-matched *env* vector (see Appendix B for the protocol and cycling conditions). This allowed creating recombinant *env* vectors that incorporated one or a few selected changes to correspond with the subject-matched *env* vector, which in turn enabled identification of the minimum changes in each subject-matched pair required to alter tropism.

4.3.3 Generation of pseudotyped viruses

293T cells were plated ml in a 100-mm dish at a density of 2.5 x 10^6 cells in 10 ml and incubated at 37°C. After 18 - 20 hours, 293T cells were transfected with 2 μg of an env expression vector (pcDNA3.1), 5 μg of pNL4-3.LucR-E- plasmid (obtained through the NIH AIDS Research and Reference Reagent Program, Division of AIDS, NIAID, NIH), and 30 μL FuGENE 6 (Promega) in serum-free DMEM. After 5 hours, the medium was replaced. After 48 hours, the medium was collected, filtered through a 0.45 μm syringe filter (Millipore), and stored at -80°C in small, single-use aliquots. Virus stocks were not subjected to multiple freeze-thaw cycles.

Virus stocks were titered on Affinofile cells induced to maximum expression of CD4 and CCR5. Infectivity was measured using a Luciferase Assay System kit (Promega) and a luminometer (Veritas), which measures in relative light units (RLU). Titration curves within the linear range of a virus dilution series were used to calculate the volume of viral stock resulting in 800,000 RLU and that volume was used for infection of Affinofile cells and MDMs.

4.3.4 Cells

293T cells were maintained in Dulbeccos modified Eagle medium (DMEM) with 4.5 g/L glucose (Cellgro) supplemented with 10% fetal bovine serum (FBS), 100 U/ml penicillin, and 100 μg/ml streptomycin (Sigma). Affinofile cells (154) were maintained in DMEM with 4.5 g/L glucose (Cellgro) supplemented with 50 mg/ml blasticidin (Invitrogen).

Monocyte-derived macrophages (MDM) were prepared as previously described (99). Briefly, blood was collected from four healthy donors. Buffy coats were prepared from whole blood by centrifugation into a Ficoll gradient (Ficoll-Paque Plus, GE Healthcare). Monocytes were isolated from the buffy coats by negative selection (EasySep human enrichment kit without CD16 depletion, StemCell Technologies). Purified monocytes were maintained in RPMI 1640 medium (Cellgro) supplemented with 10% FBS, 100 U/ml penicillin, 100 μg/ml streptomycin (Sigma), and 10 ng/ml recombinant human macrophage colony-stimulating factor (M-CSF,

Gibco).

4.3.5 Affinofile cell assay

Assays were performed as described previously (159). Briefly, a 96-well black plate (Costar) was pre-treated with poly-L-lysine by adding 75 μL of 0.1 g/L poly-L-lysine in PBS to each well, incubating at 37°C for 20 min, then removing the solution. Affinofile cells were plated at a density of 2.0 x 10^4 cells in 100 μL for each well. After 18 - 20 h, ponasterone A (Invitrogen) was added to the medium at a final concentration of 5 nM to induce maximum expression of CCR5, and doxycycline (Sigma) was added to the medium at either a final concentration of 5 ng/ml to induce maximum expression of CD4 or no doxycycline was added for minimum expression of CD4. After 20 additional hours, the medium with the chemical inducers was replaced with normal medium (i.e. lacking ponasterone A and doxycycline) and virus was added to the cells. The plates were centrifuged at 2000 rpm for 2 h at 37°C, then incubated at 37°C. After 48 hours, the medium was removed and the cells were washed once with PBS then lysed with 50 μL of Reporter lysis buffer (Promega). The lysate was stored at -80°C. Virus entry was then assessed by thawing the lysates and quantifying luciferase expression by using a luciferase assay system for firefly luciferase (Promega).

4.3.6 MDM assay

Monocyte-derived macrophages (MDMs) were plated at a density of 5.0 x 10^4 cells in 0.5 ml for each well of a 48-well plate. Five days after plating, 50% of the medium replaced. After an additional two days, viruses were added to the well and the plates were centrifuged at 2000 rpm for 2 h at 37°C. The plates were washed once with PBS, washed once with medium, then a full medium change was done to remove unbound virus. After 48 h, the cells were washed twice with PBS and lysed with 50 μL of Reporter lysis buffer (Promega), and the lysate was stored at -80°C. Virus entry was then assessed by thawing the lysates and quantifying luciferase expression by using a luciferase assay system (Promega).

4.3.7 Neutralization assays

Neutralization assays using TZM-bl cells have been previously described (215). Briefly, soluble CD4 (sCD4) or a neutralizing antibody was serially diluted across a 96-well black plate (Costar). Virus was added at a single concentration (approximately 150,000 RLU) and incubated with the antibody or sCD4 for 60 min at 37°C. TZM-bl cells were added to a density of 1.0 x 10^4 cells per well and incubated 48 h at 37°C.

4.4 Results

We made recombinants using pairs of HIV-1 *env* gene expression vectors derived from one macrophage-tropic (M-tropic) and one T cell-tropic (T-tropic) virus isolated from each of five subjects. These *env* genes have been extensively characterized by both genetic and phenotypic analyses to clearly identify the cellular tropisms of the viruses associated with the encoded Env proteins (61, 99, 276). The M-tropic viruses analyzed in this study can be clearly distinguished from the subject-matched T-tropic viruses by four criteria: (1) central nervous system compartmentalization (a viral population that is genetically and anatomically distinct from the more typical lymph/blood-associated T-tropic viral population), (2) efficient use of low CD4 densities (such as those found on macrophages) for cell entry, (3) sensitivity to neutralization by soluble CD4 (sCD4), and (4) efficient entry of monocyte-derived macrophages (MDMs). We have recently shown that the ability to use low CD4 densities for entry (i.e. efficient CD4 usage) is strongly predictive of macrophage tropism and can even detect viruses with a weak M-tropic phenotype (i.e. an intermediate phenotype between T-tropic and M-tropic viruses (276)). To measure CD4 usage, we used Affinofile cells with a range of inducible CD4 expression levels to assay for M-tropic viruses. The $CD4^{low}$ Affinofile cell assay (99, 159, 276) allows rapid screening for M-tropic viruses by using viruses to infect Affinofile cells expressing the minimum density of CD4 ($CD4^{low}$ Affinofile cells) normalized to infection of Affinofiles expressing maximum CD4 density ($CD4^{high}$ Affinofile cells).

HIV-1 *env* sequences are highly diverse (97), making sequence comparisons difficult. To demonstrate the variation in HIV-1 Env proteins, we used amino acid consensus sequences from 80 subjects with subtype B HIV-1 infection and plotted the frequency of each amino acid at each position (Figure 4.1). This plot highlights a large degree of length variation in the V1, V2, V4, and V5 regions and a substantial amount of variation in both the variable regions and in the relatively conserved C3 region.

4.4.1 Macrophage tropism is not determined by C-terminal length variation

. Three of the five M-tropic *env* genes encoded a read-through mutation of the termination codon and extended the Env protein 4 to 14 amino acids past the consensus terminus, which is rare (Figure 4.1). To test whether this 5 extension of the Env protein had any effect on macrophage tropism, we reinserted a stop codon at the subtype B HIV-1 consensus position. Parental or mutated *env* expression vectors were used to pseudotype virus particles made from an Env-deficient HIV-1 luciferase reporter construct, and the pseudotyped virions were analyzed using the $CD4^{low}$ Affinofile cell assay (Figure 4.2). Luciferase activity was measured in relative light units (RLUs) as a proxy for infection. All $CD4^{low}$ infectivity values are reported as a percentage of the $CD4^{low}$ infectivity achieved by the parental M-tropic from the same subject.

Truncation of the extra four amino acids in the T-tropic Env protein from 5002, nine in 4059, and fourteen in 4013 had no detectable effect on the ability to use low CD4 for infection ($CD4^{low}$ infectivity; Figure 4.2). Nor were there substantial differences in the specific infectivity of the viral stocks as measured by infectivity on Affinofile expressing high (permissive) levels of CD4 as a function of stock volume. Although the extra amino acids are conspicuous and enriched in these M-tropic viruses, there appears to be no effect on virus function possibly due to Env proteins being pseudotyped with unrelated structural proteins.

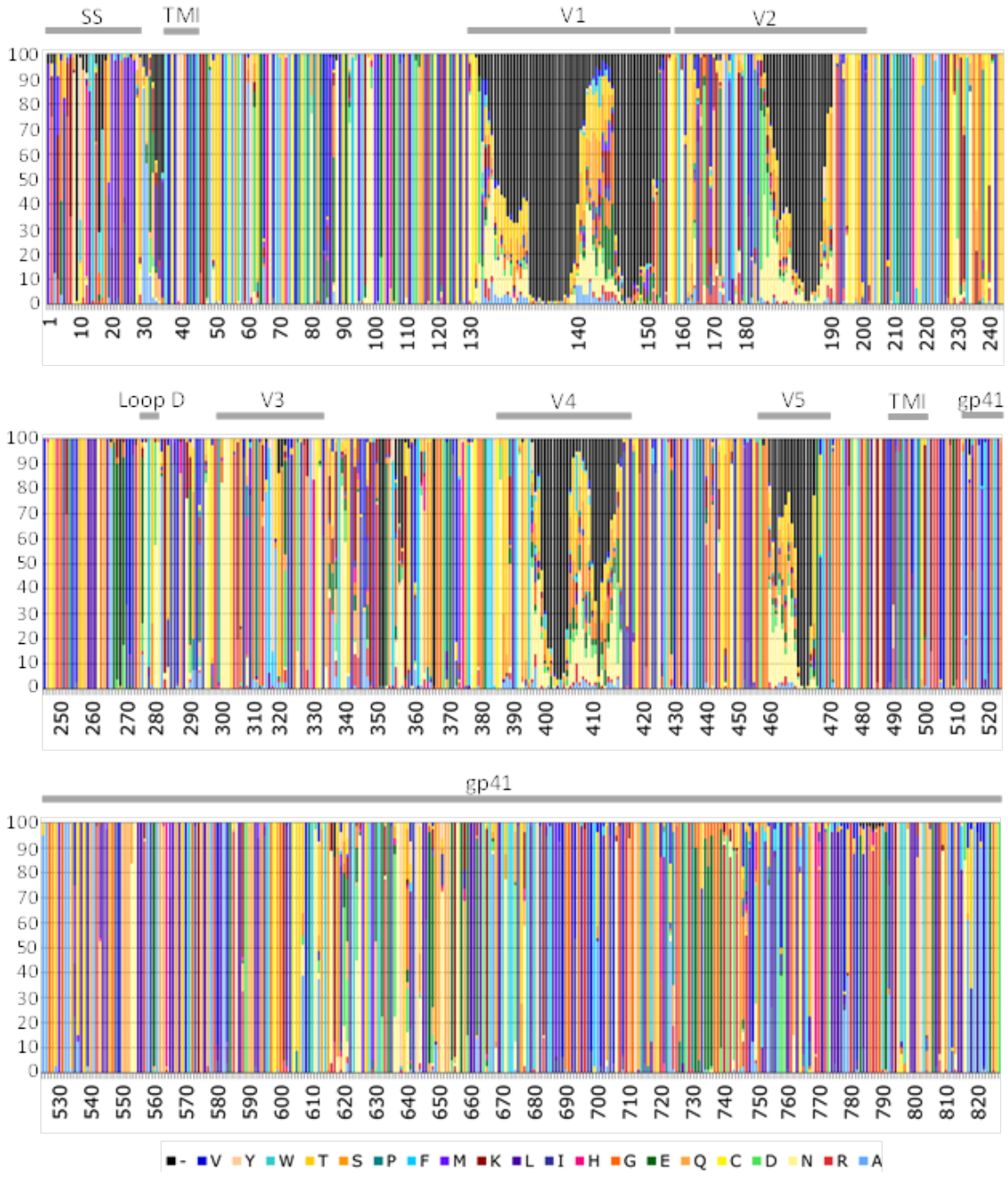

Figure 4.1: **Amino acid variation in HIV-1 Env proteins** Consensus amino acid sequences were created for 80 different subjects with subtype B HIV-1 infection. Each amino acid is represented by a different color as indicated at the bottom of the figure. The length of each bar represents the frequency of each amino acid present at that position. Black bars represent the absence of any amino acid at that position. The numbers along the X-axis indicate the amino acid position per HXB2 numbering.

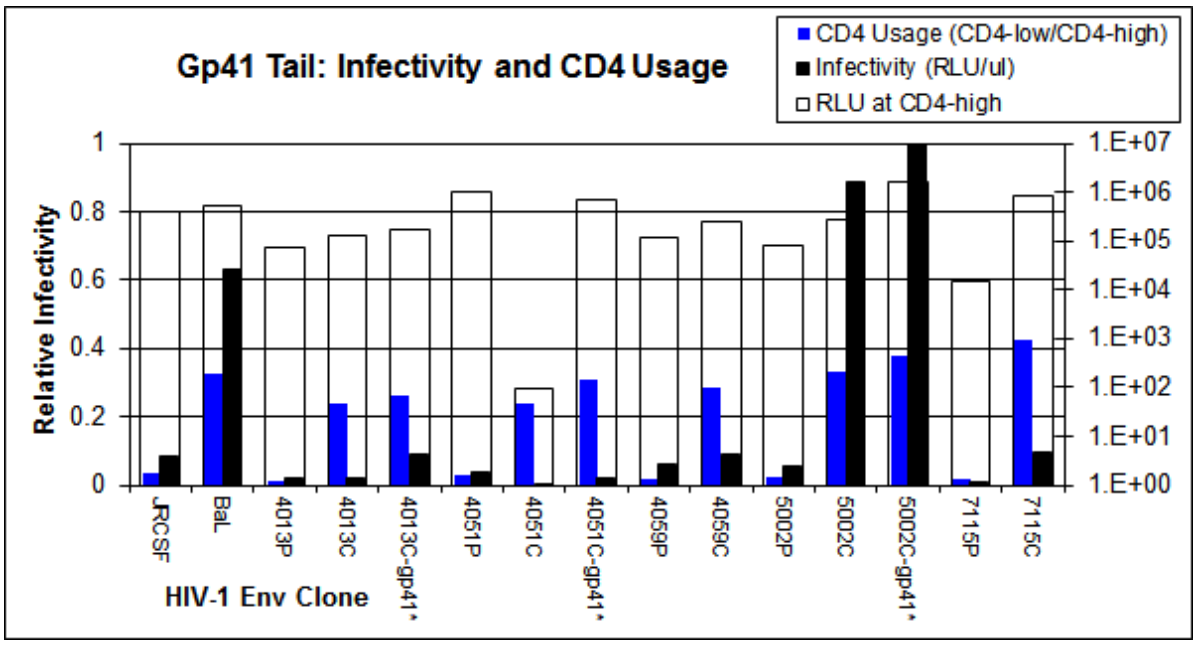

Figure 4.2: **Truncation of extra 5 length in gp41 does not affect CD4^{low} infectivity** In the three M-tropic *env* genes that had a read-through of the termination codon, the consensus termination codon was inserted to truncate the Env protein to consensus length (and to match the subject-matched T-tropic protein).

4.4.2 Recombinants between paired M- and T-tropic *env* genes map the domains responsible for macrophage tropism

To reduce the noise of subject-to-subject variation, we compared each M-tropic *env* sequence only with a subject-matched T-tropic *env* sequence, which reduced the number of coding changes to 93 changes per pair on average (Figure 4.3). To reduce the analysis of differences unrelated to tropism, we used restriction enzyme digestions and ligation to perform homologous swaps between subject-matched *env* genes, resulting in the insertion of a relatively large sequence from the M-tropic *env* gene into the T-tropic background (replacing the homologous T-tropic sequence) to create chimeric *env* expression vectors. Where possible, we made additional homologous swaps between the new chimeras and the parental T-tropic *env* genes to produce smaller M-tropic inserts. When convenient restriction sites were not available, we used overlap-extension PCR (OE-PCR) to replace regions of the parental T-tropic *env* expression vector with smaller M-tropic *env* sequences. This resulted in chimeric *env* genes

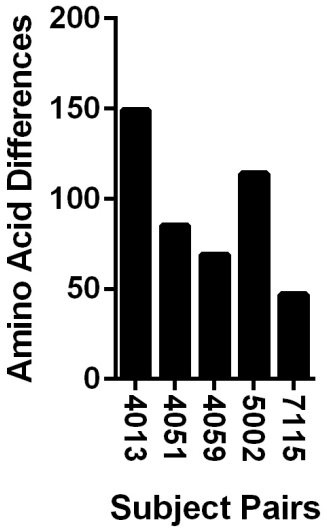

Figure 4.3: **The number of amino acid differences between subject-matched Env proteins** The number of coding changes between paired Env proteins was calculated and reported as the raw number of differences.

wherein some portion of the M-tropic sequence (represented by boxed regions; Figure 4.4) have replaced the homologous region in the subject-matched T-tropic background sequence.

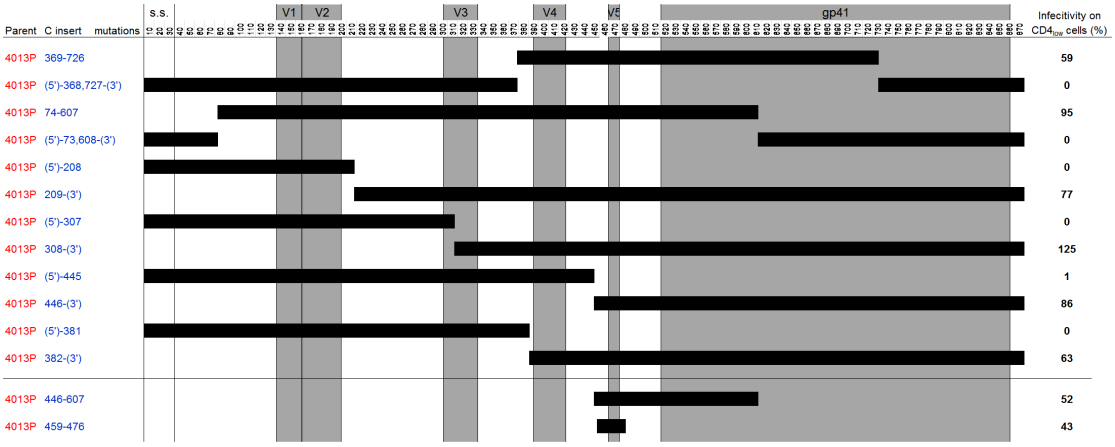
s.s.
V1
V2
V3
V4
V5
gp41
Parent C insert mutations
Infecitivity on CD4low cells (%)
4013P 369-726 59
4013P (5')-368,727-(3') 0
4013P 74-607 95
4013P (5')-73,608-(3') 0
4013P (5')-208 0
4013P 209-(3') 77
4013P (5')-307 0
4013P 308-(3') 125
4013P (5')-445 1
4013P 446-(3') 86
4013P (5')-381 0
4013P 382-(3') 63
4013P 446-607 52
4013P 459-476 43

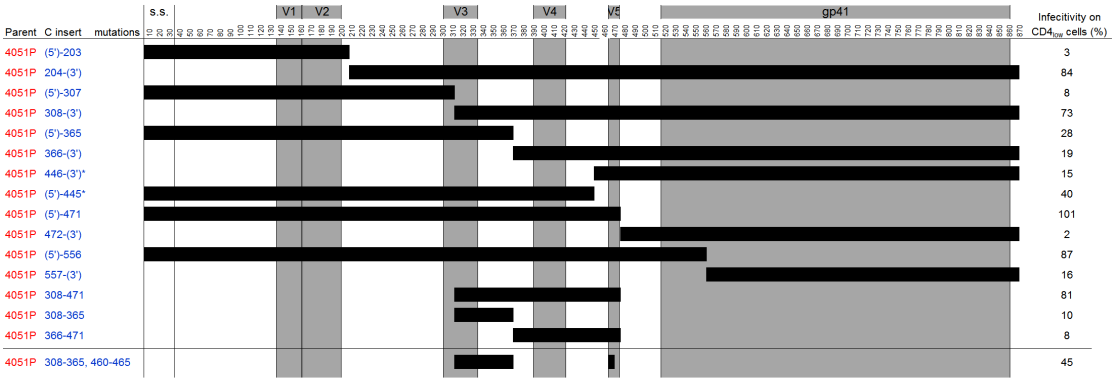
s.s.
V1
V2
V3
V4
V5
gp41
Parent C insert mutations
Infecitivity on CD4low cells (%)
4051P (5')-203 3
4051P 204-(3') 84
4051P (5')-307 8
4051P 308-(3') 73
4051P (5')-365 28
4051P 366-(3') 19
4051P 446-(3')* 15
4051P (5')-445* 40
4051P (5')-471 101
4051P 472-(3') 2
4051P (5')-556 87
4051P 557-(3') 16
4051P 308-471 81
4051P 308-365 10
4051P 366-471 8
4051P 308-365, 460-465 45

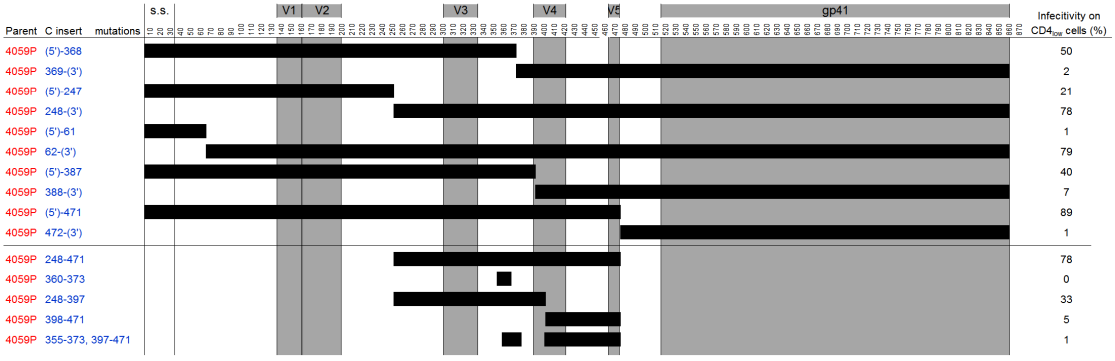
s.s.
V1
V2
V3
V4
V5
gp41
Parent C insert mutations
Infecitivity on CD4low cells (%)
4059P (5')-368 50
4059P 369-(3') 2
4059P (5')-247 21
4059P 248-(3') 78
4059P (5')-61 1
4059P 62-(3') 79
4059P (5')-387 40
4059P 388-(3') 7
4059P (5')-471 89
4059P 472-(3') 1
4059P 248-471 78
4059P 360-373 0
4059P 248-397 33
4059P 398-471 5
4059P 355-373, 397-471 1


s.s.
V1
V2
V3
V4
V5
gp41
Parent C insert mutations
Infecitivity on CD4low cells (%)
5002P (5')-61 3
5002P 62-(3')
5002P (5')-366 3
5002P 367-(3') 161
5002P 367-471 149
5002P 448-474 18

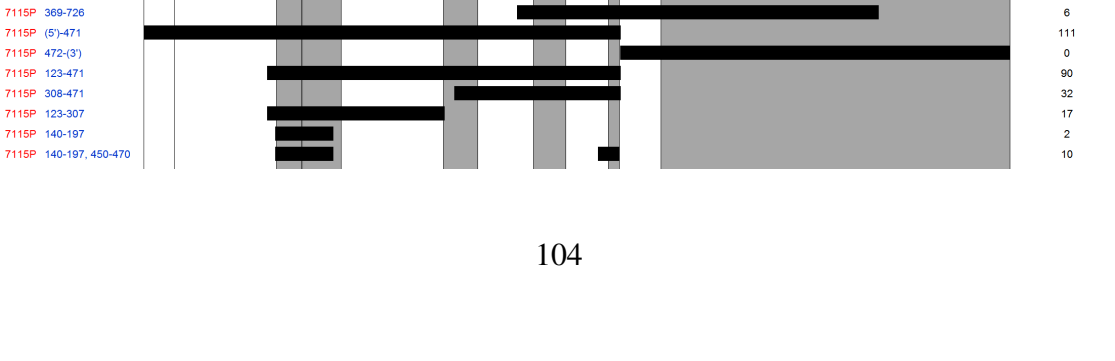
s.s.
V1
V2
V3
V4
V5
gp41
Parent C insert mutations
Infecitivity on CD4low cells (%)
7115P 74-607 96
7115P (5')-73,608-(3') 5
7115P (5')-122 0
7115P 123-(3') 100
7115P (5')-307 39
7115P 308-(3') 6
7115P (5')-368,727-(3') 28
7115P 369-726 6
7115P (5')-471 111
7115P 472-(3') 0
7115P 123-471 90
7115P 308-471 32
7115P 123-307 17
7115P 140-197 2
7115P 140-197, 450-470 10

Figure 4.4 *(previous page)*: **Chimeric Env proteins with M-tropic inserts in a T-tropic background** Restriction digestion/ligation and overlap-extension PCR (Appendix B) were used to generate chimeric *env* gene vectors. Starting with a T-tropic *env* gene, several regions were replaced with homologous sequences from subject-matched M-tropic *env* gene (black boxes). Viruses pseudotyped with these chimeric *env* genes and a Luciferase reporter construct for use in infectivity assays (see Figure 4.3).

For each subject, we compared the chimeric and parental pseudoviruses to evaluate whether each M-tropic sequence insertion was able to confer efficient $CD4^{low}$ infectivity (Figure 4.5). Several of the M-tropic insertions resulted in an all-or-none response (i.e. the chimera produced a $CD4^{low}$ infectivity similar to either the parental T-tropic or M-tropic Env-pseudotyped virus). However, in some cases, the chimera produced an intermediate $CD4^{low}$ infectivity, which indicates that there are multiple genetic determinants interacting to affect $CD4^{low}$ infectivity and suggests that $CD4^{low}$ infectivity is a continuous rather than a bimodal phenotype.

Most surprising was that, for one *env* gene pair (5002), we generated a chimera *env* gene that induced greater $CD4^{low}$ infectivity than that of the parental M-tropic *env* gene (Figure 4.5a). Although it is possible that this is an artifact of creating an artificial recombinant, it is also possible that this super-M-tropic chimera reveals $CD4^{low}$ infectivity being checked either intentionally in defense of some other function or unintentionally, suggesting that macrophage tropism is not yet fully optimized in the parental M-tropic *env* gene. The smallest region able to confer maximum $CD4^{low}$ infectivity was also found in the 5002 pair: from just upstream of V4 through V5 (amino acids 367-471). $CD4^{low}$ infectivity affected by a smaller region may suggest that the parental T-tropic *env* gene is primed for low CD4 usage by mutations present in both the parental T-tropic and M-tropic *env* gene. Alternatively, a small effector region combined with the super-$CD4^{low}$ infectivity may support the hypothesis that there exists some reason to dampen $CD4^{low}$ infectivity in the blood (from which the T-tropic *env* gene was isolated) but not in the cerebrospinal fluid (from which the M-tropic *env* gene was isolated).

In contrast, subject 7115 revealed effectors of $CD4^{low}$ infectivity spanning all five variable regions (V1-V5) from position 123-471 (Figure 4.5b). If the 7115M V1-V5 region was

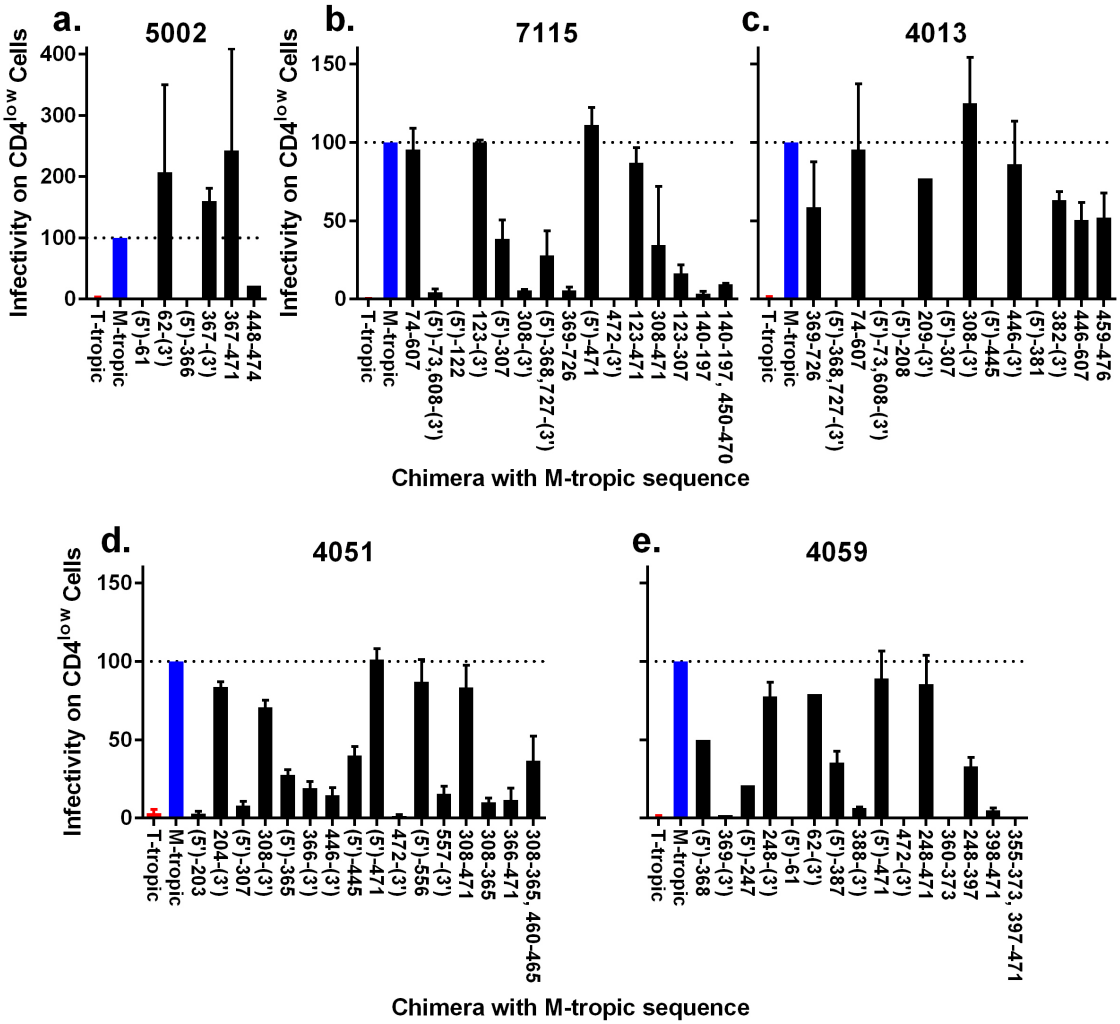

Figure 4.5: **CD4^{low} Affinofile assay of chimeric Env proteins** Viruses pseudotyped with chimeric *env* genes (black bars) were evaluated for the ability to use low levels of surface CD4 for entry in the CD4^{low} Affinofile assay compared with parental T-tropic (red bars) and parental M-tropic (blue bars) Env proteins. Each chimeric Env protein is identified by the M-tropic region (see figure 4.2). All values are normalized to the subject-matched parental M-tropic Env proteins. All chimeras were tested; bars not visible represent extremely poor relative CD4^{low} infectivity. Note: the plot of 5002 uses a different scale.

divided (e.g. within the V3), the two resulting fragments conferred a combined CD4^{low} infectivity of approximately 50% of the M-tropic parental *env* gene. Other chimeras that split the V1-V5 region in the C3 had similar effects, giving a combined CD4^{low} infectivity of only 34% compared to 90% in the chimera including the full 123-471 region. These reductions in CD4^{low} infectivity suggest a complex and interactive contribution of multiple genetic determinants to the CD4^{low} infectivity phenotype.

The remaining three subjects (4013, 4051, and 4059) required regions encompassing the V3 through V5 regions for maximum CD4^{low} infectivity (Figure 4.5c-e). Because 4013 M-tropic inserts at amino acid positions 74-607 and 308-(3) gave CD4^{low} infectivity values indistinguishable from the 4013 M-tropic parent, 308-607 is likely the full range of effectors. However, fully half of the CD4^{low} infectivity is contributed by a very relatively small range of amino acids at positions 459-476, which spans the V5 region. For subject 4051, we were able to create a chimera with M-tropic residues at positions 308-471 that was able to confer 80% of the CD4^{low} infectivity observed for the M-tropic parent. Like in 7115, however, splitting this region in either the C3 or the C4 resulted in combined CD4^{low} infectivity values of less than half of those from the 308-471 chimera. Based on the observation for 4013 in which half of the CD4^{low} infectivity could be traced to a small fraction of the whole effector region, we constructed a chimera with two M-tropic inserts at 308-365 and 460-465. The 308-365 + 460-465 combined chimera did increase the CD4^{low} infectivity, but only to 45%, indicating that we have not fully accounted for the interactions within the 308-471 region.

For subject 4059, we were also able to create a chimera able to confer nearly 80% of the infectivity observed for the M-tropic parent with a similar M-tropic region. When this region was split in the V4, the 248-397 region conferred 33% CD4^{low} infectivity and the 397-471 conferred only 5% CD4^{low} infectivity. Thus, 4059 is the only pair of the five studied in which the V5 region cannot independently contribute a substantial portion of the CD4^{low} infectivity. However, this does not rule out contributions, minor or substantial, from the V5, but it does rule out the ability to affect CD4^{low} infectivity independently. It is also possible that the

V5 mutations are not effectors at all and are actually compensatory for mutations elsewhere - perhaps mutations already incorporated but quiescent in the parental T-tropic clones from 4013, 4051, 5002, and 7115, but not 4059.

4.4.3 Site-directed mutagenesis maps specific residues involved in macrophage tropism

. Reducing the regions further resulted in chimeras with drastically reduced $CD4^{low}$ infectivity, making it difficult to detect real differences in $CD4^{low}$ infectivity among the small recombinants. Therefore, we used site-directed mutagenesis to change a single amino acid in the M-tropic *env* gene within the region identified by the previous chimeras to match the amino acid of the T-tropic *env* gene. This process resulted in approximately 24 M-tropic clones per subject (on average; range: 15 to 34) each with a single amino acid substitution. Substituting T-tropic amino acids into the M-tropic background is most likely to allow us to detect a loss in $CD4^{low}$ infectivity for positions involved in cellular tropism. These point substitutions are more likely to reveal genetic determinants, even if they are dependent upon other determinants, than would the reverse, which might be confounded if the substituted amino acid is involved in $CD4^{low}$ infectivity but is unable to effect a change in $CD4^{low}$ infectivity alone.

The singly mutated M-tropic clones were pseudotyped and assayed for $CD4^{low}$ infectivity (Figure 4.6). Because of variability in the $CD4^{low}$ assay that increases at higher $CD4^{low}$ infectivity values, we cannot distinguish a reduction by less than 10% from no reduction. These fairly insubstantial changes occurred in approximately two-thirds of all individual substitutions combined across all five pairs. The detection of several amino acid substitutions able to reduce $CD4^{low}$ infectivity 10% or more allowed us to focus on these more substantial and reproducible changes, which make up approximate one-third of all substitutions. Each of the five pairs tested had between one and five substitutions that reduced $CD4^{low}$ infectivity substantially, by more than 40%, representing only one-tenth of all individual substitutions.

4013, 4051, and 4059 all revealed genetic determinants in the both the V3 and V4 regions. 4013, 5002, and 7115 revealed genetic determinants near CD4 contact residues. 7115 is the

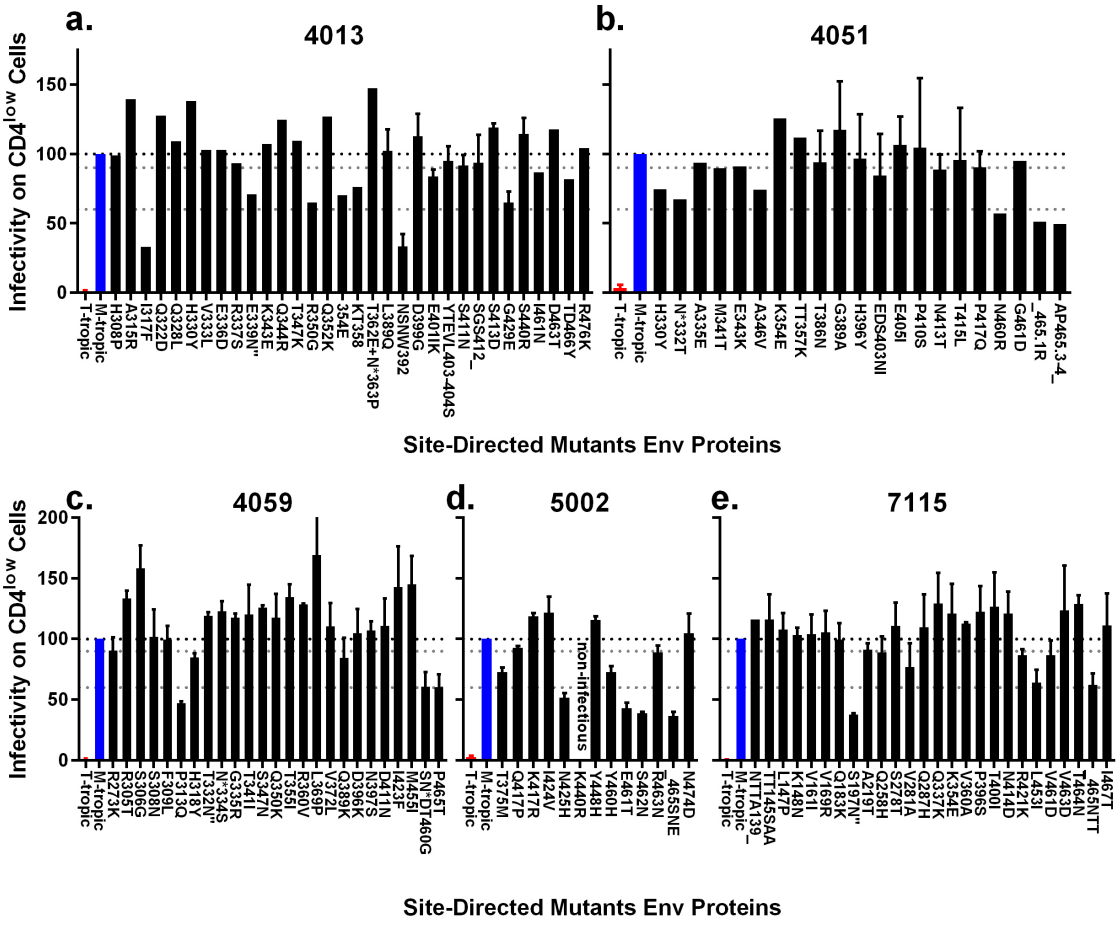

Figure 4.6: **CD4^{low} Affinofile assay of site-directed mutant M-tropic Env proteins** Viruses pseudotyped with M-tropic *env* genes mutated to encode an T-tropic amino acid substitution (black bars) were evaluated for the ability to use low levels of surface CD4 for entry in the CD4^{low} Affinofile assay compared with parental T-tropic (red bars) and parental M-tropic (blue bars) Env proteins. Each mutated Env protein is identified by the amino acid substitution. All values are normalized to the subject-matched parental M-tropic Env proteins. Note: 5002T K440R was non-infectious and so could not be evaluated for relative CD4^{low} infectivity.

only pair to reveal a determinant in the V1/V2 region, but a single mutation at that position had a substantial effect on $CD4^{low}$ infectivity. Notably, every subject-matched pair of *env* genes tested had between one and five amino acid substitutions within positions 460-465 that could modulate $CD4^{low}$ infectivity.

The substitutions in 4013M that had the greatest effect were I317F and a deletion of NSNW at position 392. Reverting the parental M-tropic Env protein to the amino acid compositions of the T-tropic Env protein at these positions resulted in a $CD4^{low}$ infectivity reduction of more than 50% each (Figure 4.6a). There were another eight substitutions that resulted in more modest reductions of $CD4^{low}$ infectivity between 10% and 40%. Four of these were in the C3 region and one was in the V4, but none of these were near the CD4 binding residues. However, a G429E substitution occurred at a CD4-interacting residue and reduced $CD4^{low}$ infectivity by 35%. The remaining two substitutions occurred in the V5 region. Mutations made in the chimera of 4013T with the M-tropic 459-476 region indicated a role for Y460R and L471I in $CD4^{low}$ infectivity (data not shown), bringing the total to four substitutions in the V5 that affect $CD4^{low}$ infectivity.

All of the substitutions in 4051 that were able to reduce $CD4^{low}$ infectivity by ¿40% were located in the V5 region (Figure 4.6b): N460R, an insertion 465.1R, and a deletion A465.3 and P465.4 (note: the fractions of positions indicate that these amino acids are positioned between numbered positions in HXB2, e.g. 465.1 is between positions 465 and 466). Deletions of A465.3 and P465.4 affect $CD4^{low}$ infectivity either individually (data not shown) or combined (Figure 4.6b at far right). Similar to 4013, substitutions with modest effects occurred in the C3 and V4 regions and were not proximal to CD4 binding residues.

The substitutions in 4059 resulting in the most substantial reductions in $CD4^{low}$ infectivity were in the V3 tip (P313Q) and in the V5 region (SN*DT460G and P465T, where * indicates a potential N-linked glycosylation site; PNGS). More modest effects resulted from substitutions H318Y (in the V3 region, near to P313Q) and Q389K (in the V4 region). This subject-matched pair of Env proteins revealed the fewest effectors of $CD4^{low}$ infectivity and so may provide the

simplest model of interaction between positions effecting CD4^{low} infectivity.

Generally, the substitutions have not significantly impacted the intrinsic infectivity of the mutant pseudotyped viruses. However, the K440R substitution in 5002 results in a virus with no detectable infectivity (Figure 4.6d). Lysine and arginine residues are fairly similar in their physical properties and are commonly substituted for one another to little effect; so it is curious that such a swap could render an Env protein completely non-functional. A N425H substitution, which is two amino acid positions away from a CD4-interacting residue, produces a substantial reduction in CD4^{low} infectivity. Another substitution T375M produces a more modest effect, but is also relatively close to CD4-interacting residues. The remaining substitutions with substantial effects are in the V5: E461T, S462N (no PNGS), and an insertion 465SNE. Two additional substitutions in the V5 with more modest effects on CD4^{low} sensitivity support involvement of the V5 region in CD4^{low} infectivity.

The 7115 pair appears to have relatively few substitutions that affect CD4^{low} infectivity. However, the effect of each substitution is minimized by the fact that the parental 7115 M-tropic Env protein achieves nearly twice CD4^{low} infectivity of the other parental M-tropic Env proteins. Thus, the 60% reduction in CD4^{low} infectivity caused by the S197N* mutation, which is located at the base of the V1/V2 structure, is even greater than it appears. A V281A in the D loop, which directly interacts with CD4, causes a more modest effect on CD4^{low} infectivity. Another substitution R421K is near CD4-interacting residues at 427 and 429, but has a fairly small effect on CD4^{low} infectivity. Three substitutions that modestly effect CD4^{low} infectivity are located C2 region and another three are in the V5 region. Thus, despite the wide region involved, a similar number of amino acids in 7115 appear to be involved in CD4^{low} infectivity (eight with a detectable effect) compared to other subject-matched Env proteins.

4.4.4 Site-directed mutagenesis to evaluate contributions of single substitutions

. For each substitution that resulted in either moderate or substantial reduction in $CD4^{low}$ infectivity, the reciprocal mutation was made in the T-tropic *env* gene (e.g. because 4013M I317F resulted in a 67% reduction, we generated a 4013T F317I mutant). This resulted in 5 to 17 (mean = 10) mutant *env* genes per T-tropic *env* gene. As before, these mutant *env* genes were pseudotyped and assayed for $CD4^{low}$ infectivity (Figure 4.7). However, most individual substitutions had only very small effect on $CD4^{low}$ infectivity, usually increasing the infectivity of the T-tropic Env-pseudotyped virus by less than 10%, relative to the parental M-tropic Env-pseudotyped virus.

For positions where a substitution had a large effect in reducing $CD4^{low}$ infectivity in an M-tropic virus but little or no effect in the paired T-tropic virus, we suspect that these positions are potentiating enhanced $CD4^{low}$ infectivity but cannot cause an effect alone. In one notable case, the H425N mutation in the 5002T background increased the $CD4^{low}$ infectivity to 23% of the parental M-tropic value. The parental 5002 T-tropic Env protein has a relatively rare amino acid at position 425 a histidine which is a positively charged residue that contains a relatively bulky aromatic ring. On the other hand, position 425 of the parental 5002 M-tropic Env protein is the typical asparagine, which is smaller, uncharged, and non-glycosylated. In this case, changing a rare variant to the typical variant caused enhancement in $CD4^{low}$ infectivity, which hints at the presence of contributing or potentiating substitutions that are shared by both the M-tropic and T-tropic Env proteins from 5002.

Based on the results generated from testing single mutations in both the T-tropic and M-tropic *env* genes, we selected substitutions that most substantially altered $CD4^{low}$ infectivity for each subject-matched pair of *env* genes (Figure 4.8). To better understand how individual substitutions interact, we used site-directed mutagenesis to create T-tropic *env* genes containing mutations for multiple amino acid substitutions, starting with the substitution that had the largest effect on $CD4^{low}$ infectivity and accumulating additional substitutions in a stepwise fashion. As a proof of principle experiment, we tested a 4013 T-tropic *env* gene mutated to

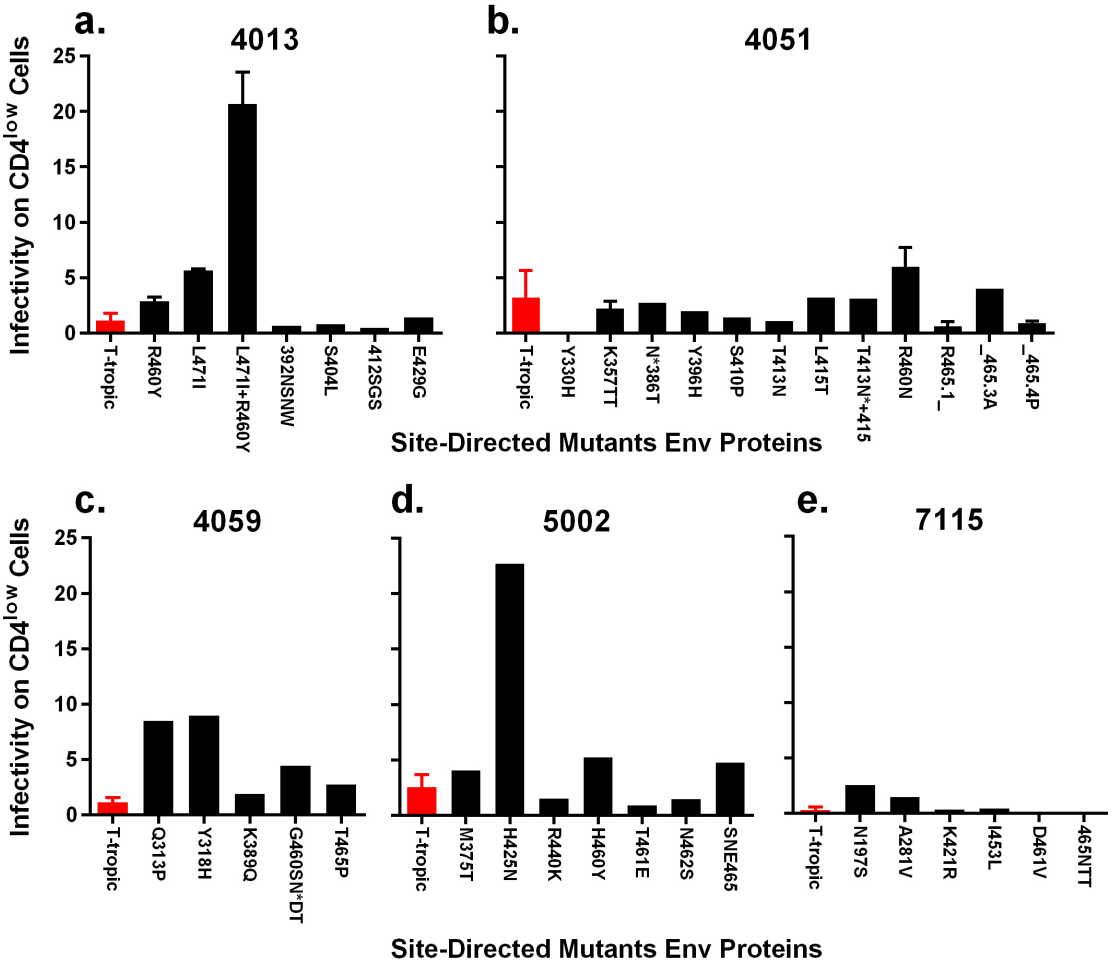

Figure 4.7: **CD4^{low} Affinofile assay of site-directed mutant T-tropic Env proteins** Viruses pseudotyped with T-tropic *env* genes mutated to encode an M-tropic amino acid substitution (black bars) were evaluated for the ability to use low levels of surface CD4 for entry in the CD4^{low} Affinofile assay compared with parental T-tropic (red bars) and parental M-tropic (blue bars) Env proteins. Each mutated Env protein is identified by the amino acid substitution. All values are normalized to the subject-matched parental M-tropic Env proteins.

encode two substitutions, R460Y and L471I, in the CD4^{low} Affinofile assay. Although individually, each substitution was only able to enhance CD4^{low} usage from 0% (i.e. parental T-tropic Env-pseudotyped virus) to 3% or 6% of that observed for the M-tropic Env-pseudotyped virus, the double mutant increased CD4^{low} infectivity to 21% of that observed for the M-tropic Env-pseudotyped virus. If each substitution was acting independently, the CD4^{low} infectivity would have been 9% (for additive effects) or less (for antagonist effects). Therefore, these two substitutions are likely acting synergistically.

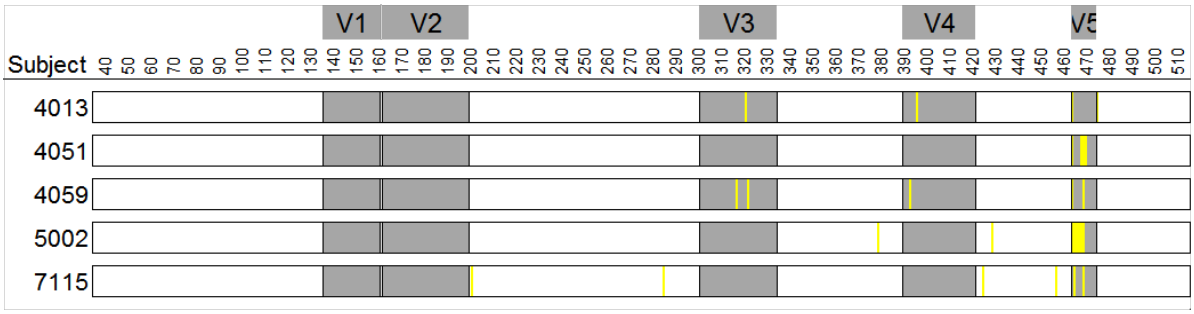

Figure 4.8: **Summary of amino acid substitutions that affect CD4^{low} infectivity** A map of the gp120 region of HIV-1 has been marked with HXB2 numbering and the five variable regions (V1-V5) have been marked in gray. The substitutions that affect CD4^{low} infectivity have been marked in yellow.

4.5 Discussion

The genetic determinants of macrophage tropism in HIV-1 have proven elusive despite genetic analyses of large cohorts of viral genomes and focused studies of a few subjects that combine genetic analysis with in vitro infection of MDMs. Identification of candidate mutations in silico has been stymied by the remarkably high variation in the HIV-1 env gene. High-throughput screening of cellular tropism in vitro has been curtailed by limited batch size and variation in MDMs. The creation of Affinofiles (154) and the development and validation of the CD4^{low} Affinofile assay (61, 99, 276) has enabled high-throughput screening of CD4 usage as a proxy for macrophage tropism with greater accuracy, higher reproducibility and increased capacity compared to MDM infection. By using the high-throughput capacity of the

$CD4^{low}$ Affinofile assay, we were able to screen each env gene comprehensively using molecular genetics methods, which was vital to capturing a majority of the genetic determinants of macrophage tropism that evolved in each subject.

Despite the lack of a single unifying amino acid substitution to form the foundation of macrophage tropism across all five subject-matched pairs, each pair had between one and five (mean = 3) substantial determinants in the amino acid positions 460-465, which perfectly describes the hypervariable region of V5. This region is also involved with binding to, and resistance against, VRC01 (1, 277, 278), which is a broadly-neutralizing antibody targeting the CD4 binding site (CD4bs), and ibalizumab, which is an antibody targeting CD4 (279). Together, these observations support interaction of the V5 region and the CD4bs in the folded protein, especially if the V5 region has been modified to be larger or more reactive with either CD4 or within the CD4 interaction site on the HIV-1 Env protein (Figure 4.9). Curiously, only three of the five pairs complemented the determinants in the V5 with major determinants directly proximal to major CD4 contacts, i.e. within 10 amino acid positions: 4013, 5002, and 7115.

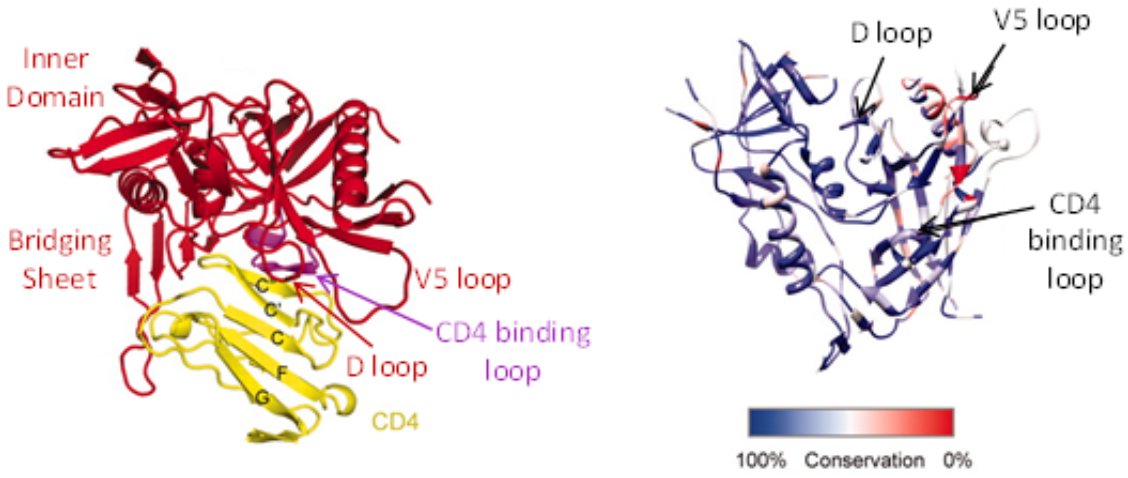

Figure 4.9: **The gp120 region of HIV-1 Env complexed with CD4 (1)** The V5 loop protrudes out over the CD4 binding site of the HIV-1 Env protein. Normally, the V5 does not directly interact with CD4, but can interact with and sometimes sterically restrict larger molecules such as antibodies. It is possible that a cluster of changes in the V5 could alter the V5 structure and bring it into closer proximity to the CD4-Env interaction.

Three pairs (4013, 4051, and 4059) complemented determinants in the V5 with determinants in the V3 and V4 regions. The V3 region has long been known to affect cellular tropism, containing the major determinants for evolving to target nave T cells (via the CXCR4 coreceptor) rather than memory T cells (via the more typical CCR5 coreceptor). For 4013, encoding a I317F substitution into the M-tropic env gene comes with the cost of an overall loss of infectivity, which may artificially enhance the loss of $CD4^{low}$ infectivity. However, there is no apparent decrease in infectivity for any other of the other substitutions in any of the pairs. The M-tropic and T-tropic env genes do not confer any detectable difference in coreceptor usage for any of the pairs tested (99), making it unclear how an amino acid substitution in the V3 might enhance CD4 usage, much less the G-P-G-R tip of V3 that interacts with the coreceptor. Nor are there any patterns in the types of substitutions (e.g. charge, size, etc.) made in different pairs. Although it is possible that the substitutions affected Env-CCR5 interactions in a way too subtle to be detected in coreceptor usage, it is more likely that mutations in the V3 and V4 are causing subtle changes in the structure of Env to enhance $CD4^{low}$ usage.

7115 is unusual in that macrophage tropism involves the V5, two CD4bs-proximal mutations (including one in the D-loop), and a mutation in the V1/V2 structure at position 197 (also identified by (271, 280). Making the S197N* substitution in the parental 7115 M-tropic env gene resulted in a substantial decrease in $CD4^{low}$ infectivity, losing 60% of the original efficiency. Changes in the V1/V2 region of Env have also been implicated in macrophage tropism as detected by antibody sensitivity (130, 276), though the mechanism is less obvious because the functions of V1/V2 that have been revealed to date include immune evasion and trimer stability. It seems likely that the full complement of V1/V2 functions has not yet been revealed. Because the 7115 M-tropic env gene can induce an absolute $CD4^{low}$ infectivity value nearly two-fold greater than all of the other M-tropic env genes in this study, it is tempting to view the 7115 M-tropic virus as further evolved toward some optimal macrophage tropism than the other M-tropic viruses assayed. However, without knowing the end point or perfectly optimized state of macrophage tropism, or whether that optimum can be reached by two dif-

ferent viral populations from two different subjects, it is difficult to compare the evolution of M-tropic env genes from different subjects.

The analysis also turned up patterns in $CD4^{low}$ infectivity resulting from single substitutions. For three of five M-tropic env genes, the reduction in $CD4^{low}$ infectivity seemed to cluster into distinct groups. For example, in the 4013 M-tropic env gene, there were four substitutions that reduced the $CD4^{low}$ infectivity by more than 65% and eight substitutions that reduced the $CD4^{low}$ infectivity by 10%-35%, but no substitutions that resulted in a reduction in the 35%-65% range. Although the relatively small number of mutations for each pair could potentially create or exaggerate this separation, it also may indicate that there are major and minor genetic determinants of macrophage tropism; i.e. that some are the primary foundation for enhanced $CD4^{low}$ infectivity and the others are supplemental. However, this model is unable to differentiate whether these minor mutations further optimize macrophage tropism or whether they are compensatory and mitigate detrimental effects caused by the primary determinants.

When making substitutions in the T-tropic background, only one substitution encoded in one subject-matched pair of env genes had a substantial effect on $CD4^{low}$ infectivity (¿ 10% relative to the parental M-tropic value). A H425N substitution encoded into the 5002 T-tropic env gene resulted in 23% $CD4^{low}$ infectivity (normalized to parental 5002 M-tropic values). The relatively bulky, aromatic ring-containing histidine encoded in the parental T-tropic env gene may have been blocking $CD4^{low}$ infectivity-enhancing substitutions that had already accumulated elsewhere in the T-tropic Env protein. Replacing the histidine with the smaller, uncharged, and unglycosylated asparagine, which is the typical amino acid at position 425, may have unblocked access to the CD4bs, allowing other mutations to enhance $CD4^{low}$ infectivity. However, this theory suggests that even the 5002 T-tropic Env had started to evolve toward macrophage tropism, but had acquired a block to that progress with unclear benefits (if any). We hypothesize that if the other mutations increased exposure of the CD4bs for enhanced $CD4^{low}$ infectivity, it is possible that the histidine was selected for to prevent against

immune access to the CD4bs and neutralization of the virus.

The evolution of M-tropic viruses to efficiently infect macrophages does not impair their ability to infect $CD4^+$ T cells. Without any apparent consequence to fitness, it is unclear why adaptations to use CD4 more efficiently are not more common. It has been hypothesized that enhanced CD4 usage was achieved through exposure of neutralization-sensitive epitopes on the HIV-1 Env protein, and so could only evolve in immunoprivileged compartments like the CNS. However, M-tropic Env proteins are not more sensitive to neutralization by polyclonal antibodies in homologous serum than T-tropic Env proteins (276). It is still possible that there are specific neutralizing epitopes that become more accessible to antibody recognition during evolution to macrophage tropism, particularly in the CD4bs. Changes in the CD4bs are supported by increased CD4 usage and increased sensitivity to sCD4 in M-tropic compared to T-tropic Env proteins. Other studies have shown potential for increased exposure of the CD4bs, which may make it more sensitivity to neutralization by CD4bs-targeting antibodies - and not other antibodies but the results have been mixed (130, 187, 207, 276).

It will be difficult to truly understand all of the mutations involved in the evolution of macrophage tropism without longitudinal sampling of HIV-1 env genes in the rare number of subjects who develop M-tropic viral populations. Furthermore, sampling must begin before the future-M-tropic population diverges from the rest of the T-tropic populations. The difficulty of obtaining such samples makes that method all but impossible. However, by mapping the major genetic determinants in existing subject samples through a combination of genetic and functional characterizations, it is possible to infer the major steps along the evolutionary pathway to macrophage tropism and may eventually enable genetic screening for M-tropic virus.

CHAPTER 5

DISCUSSION

5.1 Summary, Synthesis, and Future Directions

Macrophage tropism in HIV-1 has been refractory to detailed characterization for several reasons. First, M-tropic viruses are detected only rarely in HIV-1 infection. M-tropic viruses are most frequently observed in the central nervous system, which cannot be accessed in living subjects and is inferred using CSF. Second, the high natural genetic variation in HIV-1, compounded by the small number of examples of M-tropic virus, has prevented identification of the genetic determinants of macrophage tropism. Without an identifying genetic signature, screening for these variants is arduous and requires HIV-1 *env* genes to be isolated, cloned, expressed, and assessed phenotypically. Third, the phenotypic test (MDM infectivity), which until recently was widely used, was highly variable and allowed uncertainty in identification and was not sensitive enough to reliably identify intermediate phenotypes between that of T cell tropism and macrophage tropism. These factors have stymied attempts to clarify the genetic and phenotypic characteristics of macrophage tropism in HIV-1.

To compile a panel of viruses with indisputable cellular tropism classification, we used subject-matched pairs of T-tropic and M-tropic (or intermediate) viruses that were rigorously defined using several *in vitro* assays and relevant clinical measures. The generation of the Affinofile cell line with independently regulatable CD4 and CCR5 expression has enabled development of new methods for screening and evaluating cellular tropism. Measuring infectivity over a range of CD4 densities provides a sensitive measure of CD4 usage. Alternatively,

measuring infectivity at only the lowest density of CD4 ($CD4^{low}$ infectivity) provides an accurate detection of cellular tropism that can be using for high-throughput screening. We used $CD4^{low}$ infectivity screening to identify primary isolates with intermediate cellular tropism and to identify the determinants of macrophage tropism. We then used CD4 titration to provide detailed CD4 usage characteristics of T-tropic, M-tropic, and intermediate HIV-1 Env proteins.

We began by assessing different cell types potentially targeted by HIV-1 with different cellular tropism. We measured CD4 densities on Affinofile cells and on human memory T cells, monocytes, and monocyte-derived macrophages (MDMs) *ex vivo* using flow cytometry. Differences in CD4 usage between M-tropic and T-tropic Env proteins were correlated with the differences in CD4 receptor densities (but not CCR5 coreceptor densities) on the targeted cell type. Screening large numbers of subjects for cellular tropism variants using $CD4^{low}$ infectivity enabled identification of primary isolates with intermediate CD4 usage. Detailed analysis of CD4 usage through CD4 titration revealed that M-tropic Env proteins display increased cooperativity in interactions with CD4, though whether fewer CD4 molecules are required to activate each spike or activation of fewer spikes is required for fusion remain entangled. Infection of MDMs with a panel of primary isolates that displayed a wide range of CD4 usage phenotypes revealed that CD4 usage is strongly predictive of MDM infectivity not just categorically but linearly over a continuous range, challenging the model that cellular tropism is bimodal or categorical.

Physical changes in the CD4 binding site (CD4bs) of M-tropic Env proteins have been revealed through probing reagents targeting the CD4bs. Probing the CD4 binding site using several CD4bs antibodies, which are relatively bulky and normally sterically restricted in T-tropic Env proteins, revealed a trend toward increased access as measured by neutralization of M-tropic Env proteins. However, larger panels of viruses will need to be tested to assess whether any differences in sensitivity to CD4bs antibodies are significant, statistically and phyisologically. In contrast, a small molecule inhibitor (too small to be sterically restricted)

showed no difference in sensitivity to inhibition. A more ideal binding partner, sCD4, was vastly more inhibitory for M-tropic compared to subject-matched T-tropic Env proteins. Together, these data suggest that the M-tropic Env proteins may have reduced the steric restriction of the normally narrow pocket of the CD4bs in order to enhance interactions when CD4 when densities are low.

Surface plasmon resonance can make precise measurements of binding interactions between HIV-1 Env proteins and CD4, but has been problematic due to the difficulty in making soluble versions of the external portion of Env trimers while maintaining the functionality of the full protein structure. However, a new strategy has been recently developed to create soluble Env trimers that function more naturally (263, 281-283). It may be possible to use that strategy to develop soluble versions of our M-tropic and T-tropic clones that can be used in protein binding experiments. Alternatively, it may be possible to develop an ELISA protocol using pseudotyped viruses and purified anti-gp140 IgG conjugated to a reporter molecule. The ELISA has less accuracy than surface plasmon resonance, but may be possible with reagents already in existence. Regardless, in order to truly understand how M-tropic viruses are interacting differently with CD4, the relative binding properties of CD4 and M-tropic or T-tropic Env proteins will have to be more directly examined.

Adaptation to use the lower CD4 levels found on macrophages resulted in M-tropic Env proteins with changes in their interactions with CD4 both quantitatively and qualitatively. However, few M-tropic Env proteins appear to rely on evolving changes in or near sites of direct CD4 interaction, including contact residues clustered on either end of the V4 region and the D loop, which is just upstream of V3. Three of the five M-tropic primary isolates tested (4013, 5002, and 7115) were dependent upon peri-CD4bs substitutions that resulted in residues either smaller, in the cases of 4013 and 5002 or similar in size and charge to the original in 7115. This supports the model of reduced steric restriction in 4013 and 4051, but cannot explain the changes in 7115. Encoding substitution of the M-tropic amino acid into the T-tropic Env protein at position 425 was able to individually confer a significant increase

in CD4^{low} infectivity (23% of the parental M-tropic Env). However, none of the other four peri-CD4bs substitutions identified in 4013, 5002, or 7115 had a substantial effect on CD4^{low} infectivity individually and other substitutions produced larger effects in 4013 and 7115.

Due to the late stage of disease and the presence of an environment where M-tropic viral populations can and have emerged, it is possible that the T-tropic clones are not purely T-tropic in that their phenotype is T-tropic, but they have preparatory or permissive mutations that enable evolution of macrophage tropism. If so, these permissive mutations would be veiled by their presence is both the T-tropic and M-tropic *env* genes, but may be detected by comparing each pair of *env* genes in this study with a large cohort of *env* genes from subjects with only T-tropic viral populations. The variation patterns may be too complicated to extract additional compensatory mutations in this way, but we cannot ignore the fact that we have, necessarily, used T-tropic viruses from subjects in whom M-tropic viruses have evolved and the implications for variation in T-tropic viruses.

The V5 region was most consistently involved in CD4 usage with all five M-tropic *env* genes containing determinants in that region. Of the 31 substitutions affecting CD4^{low} infectivity across all five pairs of primary isolates tested, fifteen were located in the V5 and one was located just upstream of the V5, representing almost half of the total genetic determinants in this panel of subject-matched primary isolates. The V5 is by far the smallest of the five variable loops in the gp120 protein structure with a hypervariable region (positions 460-465) that is typically between four and ten (occasionally more) amino acids in length. The V5 is also unusual in that it is defined on each end by clusters of glycine residues rather than by disulfide-linked cysteine residues. The V5 region itself is not directly adjacent to the CD4bs, though the C5 region downstream of V5 and upstream of the gp41 interacting domain does approach the CD4bs. Unlike the substitutions in the CD4bs, V5 substitutions that enhanced CD4^{low} infectivity were larger and more hydrophobic than the original amino acid. The increased size may reach into the CD4 interaction area to produce an additional interaction with CD4 or to pull on the downstream C5 region to change potential CD4 interactions there. Al-

ternatively, changes in V5 could affect the conformational changes in the Env protein as a result of binding CD4. Even without a precise genetic signature, the consistent trend of V5 substitutions for larger and more hydrophobic amino acids can be calculated and used as a first pass to sift through *env* sequences in search of those potentially displaying macrophage tropism.

Additional genetic determinants of macrophage were identified in the V3 region, though at lower frequency (three of five pairs). The substitutions in V3 do not have any detectable effect on coreceptor usage (99) or changes in sensitivity to antibodies targeting V3 and CD4-induced epitopes (276). The positions of the substitutions are similar in two of the three pairs (4013 and 4059), but none of the substitutions result in similar changes in amino acid properties. Therefore, it seems more likely that V3 substitutions are compensatory for changes made elsewhere. Curiously, all three pairs that employ V3 substitutions also each employ a V4 substitution, though neither of the other two pairs have changes in either V3 or V4, suggesting the possibility that the V3 and V4 substitutions are working together. Experiments are currently underway to evaluate the interactions between individual substitutions by making different combinations of mutation for each pair.

Even more surprising is the involvement of the V1/V2 region in macrophage tropism. Probing with antibodies targeting the V1/V2 region showed consistent patterns of resistance in M-tropic viruses that could not be explained by known resistance mutations and which was supported by a larger study of unmatched T-tropic and M-tropic viruses (130). Furthermore, the intermediate viruses appeared to have intermediate resistance to V1/V2 antibodies, though this observation did not reach significance. Only one pair (7115) contained genetic determinants of cellular tropism in the V1/V2 structure, which has only recently been solved (133, 282). However, a single S197N* reversion substitution in the M-tropic clone to match the T-tropic and consensus amino acid at this position reduced $CD4^{low}$ usage over 60%. Interestingly, the N*197S in the T-tropic clone had little effect, suggesting that the V1/V2 substitution is interacting with one of the other determinants. The additional planned experiments will

evaluate the interaction between position 197 and other determinants of macrophage tropism in 7115, which are spread throughout the D loop, CD4bs, C4 and V5 regions. It is also important to note that when we initially narrowed down the regions that are most important for determining cellular tropism, the smaller regions did not encompass the full $CD4^{low}$ infectivity of the parental M-tropic clone, often losing 10-20% of the original $CD4^{low}$ infectivity. So although we have identified the major genetic determinants, the evolution of macrophage tropism is far more complex and involves mutations throughout the *env* gene to subtly enhance or compensate the major determinants.

The evolution of macrophage tropism in HIV-1 is complex, requiring the cooperation of a constellation of mutations throughout the *env* gene and resulting in Env proteins with a subtly altered conformation that enables using low levels of CD4 more efficiently. We have developed a panel of viruses that have been and will continue to be instrumental in examining host range variation in HIV-1 by focusing on entry and the HIV-1 *env* gene. We have also developed an assay to identify cellular tropism with sensitivity and reproducibility that could be easily standardized across labs and avoids the variation in the current assay based on MDM infection. By combining these resources we have been able to identify phenotypic correlates and genetic determinants of macrophage tropism and clarify conflicting observations that were likely due to inconsistencies in identifying macrophage tropism in primary isolates and in using tissue culture adapted lab strains to represent M-tropic viruses. We have started to unravel how M-tropic variants have altered usage of the CD4 receptor to infect a new target cell with less optimal CD4 expression and exonerated other stages of entry that are not associated with macrophage tropism despite their capacity for variation. Although the precise genetic determinants of macrophage tropism have not yet been identified, there is a trend of substitutions of larger and more hydrophobic residues in the V5 region, which may provide a rough guide for genetic screening for cellular tropism. Clues about less scrutable V1/V2 region have been uncovered and hint at potential interactions with the CD4bs. Finally, discovery of viruses with intermediate phenotypes between those of M-tropic viruses and the

canonical T-tropic viruses are starting to provide clues about how macrophage tropism might evolve. Collectively, this work has provided new information about macrophage tropism and several new tools for exploring evolution and host range variation in HIV-1.

CHAPTER 6

APPENDICES

6.1 Appendix A: Protocol for Overlap/Extension PCR of Homologous Sequences

In this modified O/E PCR, we are recombining homologous plasmids, allowing us to skip the steps for creating the insertion fragment (the insertion in the middle, flanked by target vector sequences). Instead, we will simply choose primers that will amplify regions on either side of the insertion sequence that are conserved between the inserted template and the target template.

Choosing primers:

- 30 40 conserved bases are needed on either end of the substitution/insertion sequence.
- The forward primer should match the first 20 bp of the 5 conserved sequence.
- The reverse primer should match the reverse-complement of the last 20-25 bps of the 3 conserved sequence.
- The 3 end of each primer should have at least 1 G or C residue and preferably 2 G/C residues.

Generation of the insertion construct:

1. Use primers to amplify the insertion fragment from the template to be inserted.
   (a) Any high-fidelity DNA polymerase is sufficient at this step (e.g. pfuTURBO).

(b) Use the recommended protocol, but increase to 50 100 replication cycles (spiking the reaction with additional polymerase may be needed, especially for longer fragments or more cycles).

2. Gel purify amplified insertion fragment.

   (a) Load entire PCR product + loading dye into a single well of a 1% agarose gel.

   (b) Electrophorese at 125 V until the bromophenol blue dye.

   (c) Purify with Qiagen MinELute Gel Extraction Kit.

3. Quantify DNA and calculate molarity.

   (a) Use the nanodrop to quantify DNA.

   (b) Use an online calculator to estimate the MW of the insertion fragment.

   (c) Use those two measurements to calculate the molarity of the insertion fragment.

4. Use the insertion fragment to prime PCR for insertion.

   (a) Use Phusion polymerase (it is 10x more processive than pfu polymerases).

   (b) Use the reagents in Table 6.1 (added in the order listed) for a 10-μL reaction (but larger reactions may be used if there is sufficient amounts of insertion fragment.

   (c) Use the cycling conditions in Table 6.2

5. Transform directly from insertion PCR product, because the reaction is not efficient enough to for the product to be detected by UV in an ethidium bromide gel.

6. Culture transformed bacteria, harvest cells, and extract plasmid DNA using a Qiagen miniprep kit.

7. Evaluate successful insertion by digest mapping (if possible), then by sequencing.

Table 6.1: Reagents for Overlap/Extension PCR

Reagent	1 x Volume μL
Water	(remaining volume)
5 x HF buffer	2.0
DMSO	0.3
10 mM dNTP	0.2
template DNA	(3 ng or 30 ng)
insertion fragment	(250 x molarity of template)
Phusion polymerase	0.2
Total reaction	10.0

Table 6.2: Cycling Conditions for Overlap/Extension PCR

Time (mm:ss)	Temp (°C)	Repetition
2:00	100	1x
0:30	94	50x
0:30	60	
15:00	68	
15:00	68	1x
∞	4	1x

6.2 Appendix B: Protocol for Site-Directed Mutagenesis (SDM) PCR

We have adapted the Pfu Turbo (Agilent) PCR protocol and optimized for both site-directed mutagenesis and for using HIV-1 *env* as a template.

Designing Primers

- For the region of each primer overlapping the site to be altered (target site), use the desired final sequence including any additions, deletions, and/or substitutions.
- 11-15 nucleotides (NTs) matching the template are required upstream of the target site, such that the two 5-most NTs are A/T residues.
- 25-35 NTs matching the template are required downstream of the target site from the template sequence, such that the two 3-most NTs are G/C residues.

Thus, the final primers should overlap approximately 20 base pairs and should have at least a 20 base pair 3 overhang on each end, i.e.:

- Forward: 5 - A/T - A/T - $X_{9\text{-}13}$ - (desired mutation) - $X_{23\text{-}33}$ - G/C - G/C - 3
- Reverse: 3- G/C - G/C - $X_{23\text{-}33}$ - (desired mutation) - $X_{9\text{-}13}$ - A/T - A/T - 5

Site-Directed Mutagensis PCR

1. Set up the PCR reaction on ice immediately prior to cycling.
   (a) Use Pfu Turbo (Agilent) polymerase.
   (b) Use the reagents in Table 6.4 (added in the order listed) for a 50-µL reaction:
   (c) Use the following cycling conditions:
2. Perform a digestion with DpnI (NEB; as per manufacturers protocol) to cleave the template.

Table 6.3: Reagents for Site-Directed Mutagenesis PCR

Reagent	1 x Volume (μL)
Water	(remaining volume)
10 x Turbo buffer	5.0
DMSO	4.0
10 mM dNTP	1.5
template DNA	(10 ng or 100 ng)
forward primer	1.5
reverse primer	1.5
Pfu Turbo polymerase	1.5
Total reaction	50.0

Table 6.4: Cycling Conditions for Site-Directed Mutagenesis PCR

Time (mm:ss)	Temp (°C)	Repetition
5:00	95	1x
0:30	95	
0:30	55	50x
10:00	68	
10:00	68	1x
∞	4	1x

3. Evaluate the PCR-digestion product by gel electrophoresis by migration and band intensity.

4. Transform successful PCR-digestion product into competent MAX Efficiency Stbl2 Competent Cells (Thermofisher; as per manufacturers protocol).

5. Culture transformed bacteria, harvest cells, and extract plasmid DNA using a Qiagen miniprep kit.

6. Evaluate successful insertion by digest mapping (if possible), then by sequencing.

REFERENCES

1. Zhou, T., I. Georgiev, X. Wu, Z.-Y. Yang, K. Dai, A. Finzi, Y. D. Kwon, J. F. Scheid, W. Shi, L. Xu, Y. Yang, J. Zhu, M. C. Nussenzweig, J. Sodroski, L. Shapiro, G. J. Nabel, J. R. Mascola, and P. D. Kwong. 2010. Structural basis for broad and potent neutralization of hiv-1 by antibody vrc01. Science 329:811-817.

2. Gao, F., E. Bailes, D. L. Robertson, Y. Chen, C. M. Rodenburg, S. F. Michael, L. B. Cummins, L. O. Arthur, M. Peeters, G. M. Shaw, P. M. Sharp, and B. H. Hahn. 1999. Origin of hiv-1 in the chimpanzee pan troglodytes troglodytes. Nature 397:436-441.

3. Salemi, M., K. Strimmer, W. W. Hall, M. Duffy, E. Delaporte, S. Mboup, M. Peeters, and A. M. Vandamme. 2001. Dating the common ancestor of sivcpz and hiv-1 group m and the origin of hiv-1 subtypes using a new method to uncover clock-like molecular evolution. FASEB journal: official publication of the Federation of American Societies for Experimental Biology 15:276-278.

4. Keele, B. F., F. V. Heuverswyn, Y. Li, E. Bailes, J. Takehisa, M. L. Santiago, F. Bibollet-Ruche, Y. Chen, L. V. Wain, F. Liegeois, S. Loul, E. M. Ngole, Y. Bienvenue, E. Delaporte, J. F. Y. Brookfield, P. M. Sharp, G. M. Shaw, M. Peeters, and B. H. Hahn. 2006. Chimpanzee reservoirs of pandemic and nonpandemic hiv-1. Science 313:523-526.

5. Robertson, D. L., J. P. Anderson, J. A. Bradac, J. K. Carr, B. Foley, R. K. Funkhouser, F. Gao, B. H. Hahn, M. L. Kalish, C. Kuiken, G. H. Learn, T. Leitner, F. McCutchan, S. Osmanov, M. Peeters, D. Pieniazek, M. Salminen, P. M. Sharp, S. Wolinsky, and B. Korber. 2000. Hiv-1 nomenclature proposal. Science 288:55-55.

6. Van Heuverswyn, F., and M. Peeters. 2007. The origins of hiv and implications for the global epidemic. Current Infectious Disease Reports 9:338-346.

7. Plantier, J.-C., M. Leoz, J. E. Dickerson, F. De Oliveira, F. Cordonnier, V. Leme, F. Damond, D. L. Robertson, and F. Simon. 2009. A new human immunodeficiency virus derived from gorillas. Nature Medicine 15:871-872.

8. Vallari, A., V. Holzmayer, B. Harris, J. Yamaguchi, C. Ngansop, F. Makamche, D. Mbanya, L. Kaptu, N. Ndembi, L. Grtler, S. Devare, and C. A. Brennan. 2011. Confirmation of putative hiv-1 group p in cameroon. J. Virol. 85:1403-1407.

9. D'arc, M., A. Ayouba, A. Esteban, G. H. Learn, V. Bou, F. Liegeois, L. Etienne, N. Tagg, F. H. Leendertz, C. Boesch, N. F. Madinda, M. M. Robbins, M. Gray, A. Cournil, M. Ooms, M. Letko, V. A. Simon, P. M. Sharp, B. H. Hahn, E. Delaporte, E. Mpoudi Ngole, and M. Peeters. 2015. Origin of the hiv-1 group o epidemic in western lowland gorillas. Proceedings of the National Academy of Sciences of the United States of America.

10. Wilen, C. B., J. C. Tilton, and R. W. Doms. 2012. Hiv: Cell binding and entry. Cold Spring Harbor Perspectives in Medicine 2:a006866.

11. 2013. Fields virology, 6th ed ed. Wolters Kluwer Health/Lippincott Williams & Wilkins, Philadelphia.

12. Sleasman, J. W., L. F. Aleixo, A. Morton, S. Skoda-Smith, and M. M. Goodenow. 1996. $CD4^+$ memory t cells are the predominant population of hiv-1-infected lymphocytes in neonates and children. AIDS 10:1477-1484.

13. Douek, D. C., J. M. Brenchley, M. R. Betts, D. R. Ambrozak, B. J. Hill, Y. Okamoto, J. P. Casazza, J. Kuruppu, K. Kunstman, S. Wolinsky, Z. Grossman, M. Dybul, A. Oxenius, D. A. Price, M. Connors, and R. A. Koup. 2002. Hiv preferentially infects hiv-specific $CD4^+$ t cells. Nature 417:95-98.

14. Brenchley, J. M., B. J. Hill, D. R. Ambrozak, D. A. Price, F. J. Guenaga, J. P. Casazza, J. Kuruppu, J. Yazdani, S. A. Migueles, M. Connors, M. Roederer, D. C. Douek, and R. A. Koup. 2004. T-cell subsets that harbor human immunodeficiency virus (hiv) in vivo: Implications for hiv pathogenesis. J. Virol. 78:1160-1168.

15. Peters, P. J., W. M. Sullivan, M. J. Duenas-Decamp, J. Bhattacharya, C. Ankghuambom, R. Brown, K. Luzuriaga, J. Bell, P. Simmonds, J. Ball, and P. R. Clapham. 2006. Non-macrophage-tropic human immunodeficiency virus type 1 r5 envelopes predominate in blood, lymph nodes, and semen: Implications for transmission and pathogenesis. J. Virol. 80:6324-6332.

16. Isaacman-Beck, J., E. A. Hermann, Y. Yi, S. J. Ratcliffe, J. Mulenga, S. Allen, E. Hunter, C. A. Derdeyn, and R. G. Collman. 2009. Heterosexual transmission of human immunodeficiency virus type 1 subtype c: Macrophage tropism, alternative coreceptor use, and the molecular anatomy of ccr5 utilization. J. Virol. 83:8208-8220.

17. Salazar-Gonzalez, J. F., M. G. Salazar, B. F. Keele, G. H. Learn, E. E. Giorgi, H. Li, J. M. Decker, S. Wang, J. Baalwa, M. H. Kraus, N. F. Parrish, K. S. Shaw, M. B. Guffey, K. J. Bar, K. L. Davis, C. Ochsenbauer-Jambor, J. C. Kappes, M. S. Saag, M. S. Cohen, J. Mulenga, C. A. Derdeyn, S. Allen, E. Hunter, M. Markowitz, P. Hraber, A. S. Perelson, T. Bhattacharya, B. F. Haynes, B. T. Korber, B. H. Hahn, and G. M. Shaw. 2009. Genetic identity, biological phenotype, and evolutionary pathways of transmitted/founder viruses in acute and early hiv-1 infection. The Journal of Experimental Medicine 206:1273-1289.

18. Alexander, M., R. Lynch, J. Mulenga, S. Allen, C. A. Derdeyn, and E. Hunter. 2010. Donor and recipient envs from heterosexual human immunodeficiency virus subtype c transmission pairs require high receptor levels for entry. J. Virol. 84:4100-4104.

19. Wilen, C. B., N. F. Parrish, J. M. Pfaff, J. M. Decker, E. A. Henning, H. Haim, J. E. Petersen, J. A. Wojcechowskyj, J. Sodroski, B. F. Haynes, D. C. Montefiori, J. C. Tilton, G. M. Shaw, B. H. Hahn, and R. W. Doms. 2011. Phenotypic and immunologic

comparison of clade b transmitted/founder and chronic hiv-1 envelope glycoproteins. J. Virol. 85:8514-8527.

20. Ping, L.-H., S. B. Joseph, J. A. Anderson, M.-R. Abrahams, J. F. Salazar-Gonzalez, L. P. Kincer, F. K. Treurnicht, L. Arney, S. Ojeda, M. Zhang, J. Keys, E. L. Potter, H. Chu, P. Moore, M. G. Salazar, S. Iyer, C. Jabara, J. Kirchherr, C. Mapanje, N. Ngandu, C. Seoighe, I. Hoffman, F. Gao, Y. Tang, C. Labranche, B. Lee, A. Saville, M. Vermeulen, S. Fiscus, L. Morris, S. A. Karim, B. F. Haynes, G. M. Shaw, B. T. Korber, B. H. Hahn, M. S. Cohen, D. Montefiori, C. Williamson, R. Swanstrom, and C. A. I. S. a. t. C. f. H.-A. V. I. Consortium. 2013. Comparison of viral env proteins from acute and chronic infections with subtype c human immunodeficiency virus type 1 identifies differences in glycosylation and ccr5 utilization and suggests a new strategy for immunogen design. J. Virol. 87:7218-7233.

21. Antinori, A., G. Arendt, J. T. Becker, B. J. Brew, D. A. Byrd, M. Cherner, D. B. Clifford, P. Cinque, L. G. Epstein, K. Goodkin, M. Gisslen, I. Grant, R. K. Heaton, J. Joseph, K. Marder, C. M. Marra, J. C. McArthur, M. Nunn, R. W. Price, L. Pulliam, K. R. Robertson, N. Sacktor, V. Valcour, and V. E. Wojna. 2007. Updated research nosology for hiv-associated neurocognitive disorders. Neurology 69:1789-1799.

22. Robertson, K. R., M. Smurzynski, T. D. Parsons, K. Wu, R. J. Bosch, J. Wu, J. C. McArthur, A. C. Collier, S. R. Evans, and R. J. Ellis. 2007. The prevalence and incidence of neurocognitive impairment in the haart era. AIDS (London, England) 21:1915-1921.

23. Letendre, S. L., R. J. Ellis, I. Everall, B. Ances, A. Bharti, and J. A. McCutchan. 2009. Neurologic complications of hiv disease and their treatment. Topics in HIV medicine: a publication of the International AIDS Society, USA 17:46-56.

24. Vivithanaporn, P., G. Heo, J. Gamble, H. B. Krentz, A. Hoke, M. J. Gill, and C. Power. 2010. Neurologic disease burden in treated hiv/AIDS predicts survival: A population-based study. Neurology 75:1150-1158.

25. Kim, W.-K., S. Corey, X. Alvarez, and K. Williams. 2003. Monocyte/macrophage traffic in hiv and siv encephalitis. Journal of Leukocyte Biology 74:650-656.

26. Williams, K. C., and W. F. Hickey. 2002. Central nervous system damage, monocytes and macrophages, and neurological disorders in AIDS. Annu. Rev. Neurosci. 25:537-562.

27. Ritola, K., K. Robertson, S. A. Fiscus, C. Hall, and R. Swanstrom. 2005. Increased human immunodeficiency virus type 1 (hiv-1) env compartmentalization in the presence of hiv-1-associated dementia. J. Virol. 79:10830-10834.

28. Carvalhal, A. S., S. B. Rourke, P. Belmonte-Abreu, J. Correa, and L. Z. Goldani. 2006. Evaluation of neuropsychological performance of hiv-infected patients with minor motor cognitive dysfunction treated with highly active antiretroviral therapy. Infection 34:357-360.

29. Sturdevant, C. B., A. Dow, C. B. Jabara, S. B. Joseph, G. Schnell, N. Takamune, M. Mallewa, R. S. Heyderman, A. Van Rie, and R. Swanstrom. 2012. Central nervous system compartmentalization of hiv-1 subtype c variants early and late in infection in young children. PLoS pathogens 8:e1003094.

30. Sturdevant, C. B., S. B. Joseph, G. Schnell, R. W. Price, R. Swanstrom, and S. Spudich. 2015. Compartmentalized replication of r5 t cell-tropic hiv-1 in the central nervous system early in the course of infection. PLoS Pathog 11:e1004720.

31. Gisolf, E. H., S. Jurriaans, J. Pelgrom, F. van Wanzeele, M. E. van der Ende, K. Brinkman, M. J. Borst, F. de Wolf, A. J. Japour, and S. A. Danner. 2000. The effect of treatment intensification in hiv-infection: A study comparing treatment with ritonavir/saquinavir and ritonavir/saquinavir/stavudine. Prometheus study group. AIDS (London, England) 14:405-413.

32. Gonzlez-Scarano, F., and J. Martn-Garca. 2005. The neuropathogenesis of AIDS. Nature Reviews Immunology 5:69-81.

33. Pomerantz, R. J. 2003. Reservoirs, sanctuaries, and residual disease: The hiding spots of hiv-1. HIV clinical trials 4:137-143.

34. Carvalhal, A., M. J. Gill, S. L. Letendre, A. Rachlis, T. Bekele, J. Raboud, A. Burchell, S. B. Rourke, and a. t. C. f. B. H. i. HIV/AIDS. 2015. Central nervous system penetration effectiveness of antiretroviral drugs and neuropsychological impairment in the ontario hiv treatment network cohort study. Journal of Neurovirology.

35. Letendre, S., J. Marquie-Beck, E. Capparelli, B. Best, D. Clifford, A. C. Collier, B. B. Gelman, J. C. McArthur, J. A. McCutchan, S. Morgello, D. Simpson, I. Grant, and R. J. Ellis. 2008. Validation of the cns penetration-effectiveness rank for quantifying antiretroviral penetration into the central nervous system. Arch. Neurol. 65:65-70.

36. Clements, J. E., M. Li, L. Gama, B. Bullock, L. M. Carruth, J. L. Mankowski, and M. C. Zink. 2005. The central nervous system is a viral reservoir in simian immunodeficiency virus–infected macaques on combined antiretroviral therapy: A model for human immunodeficiency virus patients on highly active antiretroviral therapy. Journal of Neurovirology 11:180-189.

37. Strazielle, N., and J.-F. Ghersi-Egea. 2005. Factors affecting delivery of antiviral drugs to the brain. Reviews in Medical Virology 15:105-133.

38. Smurzynski, M., K. Wu, S. Letendre, K. Robertson, R. J. Bosch, D. B. Clifford, S. Evans, A. C. Collier, M. Taylor, and R. Ellis. 2011. Effects of central nervous system antiretroviral penetration on cognitive functioning in the allrt cohort:. AIDS 25:357-365.

39. Rao, V. R., A. P. Ruiz, and V. R. Prasad. 2014. Viral and cellular factors underlying neuropathogenesis in hiv associated neurocognitive disorders (hand). AIDS research and therapy 11:13.

40. Spudich, S. S., A. C. Nilsson, N. D. Lollo, T. J. Liegler, C. J. Petropoulos, S. G. Deeks, E. E. Paxinos, and R. W. Price. 2005. Cerebrospinal fluid hiv infection and pleocytosis: Relation to systemic infection and antiretroviral treatment. BMC infectious diseases 5:98.

41. Koneru, R., M. F. Olive, and W. R. Tyor. 2014. Combined antiretroviral therapy reduces brain viral load and pathological features of hiv encephalitis in a mouse model. Journal of Neurovirology 20:9-17.

42. Calcagno, A., C. Atzori, A. Romito, D. Vai, S. Audagnotto, M. L. Stella, C. Montrucchio, D. Imperiale, G. Di Perri, and S. Bonora. 2015. Blood brain barrier impairment is associated with cerebrospinal fluid markers of neuronal damage in hiv-positive patients. Journal of Neurovirology.

43. Spudich, S., N. Lollo, T. Liegler, S. G. Deeks, and R. W. Price. 2006. Treatment benefit on cerebrospinal fluid hiv-1 levels in the setting of systemic virological suppression and failure. The Journal of Infectious Diseases 194:1686-1696.

44. Price, R. W., and S. Spudich. 2008. Antiretroviral therapy and central nervous system hiv type 1 infection. The Journal of Infectious Diseases 197 Suppl 3:S294-306.

45. Ferrando, S. J., J. G. Rabkin, W. van Gorp, S.-H. Lin, and M. McElhiney. 2003. Longitudinal improvement in psychomotor processing speed is associated with potent combination antiretroviral therapy in hiv-1 infection. The Journal of Neuropsychiatry and Clinical Neurosciences 15:208-214.

46. Cysique, L. A., F. Vaida, S. Letendre, S. Gibson, M. Cherner, S. P. Woods, J. A. McCutchan, R. K. Heaton, and R. J. Ellis. 2009. Dynamics of cognitive change in impaired hiv-positive patients initiating antiretroviral therapy. Neurology 73:342-348.

47. Robertson, K. R., W. T. Robertson, S. Ford, D. Watson, S. Fiscus, A. G. Harp, and C. D. M. Hall. 2004. Highly active antiretroviral therapy improves neurocognitive functioning. J. Acquir. Immune Defic. Syndr. 36:562-566.

48. Sacktor, N., M. P. McDermott, K. Marder, G. Schifitto, O. A. Selnes, J. C. McArthur, Y. Stern, S. Albert, D. Palumbo, K. Kieburtz, J. A. D. Marcaida, B. Cohen, and L. Epstein. 2002. Hiv-associated cognitive impairment before and after the advent of combination therapy. Journal of NeuroVirology 8:136-142.

49. Heaton, R. K., D. B. Clifford, D. R. Franklin, S. P. Woods, C. Ake, F. Vaida, R. J. Ellis, S. L. Letendre, T. D. Marcotte, J. H. Atkinson, M. Rivera-Mindt, O. R. Vigil, M. J. Taylor, A. C. Collier, C. M. Marra, B. B. Gelman, J. C. McArthur, S. Morgello, D. M. Simpson, J. A. McCutchan, I. Abramson, A. Gamst, C. Fennema-Notestine, T. L. Jernigan, J. Wong, I. Grant, and F. t. C. Group. 2010. Hiv-associated neurocognitive disorders persist in the era of potent antiretroviral therapy charter study. Neurology 75:2087-2096.

50. Grant, I., D. R. Franklin, R. Deutsch, S. P. Woods, F. Vaida, R. J. Ellis, S. L. Letendre, T. D. Marcotte, J. H. Atkinson, A. C. Collier, C. M. Marra, D. B. Clifford, B. B. Gelman, J. C. McArthur, S. Morgello, D. M. Simpson, J. A. McCutchan, I. Abramson, A. Gamst, C. Fennema-Notestine, D. M. Smith, R. K. Heaton, and C. Group. 2014. Asymptomatic hiv-associated neurocognitive impairment increases risk for symptomatic decline. Neurology 82:2055-2062.

51. McArthur, J. C., D. R. McClernon, M. F. Cronin, T. E. Nance-Sproson, A. J. Saah, M. St Clair, and E. R. Lanier. 1997. Relationship between human immunodeficiency virus-associated dementia and viral load in cerebrospinal fluid and brain. Annals of Neurology 42:689-698.

52. Wiley, C. A., V. Soontornniyomkij, L. Radhakrishnan, E. Masliah, J. Mellors, S. A. Hermann, P. Dailey, and C. L. Achim. 1998. Distribution of brain hiv load in AIDS. Brain Pathology (Zurich, Switzerland) 8:277-284.

53. Brew, B. J., L. Pemberton, P. Cunningham, and M. G. Law. 1997. Levels of human immunodeficiency virus type 1 rna in cerebrospinal fluid correlate with AIDS dementia stage. The Journal of Infectious Diseases 175:963-966.

54. Ellis, R. J., K. Hsia, S. A. Spector, J. A. Nelson, R. K. Heaton, M. R. Wallace, I. Abramson, J. H. Atkinson, I. Grant, and J. A. McCutchan. 1997. Cerebrospinal fluid human immunodeficiency virus type 1 rna levels are elevated in neurocognitively impaired individuals with acquired immunodeficiency syndrome. Hiv neurobehavioral research center group. Annals of Neurology 42:679-688.

55. Lamers, S. L., R. R. Gray, M. Salemi, L. C. Huysentruyt, and M. S. McGrath. 2011. Hiv-1 phylogenetic analysis shows hiv-1 transits through the meninges to brain and peripheral tissues. Infection, Genetics and Evolution: Journal of Molecular Epidemiology and Evolutionary Genetics in Infectious Diseases 11:31-37.

56. Lamers, S. L., A. F. Y. Poon, and M. S. McGrath. 2011. Hiv-1 nef protein structures associated with brain infection and dementia pathogenesis. PloS One 6:e16659.

57. Lamers, S. L., G. B. Fogel, E. J. Singer, M. Salemi, D. J. Nolan, L. C. Huysentruyt, and M. S. McGrath. 2012. Hiv-1 nef in macrophage-mediated disease pathogenesis. Int. Rev. Immunol. 31:432-450.

58. Salemi, M., S. L. Lamers, L. C. Huysentruyt, D. Galligan, R. R. Gray, A. Morris, and M. S. McGrath. 2009. Distinct patterns of hiv-1 evolution within metastatic tissues in patients with non-hodgkins lymphoma. PloS One 4:e8153.

59. Smith, D. M., S. Zrate, H. Shao, S. K. Pillai, S. L. Letendre, J. K. Wong, D. D. Richman, S. D. W. Frost, R. J. Ellis, and H. Group. 2009. Pleocytosis is associated with disruption of hiv compartmentalization between blood and cerebral spinal fluid viral populations. Virology 385:204-208.

60. Schnell, G., S. Spudich, P. Harrington, R. W. Price, and R. Swanstrom. 2009. Compartmentalized human immunodeficiency virus type 1 originates from long-lived cells in some subjects with hiv-1-associated dementia. PLoS pathogens 5:e1000395.

61. Schnell, G., S. Joseph, S. Spudich, R. W. Price, and R. Swanstrom. 2011. Hiv-1 replication in the central nervous system occurs in two distinct cell types. PLoS Pathog 7:e1002286.

62. Bednar, M. M., B. M. Hauser, L. H. Ping, E. Dukhovlinova, S. Zhou, K. T. Arrildt, I. F. Hoffman, J. J. Eron, M. S. Cohen, and R. Swanstrom. 2015. R5 macrophage-tropic hiv-1 in the male genital tract. J. Virol. 89:10688-10692.

63. Blasi, M., J. H. Carpenter, B. Balakumaran, A. Cara, F. Gao, and M. E. Klotman. 2015. Identification of hiv-1 genitourinary tract compartmentalization by analyzing the env gene sequences in urine. AIDS (London, England) 29:1651-1657.

64. Chaillon, A., S. Gianella, J. O. Wertheim, D. D. Richman, S. R. Mehta, and D. M. Smith. 2014. Hiv migration between blood and cerebrospinal fluid or semen over time. The Journal of Infectious Diseases 209:1642-1652.

65. Bull, M. E., L. M. Heath, J. L. McKernan-Mullin, K. M. Kraft, L. Acevedo, J. E. Hitti, S. E. Cohn, K. A. Tapia, S. E. Holte, J. A. Dragavon, R. W. Coombs, J. I. Mullins, and L. M. Frenkel. 2013. Human immunodeficiency viruses appear compartmentalized to the female genital tract in cross-sectional analyses but genital lineages do not persist over time. The Journal of Infectious Diseases 207:1206-1215.

66. Chaudhary, S., R. J. Noel, N. Rodrguez, S. Collado, J. Munoz, A. Kumar, and Y. Yamamura. 2011. Correlation between cd4 t cell counts and virus compartmentalization in genital and systemic compartments of hiv-infected females. Virology 417:320-326.

67. Anderson, J. A., L.-H. Ping, O. Dibben, C. B. Jabara, L. Arney, L. Kincer, Y. Tang, M. Hobbs, I. Hoffman, P. Kazembe, C. D. Jones, P. Borrow, S. Fiscus, M. S. Cohen, R. Swanstrom, and C. f. H. A. V. Immunology. 2010. Hiv-1 populations in semen arise through multiple mechanisms. PLoS pathogens 6:e1001053.

68. Diem, K., D. C. Nickle, A. Motoshige, A. Fox, S. Ross, J. I. Mullins, L. Corey, R. W. Coombs, and J. N. Krieger. 2008. Male genital tract compartmentalization of human immunodeficiency virus type 1 (hiv). AIDS research and human retroviruses 24:561-571.

69. Andreoletti, L., K. Skrabal, V. Perrin, N. Chomont, S. Saragosti, G. Gresenguet, H. Moret, J. Jacques, J. d. D. Longo, M. Matta, F. Mammano, and L. Belec. 2007. Genetic and phenotypic features of blood and genital viral populations of clinically asymptomatic and antiretroviral-treatment-naive clade a human immunodeficiency virus type 1-infected women. J. Clin. Microbiol. 45:1838-1842.

70. Sullivan, S. T., U. Mandava, T. Evans-Strickfaden, J. L. Lennox, T. V. Ellerbrock, and C. E. Hart. 2005. Diversity, divergence, and evolution of cell-free human immunodeficiency virus type 1 in vaginal secretions and blood of chronically infected women: Associations with immune status. J. Virol. 79:9799-9809.

71. Philpott, S., H. Burger, C. Tsoukas, B. Foley, K. Anastos, C. Kitchen, and B. Weiser. 2005. Human immunodeficiency virus type 1 genomic rna sequences in the female genital tract and blood: Compartmentalization and intrapatient recombination. J. Virol. 79:353-363.

72. Ghosn, J., J.-P. Viard, C. Katlama, M. de Almeida, R. Tubiana, F. Letourneur, L. Aaron, C. Goujard, D. Salmon, M. Leruez-Ville, C. Rouzioux, and M.-L. Chaix. 2004. Evidence of genotypic resistance diversity of archived and circulating viral strains in blood and semen of pre-treated hiv-infected men. AIDS (London, England) 18:447-457.

73. Kemal, K. S., B. Foley, H. Burger, K. Anastos, H. Minkoff, C. Kitchen, S. M. Philpott, W. Gao, E. Robison, S. Holman, C. Dehner, S. Beck, W. A. Meyer, A. Landay, A. Kovacs, J. Bremer, and B. Weiser. 2003. Hiv-1 in genital tract and plasma of women: Compartmentalization of viral sequences, coreceptor usage, and glycosylation. Proceedings of the National Academy of Sciences of the United States of America 100:12972-12977.

74. Sutthent, R., K. Sumrangsurp, P. Wirachsilp, P. Chaisilwattana, A. Roongpisuthipong, P. Chaiyakul, P. Nooma, M. Honda, and P. Warachit. 2001. Diversity of hiv-1 subtype e in semen and cervicovaginal secretion. Journal of Human Virology 4:260-268.

75. Gupta, P., C. Leroux, B. K. Patterson, L. Kingsley, C. Rinaldo, M. Ding, Y. Chen, K. Kulka, W. Buchanan, B. McKeon, and R. Montelaro. 2000. Human immunodeficiency virus type 1 shedding pattern in semen correlates with the compartmentalization of viral quasi species between blood and semen. The Journal of Infectious Diseases 182:79-87.

76. Poss, M., A. G. Rodrigo, J. J. Gosink, G. H. Learn, D. de Vange Panteleeff, H. L. Martin, J. Bwayo, J. K. Kreiss, and J. Overbaugh. 1998. Evolution of envelope sequences from the genital tract and peripheral blood of women infected with clade a human immunodeficiency virus type 1. J. Virol. 72:8240-8251.

77. Kiessling, A. A., L. M. Fitzgerald, D. Zhang, H. Chhay, D. Brettler, R. C. Eyre, J. Steinberg, K. McGowan, and R. A. Byrn. 1998. Human immunodeficiency virus in semen arises from a genetically distinct virus reservoir. AIDS research and human retroviruses 14 Suppl 1:S33-41.

78. Delwart, E. L., J. I. Mullins, P. Gupta, G. H. Learn, M. Holodniy, D. Katzenstein, B. D. Walker, and M. K. Singh. 1998. Human immunodeficiency virus type 1 populations in blood and semen. J. Virol. 72:617-623.

79. Coombs, R. W., C. E. Speck, J. P. Hughes, W. Lee, R. Sampoleo, S. O. Ross, J. Dragavon, G. Peterson, T. M. Hooton, A. C. Collier, L. Corey, L. Koutsky, and J. N. Krieger. 1998. Association between culturable human immunodeficiency virus type 1 (hiv-1) in

semen and hiv-1 rna levels in semen and blood: Evidence for compartmentalization of hiv-1 between semen and blood. The Journal of Infectious Diseases 177:320-330.

80. Zhu, T., N. Wang, A. Carr, D. S. Nam, R. Moor-Jankowski, D. A. Cooper, and D. D. Ho. 1996. Genetic characterization of human immunodeficiency virus type 1 in blood and genital secretions: Evidence for viral compartmentalization and selection during sexual transmission. J. Virol. 70:3098-3107.

81. Becquart, P., N. Chomont, P. Roques, A. Ayouba, M. D. Kazatchkine, L. Blec, and H. Hocini. 2002. Compartmentalization of hiv-1 between breast milk and blood of hiv-infected mothers. Virology 300:109-117.

82. Gantt, S., J. Carlsson, L. Heath, M. E. Bull, A. K. Shetty, J. Mutsvangwa, G. Musingwini, G. Woelk, L. S. Zijenah, D. A. Katzenstein, J. I. Mullins, and L. M. Frenkel. 2010. Genetic analyses of hiv-1 env sequences demonstrate limited compartmentalization in breast milk and suggest viral replication within the breast that increases with mastitis. J. Virol. 84:10812-10819.

83. Heath, L., S. Conway, L. Jones, K. Semrau, K. Nakamura, J. Walter, W. D. Decker, J. Hong, T. Chen, M. Heil, M. Sinkala, C. Kankasa, D. M. Thea, L. Kuhn, J. I. Mullins, and G. M. Aldrovandi. 2010. Restriction of hiv-1 genotypes in breast milk does not account for the population transmission genetic bottleneck that occurs following transmission. PloS One 5:e10213.

84. Marras, D., L. A. Bruggeman, F. Gao, N. Tanji, M. M. Mansukhani, A. Cara, M. D. Ross, G. L. Gusella, G. Benson, V. D. D'Agati, B. H. Hahn, M. E. Klotman, and P. E. Klotman. 2002. Replication and compartmentalization of hiv-1 in kidney epithelium of patients with hiv-associated nephropathy. Nature Medicine 8:522-526.

85. Singh, A., G. Besson, A. Mobasher, and R. G. Collman. 1999. Patterns of chemokine receptor fusion cofactor utilization by human immunodeficiency virus type 1 variants from the lungs and blood. J. Virol. 73:6680-6690.

86. Heath, L., A. Fox, J. McClure, K. Diem, A. B. van 't Wout, H. Zhao, D. R. Park, J. T. Schouten, H. L. Twigg, L. Corey, J. I. Mullins, and J. E. Mittler. 2009. Evidence for limited genetic compartmentalization of hiv-1 between lung and blood. PloS One 4:e6949.

87. Gartner, S., P. Markovits, D. M. Markovitz, M. H. Kaplan, R. C. Gallo, and M. Popovic. 1986. The role of mononuclear phagocytes in htlv-iii/lav infection. Science (New York, N.Y.) 233:215-219.

88. Salazar-Gonzalez, J. F., M. G. Salazar, G. H. Learn, G. G. Fouda, H. H. Kang, T. Mahlokozera, A. B. Wilks, R. V. Lovingood, A. Stacey, L. Kalilani, S. R. Meshnick, P. Borrow, D. C. Montefiori, T. N. Denny, N. L. Letvin, G. M. Shaw, B. H. Hahn, S. R. Permar, and C. f. H. A. V. I. A0167854. 2011. Origin and evolution of hiv-1 in breast milk determined by single-genome amplification and sequencing. J. Virol. 85:2751-2763.

89. Blackard, J. T., G. Ma, C. M. Martin, S. D. Rouster, M. T. Shata, and K. E. Sherman. 2011. Hiv variability in the liver and evidence of possible compartmentalization. AIDS research and human retroviruses 27:1117-1126.

90. Penton, P. K., and J. T. Blackard. 2014. Analysis of hiv quasispecies suggests compartmentalization in the liver. AIDS research and human retroviruses 30:394-402.

91. van der Hoek, L., C. J. Sol, J. Maas, V. V. Lukashov, C. L. Kuiken, and J. Goudsmit. 1998. Genetic differences between human immunodeficiency virus type 1 subpopulations in faeces and serum. The Journal of General Virology 79 (Pt 2):259-267.

92. Poles, M. A., J. Elliott, J. Vingerhoets, L. Michiels, A. Scholliers, S. Bloor, B. Larder, K. Hertogs, and P. A. Anton. 2001. Despite high concordance, distinct mutational and phenotypic drug resistance profiles in human immunodeficiency virus type 1 rna are observed in gastrointestinal mucosal biopsy specimens and peripheral blood mononuclear cells compared with plasma. The Journal of Infectious Diseases 183:143-148.

93. Wang, T. H., Y. K. Donaldson, R. P. Brettle, J. E. Bell, and P. Simmonds. 2001. Identification of shared populations of human immunodeficiency virus type 1 infecting microglia and tissue macrophages outside the central nervous system. J. Virol. 75:11686-11699.

94. van Marle, G., M. J. Gill, D. Kolodka, L. McManus, T. Grant, and D. L. Church. 2007. Compartmentalization of the gut viral reservoir in hiv-1 infected patients. Retrovirology 4:87.

95. Lewis, M. J., P. Frohnen, F. J. Ibarrondo, D. Reed, V. Iyer, H. L. Ng, J. Elliott, O. O. Yang, and P. Anton. 2013. Hiv-1 nef sequence and functional compartmentalization in the gut is not due to differential cytotoxic t lymphocyte selective pressure. PloS One 8:e75620.

96. Bednar, M. M., B. M. Hauser, L.-H. Ping, E. Dukhovlinova, S. Zhou, K. T. Arrildt, I. F. Hoffman, J. J. Eron, M. S. Cohen, and R. Swanstrom. 2015. R5 macrophage-tropic hiv-1 in the male genital tract. J. Virol.

97. Leitner, T., S. Kumar, and J. Albert. 1997. Tempo and mode of nucleotide substitutions in gag and env gene fragments in human immunodeficiency virus type 1 populations with a known transmission history. J. Virol. 71:4761-4770.

98. Li, M., J. F. Salazar-Gonzalez, C. A. Derdeyn, L. Morris, C. Williamson, J. E. Robinson, J. M. Decker, Y. Li, M. G. Salazar, V. R. Polonis, K. Mlisana, S. A. Karim, K. Hong, K. M. Greene, M. Bilska, J. Zhou, S. Allen, E. Chomba, J. Mulenga, C. Vwalika, F. Gao, M. Zhang, B. T. M. Korber, E. Hunter, B. H. Hahn, and D. C. Montefiori. 2006. Genetic and neutralization properties of subtype c human immunodeficiency virus type 1 molecular env clones from acute and early heterosexually acquired infections in southern africa. J. Virol. 80:11776-11790.

99. Joseph, S. B., K. T. Arrildt, A. E. Swanstrom, G. Schnell, B. Lee, J. A. Hoxie, and R. Swanstrom. 2014. Quantification of entry phenotypes of macrophage-tropic hiv-1 across a wide range of cd4 densities. J. Virol. 88:1858-1869.

100. Perelson, A. S., A. U. Neumann, M. Markowitz, J. M. Leonard, and D. D. Ho. 1996. Hiv-1 dynamics in vivo: Virion clearance rate, infected cell life-span, and viral generation time. Science (New York, N.Y.) 271:1582-1586.

101. Herz, A. V., S. Bonhoeffer, R. M. Anderson, R. M. May, and M. A. Nowak. 1996. Viral dynamics in vivo: Limitations on estimates of intracellular delay and virus decay. Proceedings of the National Academy of Sciences of the United States of America 93:7247-7251.

102. Finzi, D., M. Hermankova, T. Pierson, L. M. Carruth, C. Buck, R. E. Chaisson, T. C. Quinn, K. Chadwick, J. Margolick, R. Brookmeyer, J. Gallant, M. Markowitz, D. D. Ho, D. D. Richman, and R. F. Siliciano. 1997. Identification of a reservoir for hiv-1 in patients on highly active antiretroviral therapy. Science (New York, N.Y.) 278:1295-1300.

103. Ho, Y.-C., L. Shan, N. N. Hosmane, J. Wang, S. B. Laskey, D. I. S. Rosenbloom, J. Lai, J. N. Blankson, J. D. Siliciano, and R. F. Siliciano. 2013. Replication-competent noninduced proviruses in the latent reservoir increase barrier to hiv-1 cure. Cell 155:540-551.

104. Wong, J. K., C. C. Ignacio, F. Torriani, D. Havlir, N. J. Fitch, and D. D. Richman. 1997. In vivo compartmentalization of human immunodeficiency virus: Evidence from the examination of pol sequences from autopsy tissues. J. Virol. 71:2059-2071.

105. Chun, T. W., L. Stuyver, S. B. Mizell, L. A. Ehler, J. A. Mican, M. Baseler, A. L. Lloyd, M. A. Nowak, and A. S. Fauci. 1997. Presence of an inducible hiv-1 latent reservoir during highly active antiretroviral therapy. Proceedings of the National Academy of Sciences of the United States of America 94:13193-13197.

106. Brinchmann, J. E., J. Albert, and F. Vartdal. 1991. Few infected $CD4^+$ t cells but a high proportion of replication-competent provirus copies in asymptomatic human immunodeficiency virus type 1 infection. J. Virol. 65:2019-2023.

107. Psallidopoulos, M. C., S. M. Schnittman, L. M. Thompson, M. Baseler, A. S. Fauci, H. C. Lane, and N. P. Salzman. 1989. Integrated proviral human immunodeficiency virus type 1 is present in $CD4^+$ peripheral blood lymphocytes in healthy seropositive individuals. J. Virol. 63:4626-4631.

108. Schnittman, S. M., M. C. Psallidopoulos, H. C. Lane, L. Thompson, M. Baseler, F. Massari, C. H. Fox, N. P. Salzman, and A. S. Fauci. 1989. The reservoir for hiv-1 in human peripheral blood is a t cell that maintains expression of cd4. Science (New York, N.Y.) 245:305-308.

109. Heinzinger, N. K., M. I. Bukrinsky, S. A. Haggerty, A. M. Ragland, V. Kewalramani, M. A. Lee, H. E. Gendelman, L. Ratner, M. Stevenson, and M. Emerman. 1994. The

vpr protein of human immunodeficiency virus type 1 influences nuclear localization of viral nucleic acids in nondividing host cells. Proceedings of the National Academy of Sciences of the United States of America 91:7311-7315.

110. Vodicka, M. A., D. M. Koepp, P. A. Silver, and M. Emerman. 1998. Hiv-1 vpr interacts with the nuclear transport pathway to promote macrophage infection. Genes Dev. 12:175-185.

111. Rogel, M. E., L. I. Wu, and M. Emerman. 1995. The human immunodeficiency virus type 1 vpr gene prevents cell proliferation during chronic infection. J. Virol. 69:882-888.

112. Jowett, J. B., V. Planelles, B. Poon, N. P. Shah, M. L. Chen, and I. S. Chen. 1995. The human immunodeficiency virus type 1 vpr gene arrests infected t cells in the g2 + m phase of the cell cycle. J. Virol. 69:6304-6313.

113. Re, F., D. Braaten, E. K. Franke, and J. Luban. 1995. Human immunodeficiency virus type 1 vpr arrests the cell cycle in g2 by inhibiting the activation of p34cdc2-cyclin b. J. Virol. 69:6859-6864.

114. He, J., S. Choe, R. Walker, P. Di Marzio, D. O. Morgan, and N. R. Landau. 1995. Human immunodeficiency virus type 1 viral protein r (vpr) arrests cells in the g2 phase of the cell cycle by inhibiting p34cdc2 activity. J. Virol. 69:6705-6711.

115. Schwartz, O., V. Marchal, S. Le Gall, F. Lemonnier, and J. M. Heard. 1996. Endocytosis of major histocompatibility complex class i molecules is induced by the hiv-1 nef protein. Nature Medicine 2:338-342.

116. Garcia, J. V., and A. D. Miller. 1992. Downregulation of cell surface cd4 by nef. Res. Virol. 143:52-55.

117. Aiken, C., J. Konner, N. R. Landau, M. E. Lenburg, and D. Trono. 1994. Nef induces cd4 endocytosis: Requirement for a critical dileucine motif in the membrane-proximal cd4 cytoplasmic domain. Cell 76:853-864.

118. Lama, J., A. Mangasarian, and D. Trono. 1999. Cell-surface expression of cd4 reduces hiv-1 infectivity by blocking env incorporation in a nef- and vpu-inhibitable manner. Current biology: CB 9:622-631.

119. Ross, T. M., A. E. Oran, and B. R. Cullen. 1999. Inhibition of hiv-1 progeny virion release by cell-surface cd4 is relieved by expression of the viral nef protein. Current biology: CB 9:613-621.

120. Klimkait, T., K. Strebel, M. D. Hoggan, M. A. Martin, and J. M. Orenstein. 1990. The human immunodeficiency virus type 1-specific protein vpu is required for efficient virus maturation and release. J. Virol. 64:621-629.

121. Neil, S. J. D., T. Zang, and P. D. Bieniasz. 2008. Tetherin inhibits retrovirus release and is antagonized by hiv-1 vpu. Nature 451:425-430.

122. Sheehy, A. M., N. C. Gaddis, J. D. Choi, and M. H. Malim. 2002. Isolation of a human gene that inhibits hiv-1 infection and is suppressed by the viral vif protein. Nature 418:646-650.

123. Yu, X., Y. Yu, B. Liu, K. Luo, W. Kong, P. Mao, and X.-F. Yu. 2003. Induction of apobec3g ubiquitination and degradation by an hiv-1 vif-cul5-scf complex. Science (New York, N.Y.) 302:1056-1060.

124. Koot, M., I. P. Keet, A. H. Vos, R. E. de Goede, M. T. Roos, R. A. Coutinho, F. Miedema, P. T. Schellekens, and M. Tersmette. 1993. Prognostic value of hiv-1 syncytium-inducing phenotype for rate of $CD4^+$ cell depletion and progression to AIDS. Annals of Internal Medicine 118:681-688.

125. Connor, R. I., K. E. Sheridan, D. Ceradini, S. Choe, and N. R. Landau. 1997. Change in coreceptor use correlates with disease progression in hiv-1–infected individuals. The Journal of Experimental Medicine 185:621-628.

126. Tscherning, C., A. Alaeus, R. Fredriksson, A. Bjrndal, H. Deng, D. R. Littman, E. M. Feny, and J. Albert. 1998. Differences in chemokine coreceptor usage between genetic subtypes of hiv-1. Virology 241:181-188.

127. Mascola, J. R., S. W. Snyder, O. S. Weislow, S. M. Belay, R. B. Belshe, D. H. Schwartz, M. L. Clements, R. Dolin, B. S. Graham, G. J. Gorse, M. C. Keefer, M. J. McElrath, M. C. Walker, K. F. Wagner, J. G. McNeil, F. E. McCutchan, and D. S. Burke. 1996. Immunization with envelope subunit vaccine products elicits neutralizing antibodies against laboratory-adapted but not primary isolates of human immunodeficiency virus type 1. The national institute of allergy and infectious diseases AIDS vaccine evaluation group. The Journal of Infectious Diseases 173:340-348.

128. Merk, A., and S. Subramaniam. 2013. Hiv-1 envelope glycoprotein structure. Current opinion in structural biology 23:268-276.

129. Means, R. E., T. Greenough, and R. C. Desrosiers. 1997. Neutralization sensitivity of cell culture-passaged simian immunodeficiency virus. J. Virol. 71:7895-7902.

130. O'Connell, O., A. Repik, J. D. Reeves, M. P. Gonzalez-Perez, B. Quitadamo, E. D. Anton, M. Duenas-Decamp, P. Peters, R. Lin, S. Zolla-Pazner, D. Corti, A. Wallace, S. Wang, X.-P. Kong, S. Lu, and P. R. Clapham. 2013. Efficiency of bridging-sheet recruitment explains hiv-1 r5 envelope glycoprotein sensitivity to soluble cd4 and macrophage tropism. J. Virol. 87:187-198.

131. Liu, S., W. Jing, B. Cheung, H. Lu, J. Sun, X. Yan, J. Niu, J. Farmar, S. Wu, and S. Jiang. 2007. Hiv gp41 c-terminal heptad repeat contains multifunctional domains. Relation to mechanisms of action of anti-hiv peptides. The Journal of Biological Chemistry 282:9612-9620.

132. Lee, B., M. Sharron, L. J. Montaner, D. Weissman, and R. W. Doms. 1999. Quantification of cd4, ccr5, and cxcr4 levels on lymphocyte subsets, dendritic cells, and

differentially conditioned monocyte-derived macrophages. Proceedings of the National Academy of Sciences of the United States of America 96:5215-5220.

133. McLellan, J. S., M. Pancera, C. Carrico, J. Gorman, J.-P. Julien, R. Khayat, R. Louder, R. Pejchal, M. Sastry, K. Dai, S. ODell, N. Patel, S. Shahzad-ul-Hussan, Y. Yang, B. Zhang, T. Zhou, J. Zhu, J. C. Boyington, G.-Y. Chuang, D. Diwanji, I. Georgiev, Y. Do Kwon, D. Lee, M. K. Louder, S. Moquin, S. D. Schmidt, Z.-Y. Yang, M. Bonsignori, J. A. Crump, S. H. Kapiga, N. E. Sam, B. F. Haynes, D. R. Burton, W. C. Koff, L. M. Walker, S. Phogat, R. Wyatt, J. Orwenyo, L.-X. Wang, J. Arthos, C. A. Bewley, J. R. Mascola, G. J. Nabel, W. R. Schief, A. B. Ward, I. A. Wilson, and P. D. Kwong. 2011. Structure of hiv-1 gp120 v1/v2 domain with broadly neutralizing antibody pg9. Nature 480:336-343.

134. Arrildt, K. T., S. B. Joseph, and R. Swanstrom. 2012. The hiv-1 env protein: A coat of many colors. Current HIV/AIDS reports 9:52-63.

135. Zamarchi, R., P. Allavena, A. Borsetti, L. Stievano, V. Tosello, N. Marcato, G. Esposito, V. Roni, C. Paganin, G. Bianchi, F. Titti, P. Verani, G. Gerosa, and A. Amadori. 2002. Expression and functional activity of cxcr-4 and ccr-5 chemokine receptors in human thymocytes. Clin. Exp. Immunol. 127:321-330.

136. Pace, M. J., L. Agosto, and U. O'Doherty. 2011. R5 hiv env and vesicular stomatitis virus g protein cooperate to mediate fusion to naive $CD4^+$ t cells. J. Virol. 85:644-648.

137. van't Wout, A. B., N. A. Kootstra, G. A. Mulder-Kampinga, N. Albrecht-van Lent, H. J. Scherpbier, J. Veenstra, K. Boer, R. A. Coutinho, F. Miedema, and H. Schuitemaker. 1994. Macrophage-tropic variants initiate human immunodeficiency virus type 1 infection after sexual, parenteral, and vertical transmission. The Journal of Clinical Investigation 94:2060-2067.

138. Zhu, T., H. Mo, N. Wang, D. S. Nam, Y. Cao, R. A. Koup, and D. D. Ho. 1993. Genotypic and phenotypic characterization of hiv-1 patients with primary infection. Science 261:1179-1181.

139. Braathen, L. R., G. Ramirez, R. O. Kunze, and H. Gelderblom. 1987. Langerhans cells as primary target cells for hiv infection. Lancet (London, England) 2:1094.

140. Palacio, J., B. E. Souberbielle, R. J. Shattock, G. Robinson, I. Manyonda, and G. E. Griffin. 1994. In vitro hiv1 infection of human cervical tissue. Res. Virol. 145:155-161.

141. Li, H., K. J. Bar, S. Wang, J. M. Decker, Y. Chen, C. Sun, J. F. Salazar-Gonzalez, M. G. Salazar, G. H. Learn, C. J. Morgan, J. E. Schumacher, P. Hraber, E. E. Giorgi, T. Bhattacharya, B. T. Korber, A. S. Perelson, J. J. Eron, M. S. Cohen, C. B. Hicks, B. F. Haynes, M. Markowitz, B. F. Keele, B. H. Hahn, and G. M. Shaw. 2010. High multiplicity infection by hiv-1 in men who have sex with men. PLoS pathogens 6:e1000890.

142. Ochsenbauer, C., T. G. Edmonds, H. Ding, B. F. Keele, J. Decker, M. G. Salazar, J. F. Salazar-Gonzalez, R. Shattock, B. F. Haynes, G. M. Shaw, B. H. Hahn, and J. C. Kappes. 2012. Generation of transmitted/founder hiv-1 infectious molecular clones and characterization of their replication capacity in cd4 t lymphocytes and monocyte-derived macrophages. J. Virol. 86:2715-2728.

143. Dunfee, R., E. R. Thomas, P. R. Gorry, J. Wang, P. Ancuta, and D. Gabuzda. 2006. Mechanisms of hiv-1 neurotropism. Current HIV research 4:267-278.

144. Dunfee, R. L., E. R. Thomas, and D. Gabuzda. 2009. Enhanced macrophage tropism of hiv in brain and lymphoid tissues is associated with sensitivity to the broadly neutralizing cd4 binding site antibody b12. Retrovirology 6:69.

145. Duenas-Decamp, M. J., P. J. Peters, D. Burton, and P. R. Clapham. 2009. Determinants flanking the cd4 binding loop modulate macrophage tropism of human immunodeficiency virus type 1 r5 envelopes. J. Virol. 83:2575-2583.

146. Gorry, P. R., J. Taylor, G. H. Holm, A. Mehle, T. Morgan, M. Cayabyab, M. Farzan, H. Wang, J. E. Bell, K. Kunstman, J. P. Moore, S. M. Wolinsky, and D. Gabuzda. 2002. Increased ccr5 affinity and reduced ccr5/cd4 dependence of a neurovirulent primary human immunodeficiency virus type 1 isolate. J. Virol. 76:6277-6292.

147. Martn-Garca, J., W. Cao, A. Varela-Rohena, M. L. Plassmeyer, and F. Gonzlez-Scarano. 2006. Hiv-1 tropism for the central nervous system: Brain-derived envelope glycoproteins with lower cd4 dependence and reduced sensitivity to a fusion inhibitor. Virology 346:169-179.

148. Peters, P. J., J. Bhattacharya, S. Hibbitts, M. T. Dittmar, G. Simmons, J. Bell, P. Simmonds, and P. R. Clapham. 2004. Biological analysis of human immunodeficiency virus type 1 r5 envelopes amplified from brain and lymph node tissues of AIDS patients with neuropathology reveals two distinct tropism phenotypes and identifies envelopes in the brain that confer an enhanced tropism and fusigenicity for macrophages. J. Virol. 78:6915-6926.

149. Gorry, P. R., G. Bristol, J. A. Zack, K. Ritola, R. Swanstrom, C. J. Birch, J. E. Bell, N. Bannert, K. Crawford, H. Wang, D. Schols, E. D. Clercq, K. Kunstman, S. M. Wolinsky, and D. Gabuzda. 2001. Macrophage tropism of human immunodeficiency virus type 1 isolates from brain and lymphoid tissues predicts neurotropism independent of coreceptor specificity. J. Virol. 75:10073-10089.

150. Koyanagi, Y., S. Miles, R. T. Mitsuyasu, J. E. Merrill, H. V. Vinters, and I. S. Chen. 1987. Dual infection of the central nervous system by AIDS viruses with distinct cellular tropisms. Science 236:819-822.

151. Li, S., J. Juarez, M. Alali, D. Dwyer, R. Collman, A. Cunningham, and H. M. Naif. 1999. Persistent ccr5 utilization and enhanced macrophage tropism by primary blood human immunodeficiency virus type 1 isolates from advanced stages of disease and comparison to tissue-derived isolates. J. Virol. 73:9741-9755.

152. Gray, L., J. Sterjovski, M. Churchill, P. Ellery, N. Nasr, S. R. Lewin, S. M. Crowe, S. L. Wesselingh, A. L. Cunningham, and P. R. Gorry. 2005. Uncoupling coreceptor usage of human immunodeficiency virus type 1 (hiv-1) from macrophage tropism reveals biological properties of ccr5-restricted hiv-1 isolates from patients with acquired immunodeficiency syndrome. Virology 337:384-398.

153. Churchill, M., and A. Nath. 2013. Where does hiv hide? A focus on the central nervous system. Current opinion in HIV and AIDS 8:165-169.

154. Johnston, S. H., M. A. Lobritz, S. Nguyen, K. Lassen, S. Delair, F. Posta, Y. J. Bryson, E. J. Arts, T. Chou, and B. Lee. 2009. A quantitative affinity-profiling system that reveals distinct cd4/ccr5 usage patterns among human immunodeficiency virus type 1 and simian immunodeficiency virus strains. J. Virol. 83:11016-11026.

155. Staprans, S., N. Marlowe, D. Glidden, T. Novakovic-Agopian, R. M. Grant, M. Heyes, F. Aweeka, S. Deeks, and R. W. Price. 1999. Time course of cerebrospinal fluid responses to antiretroviral therapy: Evidence for variable compartmentalization of infection. AIDS (London, England) 13:1051-1061.

156. Abrahams, M.-R., J. A. Anderson, E. E. Giorgi, C. Seoighe, K. Mlisana, L.-H. Ping, G. S. Athreya, F. K. Treurnicht, B. F. Keele, N. Wood, J. F. Salazar-Gonzalez, T. Bhattacharya, H. Chu, I. Hoffman, S. Galvin, C. Mapanje, P. Kazembe, R. Thebus, S. Fiscus, W. Hide, M. S. Cohen, S. A. Karim, B. F. Haynes, G. M. Shaw, B. H. Hahn, B. T. Korber, R. Swanstrom, C. Williamson, C. A. I. S. Team, and C. f. H.-A. V. I. Consortium. 2009. Quantitating the multiplicity of infection with human immunodeficiency virus type 1 subtype c reveals a non-poisson distribution of transmitted variants. J. Virol. 83:3556-3567.

157. Keele, B. F., E. E. Giorgi, J. F. Salazar-Gonzalez, J. M. Decker, K. T. Pham, M. G. Salazar, C. Sun, T. Grayson, S. Wang, H. Li, X. Wei, C. Jiang, J. L. Kirchherr, F. Gao, J. A. Anderson, L.-H. Ping, R. Swanstrom, G. D. Tomaras, W. A. Blattner, P. A. Goepfert, J. M. Kilby, M. S. Saag, E. L. Delwart, M. P. Busch, M. S. Cohen, D. C. Montefiori, B. F. Haynes, B. Gaschen, G. S. Athreya, H. Y. Lee, N. Wood, C. Seoighe, A. S. Perelson, T. Bhattacharya, B. T. Korber, B. H. Hahn, and G. M. Shaw. 2008. Identification and characterization of transmitted and early founder virus envelopes in primary hiv-1 infection. Proceedings of the National Academy of Sciences of the United States of America 105:7552-7557.

158. Salazar-Gonzalez, J. F., E. Bailes, K. T. Pham, M. G. Salazar, M. B. Guffey, B. F. Keele, C. A. Derdeyn, P. Farmer, E. Hunter, S. Allen, O. Manigart, J. Mulenga, J. A. Anderson, R. Swanstrom, B. F. Haynes, G. S. Athreya, B. T. M. Korber, P. M. Sharp, G. M. Shaw, and B. H. Hahn. 2008. Deciphering human immunodeficiency virus type 1 transmission and early envelope diversification by single-genome amplification and sequencing. J. Virol. 82:3952-3970.

159. Joseph, S. B., B. Lee, and R. Swanstrom. 2014. Affinofile assay for identifying macrophage-tropic hiv-1. Bio-protocol 4:e1184.http://www.bio-protocol.org/e1184

160. Del Prete, G. Q., B. Haggarty, G. J. Leslie, A. P. O. Jordan, J. Romano, N. Wang, J. Wang, M. C. Holmes, D. C. Montefiori, and J. A. Hoxie. 2009. Derivation and characterization of a simian immunodeficiency virus sivmac239 variant with tropism for cxcr4. J. Virol. 83:9911-9922.

161. Rucker, J., B. J. Doranz, A. L. Edinger, D. Long, J. F. Berson, and R. W. Doms. 1997. Cell-cell fusion assay to study role of chemokine receptors in human immunodeficiency virus type 1 entry. Methods Enzymol. 288:118-133.

162. Naif, H. M., S. Li, M. Alali, A. Sloane, L. Wu, M. Kelly, G. Lynch, A. Lloyd, and A. L. Cunningham. 1998. Ccr5 expression correlates with susceptibility of maturing monocytes to human immunodeficiency virus type 1 infection. J. Virol. 72:830-836.

163. Sonza, S., A. Maerz, S. Uren, A. Violo, S. Hunter, W. Boyle, and S. Crowe. 1995. Susceptibility of human monocytes to hiv type 1 infection in vitro is not dependent on their level of cd4 expression. AIDS research and human retroviruses 11:769-776.

164. Wynn, T. A., A. Chawla, and J. W. Pollard. 2013. Macrophage biology in development, homeostasis and disease. Nature 496:445-455.

165. Polazzi, E., and B. Monti. 2010. Microglia and neuroprotection: From in vitro studies to therapeutic applications. Prog. Neurobiol. 92:293-315.

166. Ginhoux, F., M. Greter, M. Leboeuf, S. Nandi, P. See, S. Gokhan, M. F. Mehler, S. J. Conway, L. G. Ng, E. R. Stanley, I. M. Samokhvalov, and M. Merad. 2010. Fate mapping analysis reveals that adult microglia derive from primitive macrophages. Science (New York, N.Y.) 330:841-845.

167. Schulz, C., E. Gomez Perdiguero, L. Chorro, H. Szabo-Rogers, N. Cagnard, K. Kierdorf, M. Prinz, B. Wu, S. E. W. Jacobsen, J. W. Pollard, J. Frampton, K. J. Liu, and F. Geissmann. 2012. A lineage of myeloid cells independent of myb and hematopoietic stem cells. Science (New York, N.Y.) 336:86-90.

168. Paolicelli, R. C., G. Bolasco, F. Pagani, L. Maggi, M. Scianni, P. Panzanelli, M. Giustetto, T. A. Ferreira, E. Guiducci, L. Dumas, D. Ragozzino, and C. T. Gross. 2011. Synaptic pruning by microglia is necessary for normal brain development. Science (New York, N.Y.) 333:1456-1458.

169. Sierra, A., J. M. Encinas, J. J. P. Deudero, J. H. Chancey, G. Enikolopov, L. S. Overstreet-Wadiche, S. E. Tsirka, and M. Maletic-Savatic. 2010. Microglia shape adult hippocampal neurogenesis through apoptosis-coupled phagocytosis. Cell Stem Cell 7:483-495.

170. Unger, E. R., J. H. Sung, J. C. Manivel, M. L. Chenggis, B. R. Blazar, and W. Krivit. 1993. Male donor-derived cells in the brains of female sex-mismatched bone marrow transplant recipients: A y-chromosome specific in situ hybridization study. J. Neuropathol. Exp. Neurol. 52:460-470.

171. Williams, K. C., S. Corey, S. V. Westmoreland, D. Pauley, H. Knight, C. deBakker, X. Alvarez, and A. A. Lackner. 2001. Perivascular macrophages are the primary cell type productively infected by simian immunodeficiency virus in the brains of macaques: Implications for the neuropathogenesis of AIDS. The Journal of Experimental Medicine 193:905-915.

172. Klein, I., J. C. Cornejo, N. K. Polakos, B. John, S. A. Wuensch, D. J. Topham, R. H. Pierce, and I. N. Crispe. 2007. Kupffer cell heterogeneity: Functional properties of bone marrow derived and sessile hepatic macrophages. Blood 110:4077-4085.

173. Murray, P. J., and T. A. Wynn. 2011. Protective and pathogenic functions of macrophage subsets. Nature Reviews. Immunology 11:723-737.

174. London, A., M. Cohen, and M. Schwartz. 2013. Microglia and monocyte-derived macrophages: Functionally distinct populations that act in concert in cns plasticity and repair. Frontiers in Cellular Neuroscience 7:34.

175. !!! INVALID CITATION !!!

176. Mosser, D. M., and J. P. Edwards. 2008. Exploring the full spectrum of macrophage activation. Nature Reviews. Immunology 8:958-969.

177. Crain, J. M., M. Nikodemova, and J. J. Watters. 2013. Microglia express distinct m1 and m2 phenotypic markers in the postnatal and adult central nervous system in male and female mice. J. Neurosci. Res. 91:1143-1151.

178. Gibbings, D., and A. D. Befus. 2009. Cd4 and cd8: An inside-out coreceptor model for innate immune cells. Journal of Leukocyte Biology 86:251-259.

179. Crocker, P. R., W. A. Jefferies, S. J. Clark, L. P. Chung, and S. Gordon. 1987. Species heterogeneity in macrophage expression of the cd4 antigen. The Journal of Experimental Medicine 166:613-618.

180. Duncan, C. J. A., and Q. J. Sattentau. 2011. Viral determinants of hiv-1 macrophage tropism. Viruses 3:2255-2279.

181. Thomas, E. R., R. L. Dunfee, J. Stanton, D. Bogdan, J. Taylor, K. Kunstman, J. E. Bell, S. M. Wolinsky, and D. Gabuzda. 2007. Macrophage entry mediated by hiv envs from brain and lymphoid tissues is determined by the capacity to use low cd4 levels and overall efficiency of fusion. Virology 360:105-119.

182. Gendelman, H. E., J. M. Orenstein, M. A. Martin, C. Ferrua, R. Mitra, T. Phipps, L. A. Wahl, H. C. Lane, A. S. Fauci, and D. S. Burke. 1988. Efficient isolation and propagation of human immunodeficiency virus on recombinant colony-stimulating factor 1-treated monocytes. The Journal of Experimental Medicine 167:1428-1441.

183. Li, Y., J. C. Kappes, J. A. Conway, R. W. Price, G. M. Shaw, and B. H. Hahn. 1991. Molecular characterization of human immunodeficiency virus type 1 cloned directly from uncultured human brain tissue: Identification of replication-competent and -defective viral genomes. J. Virol. 65:3973-3985.

184. Salimi, H., M. Roche, N. Webb, L. R. Gray, K. Chikere, J. Sterjovski, A. Ellett, S. L. Wesselingh, P. A. Ramsland, B. Lee, M. J. Churchill, and P. R. Gorry. 2013. Macrophage-tropic hiv-1 variants from brain demonstrate alterations in the way gp120 engages both cd4 and ccr5. Journal of Leukocyte Biology 93:113-126.

185. Ortiz, A. M., N. R. Klatt, B. Li, Y. Yi, B. Tabb, X. P. Hao, L. Sternberg, B. Lawson, P. M. Carnathan, E. M. Cramer, J. C. Engram, D. M. Little, E. Ryzhova, F. Gonzalez-Scarano, M. Paiardini, A. A. Ansari, S. Ratcliffe, J. G. Else, J. M. Brenchley, R. G. Collman, J. D. Estes, C. A. Derdeyn, and G. Silvestri. 2011. Depletion of cd4 t cells abrogates post-peak decline of viremia in siv-infected rhesus macaques. The Journal of Clinical Investigation 121:4433-4445.

186. Igarashi, T., C. R. Brown, Y. Endo, A. Buckler-White, R. Plishka, N. Bischofberger, V. Hirsch, and M. A. Martin. 2001. Macrophage are the principal reservoir and sustain high virus loads in rhesus macaques after the depletion of $CD4^+$ t cells by a highly pathogenic simian immunodeficiency virus/hiv type 1 chimera (shiv): Implications for hiv-1 infections of humans. Proceedings of the National Academy of Sciences of the United States of America 98:658-663.

187. Peters, P. J., M. J. Duenas-Decamp, W. M. Sullivan, R. Brown, C. Ankghuambom, K. Luzuriaga, J. Robinson, D. R. Burton, J. Bell, P. Simmonds, J. Ball, and P. R. Clapham. 2008. Variation in hiv-1 r5 macrophage-tropism correlates with sensitivity to reagents that block envelope: Cd4 interactions but not with sensitivity to other entry inhibitors. Retrovirology 5:5.

188. Churchill, M. J., S. L. Wesselingh, D. Cowley, C. A. Pardo, J. C. McArthur, B. J. Brew, and P. R. Gorry. 2009. Extensive astrocyte infection is prominent in human immunodeficiency virus-associated dementia. Annals of Neurology 66:253-258.

189. Bruggeman, L. A., M. D. Ross, N. Tanji, A. Cara, S. Dikman, R. E. Gordon, G. C. Burns, V. D. D'Agati, J. A. Winston, M. E. Klotman, and P. E. Klotman. 2000. Renal epithelium is a previously unrecognized site of hiv-1 infection. Journal of the American Society of Nephrology: JASN 11:2079-2087.

190. Gorry, P. R., C. Ong, J. Thorpe, S. Bannwarth, K. A. Thompson, A. Gatignol, S. L. Vesselingh, and D. F. J. Purcell. 2003. Astrocyte infection by hiv-1: Mechanisms of restricted virus replication, and role in the pathogenesis of hiv-1-associated dementia. Current HIV research 1:463-473.

191. Thompson, K. A., M. J. Churchill, P. R. Gorry, J. Sterjovski, R. B. Oelrichs, S. L. Wesselingh, and C. A. McLean. 2004. Astrocyte specific viral strains in hiv dementia. Annals of Neurology 56:873-877.

192. Zhu, T., D. Muthui, S. Holte, D. Nickle, F. Feng, S. Brodie, Y. Hwangbo, J. I. Mullins, and L. Corey. 2002. Evidence for human immunodeficiency virus type 1 replication in vivo in cd14(+) monocytes and its potential role as a source of virus in patients on highly active antiretroviral therapy. J. Virol. 76:707-716.

193. Gulick, R. M., J. Lalezari, J. Goodrich, N. Clumeck, E. DeJesus, A. Horban, J. Nadler, B. Clotet, A. Karlsson, M. Wohlfeiler, J. B. Montana, M. McHale, J. Sullivan, C. Ridgway, S. Felstead, M. W. Dunne, E. van der Ryst, H. Mayer, and M. S. Teams. 2008. Maraviroc for previously treated patients with r5 hiv-1 infection. The New England Journal of Medicine 359:1429-1441.

194. Stephenson, J. 2007. Researchers buoyed by novel hiv drugs: Will expand drug arsenal against resistant virus. JAMA 297:1535-1536.

195. Huang, W., S. H. Eshleman, J. Toma, S. Fransen, E. Stawiski, E. E. Paxinos, J. M. Whitcomb, A. M. Young, D. Donnell, F. Mmiro, P. Musoke, L. A. Guay, J. B. Jackson, N. T. Parkin, and C. J. Petropoulos. 2007. Coreceptor tropism in human immunodeficiency virus type 1 subtype d: High prevalence of cxcr4 tropism and heterogeneous composition of viral populations. J. Virol. 81:7885-7893.

196. Ho, S.-h., L. Shek, A. Gettie, J. Blanchard, and C. Cheng-Mayer. 2005. V3 loop-determined coreceptor preference dictates the dynamics of $CD4^+$-t-cell loss in simian-human immunodeficiency virus-infected macaques. J. Virol. 79:12296-12303.

197. Nishimura, Y., T. Igarashi, O. K. Donau, A. Buckler-White, C. Buckler, B. A. P. Lafont, R. M. Goeken, S. Goldstein, V. M. Hirsch, and M. A. Martin. 2004. Highly pathogenic shivs and sivs target different $CD4^+$ t cell subsets in rhesus monkeys, explaining their divergent clinical courses. Proceedings of the National Academy of Sciences of the United States of America 101:12324-12329.

198. Bleul, C. C., L. Wu, J. A. Hoxie, T. A. Springer, and C. R. Mackay. 1997. The hiv coreceptors cxcr4 and ccr5 are differentially expressed and regulated on human t lymphocytes. Proceedings of the National Academy of Sciences of the United States of America 94:1925-1930.

199. Lewin, S., S. Sonza, L. Irving, C. McDonald, J. Mills, and S. Crowe. 1996. Surface cd4 is critical to in vitro hiv infection of human alveolar macrophages. AIDS Research and Human Retroviruses 12:877-883.

200. Yi, Y., W. Chen, I. Frank, J. Cutilli, A. Singh, L. Starr-Spires, J. Sulcove, D. L. Kolson, and R. G. Collman. 2003. An unusual syncytia-inducing human immunodeficiency virus type 1 primary isolate from the central nervous system that is restricted to cxcr4, replicates efficiently in macrophages, and induces neuronal apoptosis. Journal of Neurovirology 9:432-441.

201. Kabat, D., S. L. Kozak, K. Wehrly, and B. Chesebro. 1994. Differences in cd4 dependence for infectivity of laboratory-adapted and primary patient isolates of human immunodeficiency virus type 1. J. Virol. 68:2570-2577.

202. Dunfee, R. L., E. R. Thomas, P. R. Gorry, J. Wang, J. Taylor, K. Kunstman, S. M. Wolinsky, and D. Gabuzda. 2006. The hiv env variant n283 enhances macrophage tropism and is associated with brain infection and dementia. Proceedings of the National Academy of Sciences of the United States of America 103:15160-15165.

203. Musich, T., P. J. Peters, M. J. Duenas-Decamp, M. P. Gonzalez-Perez, J. Robinson, S. Zolla-Pazner, J. K. Ball, K. Luzuriaga, and P. R. Clapham. 2011. A conserved determinant in the v1 loop of hiv-1 modulates the v3 loop to prime low cd4 use and macrophage infection. J. Virol. 85:2397-2405.

204. Gonzalez-Perez, M. P., O. O'Connell, R. Lin, W. M. Sullivan, J. Bell, P. Simmonds, and P. R. Clapham. 2012. Independent evolution of macrophage-tropism and increased charge between hiv-1 r5 envelopes present in brain and immune tissue. Retrovirology 9:20.

205. Cashin, K., M. Roche, J. Sterjovski, A. Ellett, L. R. Gray, A. L. Cunningham, P. A. Ramsland, M. J. Churchill, and P. R. Gorry. 2011. Alternative coreceptor requirements for efficient ccr5- and cxcr4-mediated hiv-1 entry into macrophages . J. Virol. 85:10699-10709.

206. Duenas-Decamp, M. J., P. Peters, D. Burton, and P. R. Clapham. 2008. Natural resistance of human immunodeficiency virus type 1 to the cd4bs antibody b12 conferred by a glycan and an arginine residue close to the cd4 binding loop. J. Virol. 82:5807-5814.

207. Dunfee, R. L., E. R. Thomas, J. Wang, K. Kunstman, S. M. Wolinsky, and D. Gabuzda. 2007. Loss of the n-linked glycosylation site at position 386 in the hiv envelope v4 region enhances macrophage tropism and is associated with dementia. Virology 367:222-234.

208. Ouyang, Y., L. Liu, Y. Zhang, L. Yuan, Z. Liu, S. Yang, F. Wei, L. Qiao, and D. Chen. 2014. Discordant patterns of tissue-specific genetic characteristics in the hiv-1 env gene from hiv-associated neurocognitive disorder (hand) and non-hand patients. Journal of Neurovirology 20:332-340.

209. Harrington, P. R., M. J. Connell, R. B. Meeker, P. R. Johnson, and R. Swanstrom. 2007. Dynamics of simian immunodeficiency virus populations in blood and cerebrospinal fluid over the full course of infection. The Journal of Infectious Diseases 196:1058-1067.

210. Rossi, F., B. Querido, M. Nimmagadda, S. Cocklin, S. Navas-Martn, and J. Martn-Garcia. 2008. The v1-v3 region of a brain-derived hiv-1 envelope glycoprotein determines macrophage tropism, low cd4 dependence, increased fusogenicity and altered sensitivity to entry inhibitors. Retrovirology 2008:89.

211. Evering, T. H., E. Kamau, L. S. Bernard, C. B. Farmer, X.-P. Kong, and M. Markowitz. 2014. Single genome analysis reveals genetic characteristics of neuroadaptation across hiv-1 envelope. Retrovirology 11:65.

212. Sterjovski, J., M. J. Churchill, A. Ellett, L. R. Gray, M. J. Roche, R. L. Dunfee, D. F. J. Purcell, N. Saksena, B. Wang, S. Sonza, S. L. Wesselingh, I. Karlsson, E.-M. Fenyo, D. Gabuzda, A. L. Cunningham, and P. R. Gorry. 2007. Asn 362 in gp120 contributes to enhanced fusogenicity by ccr5-restricted hiv-1 envelope glycoprotein variants from patients with AIDS. Retrovirology 4:89.

213. Richards, K. H., M. M. Aasa-Chapman, . McKnight, and P. R. Clapham. 2010. Modulation of hiv-1 macrophage-tropism among r5 envelopes occurs before detection of neutralizing antibodies. Retrovirology 7:48.

214. Wei, X., J. M. Decker, H. Liu, Z. Zhang, R. B. Arani, J. M. Kilby, M. S. Saag, X. Wu, G. M. Shaw, and J. C. Kappes. 2002. Emergence of resistant human immunodeficiency virus type 1 in patients receiving fusion inhibitor (t-20) monotherapy. Antimicrobial Agents and Chemotherapy 46:1896-1905.

215. Montefiori, D. C. 2005. Evaluating neutralizing antibodies against hiv, siv, and shiv in luciferase reporter gene assays. Current Protocols in Immunology / Edited by John E. Coligan ... [et Al.] Chapter 12:Unit 12.11.

216. Burton, D. R., C. F. Barbas, M. A. Persson, S. Koenig, R. M. Chanock, and R. A. Lerner. 1991. A large array of human monoclonal antibodies to type 1 human immunodeficiency virus from combinatorial libraries of asymptomatic seropositive individuals. Proceedings of the National Academy of Sciences 88:10134-10137.

217. Wu, X., Z.-Y. Yang, Y. Li, C.-M. Hogerkorp, W. R. Schief, M. S. Seaman, T. Zhou, S. D. Schmidt, L. Wu, L. Xu, N. S. Longo, K. McKee, S. ODell, M. K. Louder, D. L. Wycuff, Y. Feng, M. Nason, N. Doria-Rose, M. Connors, P. D. Kwong, M. Roederer, R. T. Wyatt, G. J. Nabel, and J. R. Mascola. 2010. Rational design of envelope identifies broadly neutralizing human monoclonal antibodies to hiv-1. Science 329:856-861.

218. Wu, X., T. Zhou, J. Zhu, B. Zhang, I. Georgiev, C. Wang, X. Chen, N. S. Longo, M. Louder, K. McKee, S. ODell, S. Perfetto, S. D. Schmidt, W. Shi, L. Wu, Y. Yang, Z.-Y. Yang, Z. Yang, Z. Zhang, M. Bonsignori, J. A. Crump, S. H. Kapiga, N. E. Sam, B. F. Haynes, M. Simek, D. R. Burton, W. C. Koff, N. A. Doria-Rose, M. Connors, J. C. Mullikin, G. J. Nabel, M. Roederer, L. Shapiro, P. D. Kwong, and J. R. Mascola. 2011. Focused evolution of hiv-1 neutralizing antibodies revealed by structures and deep sequencing. Science 333:1593-1602.

219. Si, Z., N. Madani, J. M. Cox, J. J. Chruma, J. C. Klein, A. Schn, N. Phan, L. Wang, A. C. Biorn, S. Cocklin, I. Chaiken, E. Freire, A. B. Smith, and J. G. Sodroski. 2004. Small-molecule inhibitors of hiv-1 entry block receptor-induced conformational changes in the viral envelope glycoproteins. Proceedings of the National Academy of Sciences of the United States of America 101:5036-5041.

220. Nowicka-Sans, B., Y.-F. Gong, B. McAuliffe, I. Dicker, H.-T. Ho, N. Zhou, B. Eggers, P.-F. Lin, N. Ray, M. Wind-Rotolo, L. Zhu, A. Majumdar, D. Stock, M. Lataillade, G. J. Hanna, J. D. Matiskella, Y. Ueda, T. Wang, J. F. Kadow, N. A. Meanwell, and M. Krystal. 2012. In vitro antiviral characteristics of hiv-1 attachment inhibitor bms-626529, the active component of the prodrug bms-663068. Antimicrobial Agents and Chemotherapy 56:3498-3507.

221. Walker, L. M., S. K. Phogat, P.-Y. Chan-Hui, D. Wagner, P. Phung, J. L. Goss, T. Wrin, M. D. Simek, S. Fling, J. L. Mitcham, J. K. Lehrman, F. H. Priddy, O. A. Olsen, S. M.

Frey, P. W. Hammond, S. Kaminsky, T. Zamb, M. Moyle, W. C. Koff, P. Poignard, and D. R. Burton. 2009. Broad and potent neutralizing antibodies from an african donor reveal a new hiv-1 vaccine target. Science 326:285-289.

222. Bonsignori, M., K.-K. Hwang, X. Chen, C.-Y. Tsao, L. Morris, E. Gray, D. J. Marshall, J. A. Crump, S. H. Kapiga, N. E. Sam, F. Sinangil, M. Pancera, Y. Yongping, B. Zhang, J. Zhu, P. D. Kwong, S. O'Dell, J. R. Mascola, L. Wu, G. J. Nabel, S. Phogat, M. S. Seaman, J. F. Whitesides, M. A. Moody, G. Kelsoe, X. Yang, J. Sodroski, G. M. Shaw, D. C. Montefiori, T. B. Kepler, G. D. Tomaras, S. M. Alam, H.-X. Liao, and B. F. Haynes. 2011. Analysis of a clonal lineage of hiv-1 envelope v2/v3 conformational epitope-specific broadly neutralizing antibodies and their inferred unmutated common ancestors. J. Virol. 85:9998-10009.

223. Sanders, R. W., M. Venturi, L. Schiffner, R. Kalyanaraman, H. Katinger, K. O. Lloyd, P. D. Kwong, and J. P. Moore. 2002. The mannose-dependent epitope for neutralizing antibody 2g12 on human immunodeficiency virus type 1 glycoprotein gp120. J. Virol. 76:7293-7305.

224. Buchacher, A., R. Predl, K. Strutzenberger, W. Steinfellner, A. Trkola, M. Purtscher, G. Gruber, C. Tauer, F. Steindl, and A. Jungbauer. 1994. Generation of human monoclonal antibodies against hiv-1 proteins; electrofusion and epstein-barr virus transformation for peripheral blood lymphocyte immortalization. AIDS research and human retroviruses 10:359-369.

225. Thali, M., J. P. Moore, C. Furman, M. Charles, D. D. Ho, J. Robinson, and J. Sodroski. 1993. Characterization of conserved human immunodeficiency virus type 1 gp120 neutralization epitopes exposed upon gp120-cd4 binding. J. Virol. 67:3978-3988.

226. Buchbinder, A., S. Zolla-Pazner, S. Karwowska, M. K. Gorny, and S. T. Burda. 1992. Synergy between human monoclonal antibodies to hiv extends their effective biologic activity against homologous and divergent strains. AIDS research and human retroviruses 8:1395.

227. Moore, J. P., Y. Cao, L. Qing, Q. J. Sattentau, J. Pyati, R. Koduri, J. Robinson, C. F. Barbas, D. R. Burton, and D. D. Ho. 1995. Primary isolates of human immunodeficiency virus type 1 are relatively resistant to neutralization by monoclonal antibodies to gp120, and their neutralization is not predicted by studies with monomeric gp120. J. Virol. 69:101-109.

228. Seaman, M. S., H. Janes, N. Hawkins, L. E. Grandpre, C. Devoy, A. Giri, R. T. Coffey, L. Harris, B. Wood, M. G. Daniels, T. Bhattacharya, A. Lapedes, V. R. Polonis, F. E. McCutchan, P. B. Gilbert, S. G. Self, B. T. Korber, D. C. Montefiori, and J. R. Mascola. 2010. Tiered categorization of a diverse panel of hiv-1 env pseudoviruses for assessment of neutralizing antibodies. J. Virol. 84:1439-1452.

229. Keir, G., and E. J. Thompson. 1986. Proteins as parameters in the discrimination between different blood-csf barriers. J. Neurol. Sci. 75:245-253.

230. Singer, E. J., K. Syndulko, B. N. Fahy-Chandon, P. Shapshak, L. Resnick, P. Schmid, A. J. Conrad, and W. W. Tourtellotte. 1994. Cerebrospinal fluid p24 antigen levels and intrathecal immunoglobulin g synthesis are associated with cognitive disease severity in hiv-1. AIDS 8:197-204.

231. Anthony, I. C., D. H. Crawford, and J. E. Bell. 2003. B lymphocytes in the normal brain: Contrasts with hivassociated lymphoid infiltrates and lymphomas. Brain 126:1058-1067.

232. Meira, C. S., J. E. Vidal, T. A. Costa-Silva, G. Motoie, R. Gava, R. M. Hiramoto, and V. L. Pereira-Chioccola. 2013. Igg4 specific to toxoplasma gondii excretory/secretory antigens in serum and/or cerebrospinal fluid support the cerebral toxoplasmosis diagnosis in hiv-infected patients. Journal of Immunological Methods 395:21-28.

233. Mahalanabis, M., P. Jayaraman, T. Miura, F. Pereyra, E. M. Chester, B. Richardson, B. Walker, and N. L. Haigwood. 2009. Continuous viral escape and selection by autologous neutralizing antibodies in drug-nave human immunodeficiency virus controllers. J. Virol. 83:662-672.

234. Bunnik, E. M., L. Pisas, A. C. v. Nuenen, and H. Schuitemaker. 2008. Autologous neutralizing humoral immunity and evolution of the viral envelope in the course of subtype b human immunodeficiency virus type 1 infection. J. Virol. 82:7932-7941.

235. Gray, E. S., P. L. Moore, I. A. Choge, J. M. Decker, F. Bibollet-Ruche, H. Li, N. Leseka, F. Treurnicht, K. Mlisana, G. M. Shaw, S. S. A. Karim, C. Williamson, L. Morris, and a. t. C. S. Team. 2007. Neutralizing antibody responses in acute human immunodeficiency virus type 1 subtype c infection. J. Virol. 81:6187-6196.

236. Deeks, S. G., B. Schweighardt, T. Wrin, J. Galovich, R. Hoh, E. Sinclair, P. Hunt, J. M. McCune, J. N. Martin, C. J. Petropoulos, and F. M. Hecht. 2006. Neutralizing antibody responses against autologous and heterologous viruses in acute versus chronic human immunodeficiency virus (hiv) infection: Evidence for a constraint on the ability of hiv to completely evade neutralizing antibody responses. J. Virol. 80:6155-6164.

237. Frost, S. D. W., T. Wrin, D. M. Smith, S. L. K. Pond, Y. Liu, E. Paxinos, C. Chappey, J. Galovich, J. Beauchaine, C. J. Petropoulos, S. J. Little, and D. D. Richman. 2005. Neutralizing antibody responses drive the evolution of human immunodeficiency virus type 1 envelope during recent hiv infection. Proc. Natl. Acad. Sci. U. S. A. 102:18514-18519.

238. Aasa-Chapman, M. M. I., A. Hayman, P. Newton, D. Cornforth, I. Williams, P. Borrow, P. Balfe, and A. McKnight. 2004. Development of the antibody response in acute hiv-1 infection. AIDS (London, England) 18:371-381.

239. Richman, D. D., T. Wrin, S. J. Little, and C. J. Petropoulos. 2003. Rapid evolution of the neutralizing antibody response to hiv type 1 infection. Proceedings of the National Academy of Sciences 100:4144-4149.

240. Wei, X., J. M. Decker, S. Wang, H. Hui, J. C. Kappes, X. Wu, J. F. Salazar-Gonzalez, M. G. Salazar, J. M. Kilby, M. S. Saag, N. L. Komarova, M. A. Nowak, B. H. Hahn, P. D. Kwong, and G. M. Shaw. 2003. Antibody neutralization and escape by hiv-1. Nature 422:307-312.

241. Pilgrim, A. K., G. Pantaleo, O. J. Cohen, L. M. Fink, J. Y. Zhou, J. T. Zhou, D. P. Bolognesi, A. S. Fauci, and D. C. Montefiori. 1997. Neutralizing antibody responses to human immunodeficiency virus type 1 in primary infection and long-term-nonprogressive infection. The Journal of Infectious Diseases 176:924-932.

242. Moog, C., H. J. Fleury, I. Pellegrin, A. Kirn, and A. M. Aubertin. 1997. Autologous and heterologous neutralizing antibody responses following initial seroconversion in human immunodeficiency virus type 1-infected individuals. J. Virol. 71:3734-3741.

243. Moore, P. L., E. S. Gray, and L. Morris. 2009. Specificity of the autologous neutralizing antibody response:. Current Opinion in HIV and AIDS 4:358-363.

244. Agrawal, N., D. P. Leaman, E. Rowcliffe, H. Kinkead, R. Nohria, J. Akagi, K. Bauer, S. X. Du, R. G. Whalen, D. R. Burton, and M. B. Zwick. 2011. Functional stability of unliganded envelope glycoprotein spikes among isolates of human immunodeficiency virus type 1 (hiv-1). PloS One 6:e21339.

245. Platt, E. J., S. L. Kozak, J. P. Durnin, T. J. Hope, and D. Kabat. 2010. Rapid dissociation of hiv-1 from cultured cells severely limits infectivity assays, causes the inactivation ascribed to entry inhibitors, and masks the inherently high level of infectivity of virions. J. Virol. 84:3106-3110.

246. Tedbury, P. R., and E. O. Freed. 2014. The role of matrix in hiv-1 envelope glycoprotein incorporation. Trends Microbiol. 22:372-378.

247. Aquino-De Jesus, M. J., C. Anders, G. Miller, J. W. Sleasman, M. M. Goodenow, and W. A. Andiman. 2000. Genetically and epidemiologically related "non-syncytium-inducing" isolates of hiv-1 display heterogeneous growth patterns in macrophages. Journal of Medical Virology 61:171-180.

248. Platt, E. J., K. Wehrly, S. E. Kuhmann, B. Chesebro, and D. Kabat. 1998. Effects of ccr5 and cd4 cell surface concentrations on infections by macrophagetropic isolates of human immunodeficiency virus type 1. J. Virol. 72:2855-2864.

249. Walter, B. L., K. Wehrly, R. Swanstrom, E. Platt, D. Kabat, and B. Chesebro. 2005. Role of low cd4 levels in the influence of human immunodeficiency virus type 1 envelope v1 and v2 regions on entry and spread in macrophages. J. Virol. 79:4828-4837.

250. Chen, L., Y. D. Kwon, T. Zhou, X. Wu, S. O'Dell, L. Cavacini, A. J. Hessell, M. Pancera, M. Tang, L. Xu, Z.-Y. Yang, M.-Y. Zhang, J. Arthos, D. R. Burton, D. S. Dimitrov, G. J. Nabel, M. R. Posner, J. Sodroski, R. Wyatt, J. R. Mascola, and P. D. Kwong. 2009. Structural basis of immune evasion at the site of cd4 attachment on hiv-1 gp120. Science (New York, N.Y.) 326:1123-1127.

251. Tran, K., C. Poulsen, J. Guenaga, N. d. Val, R. Wilson, C. Sundling, Y. Li, R. L. Stanfield, I. A. Wilson, A. B. Ward, G. B. K. Hedestam, and R. T. Wyatt. 2014. Vaccine-elicited primate antibodies use a distinct approach to the hiv-1 primary receptor binding site informing vaccine redesign. Proceedings of the National Academy of Sciences 111:E738-E747.

252. Li, Y., S. O'Dell, L. M. Walker, X. Wu, J. Guenaga, Y. Feng, S. D. Schmidt, K. McKee, M. K. Louder, J. E. Ledgerwood, B. S. Graham, B. F. Haynes, D. R. Burton, R. T. Wyatt, and J. R. Mascola. 2011. Mechanism of neutralization by the broadly neutralizing hiv-1 monoclonal antibody vrc01. J. Virol. 85:8954-8967.

253. Zhang, Y.-j., R. Fredriksson, J. A. McKeating, and E. M. Feny. 1997. Passage of hiv-1 molecular clones into different cell lines confers differential sensitivity to neutralization. Virology 238:254-264.

254. Trkola, A., T. Ketas, V. N. KewalRamani, F. Endorf, J. M. Binley, H. Katinger, J. Robinson, D. R. Littman, and J. P. Moore. 1998. Neutralization sensitivity of human immunodeficiency virus type 1 primary isolates to antibodies and cd4-based reagents is independent of coreceptor usage. J. Virol. 72:1876-1885.

255. Beddows, S., S. Louisirirotchanakul, R. Cheingsong-Popov, P. J. Easterbrook, P. Simmonds, and J. Weber. 1998. Neutralization of primary and t-cell line adapted isolates of human immunodeficiency virus type 1: Role of v3-specific antibodies. The Journal of General Virology 79 (Pt 1):77-82.

256. Hoffman, T. L., C. C. LaBranche, W. Zhang, G. Canziani, J. Robinson, I. Chaiken, J. A. Hoxie, and R. W. Doms. 1999. Stable exposure of the coreceptor-binding site in a cd4-independent hiv-1 envelope protein. Proceedings of the National Academy of Sciences of the United States of America 96:6359-6364.

257. Pugach, P., S. E. Kuhmann, J. Taylor, A. J. Marozsan, A. Snyder, T. Ketas, S. M. Wolinsky, B. T. Korber, and J. P. Moore. 2004. The prolonged culture of human immunodeficiency virus type 1 in primary lymphocytes increases its sensitivity to neutralization by soluble cd4. Virology 321:8-22.

258. Shieh, J. T., J. Martn, G. Baltuch, M. H. Malim, and F. Gonzlez-Scarano. 2000. Determinants of syncytium formation in microglia by human immunodeficiency virus type 1: Role of the v1/v2 domains. J. Virol. 74:693-701.

259. Daar, E. S., X. L. Li, T. Moudgil, and D. D. Ho. 1990. High concentrations of recombinant soluble cd4 are required to neutralize primary human immunodeficiency virus type 1 isolates. Proceedings of the National Academy of Sciences of the United States of America 87:6574-6578.

260. O'Brien, W. A., S. H. Mao, Y. Cao, and J. P. Moore. 1994. Macrophage-tropic and t-cell line-adapted chimeric strains of human immunodeficiency virus type 1 differ in their susceptibilities to neutralization by soluble cd4 at different temperatures. J. Virol. 68:5264-5269.

261. Moore, J. P., L. C. Burkly, R. I. Connor, Y. Cao, R. Tizard, D. D. Ho, and R. A. Fisher. 1993. Adaptation of two primary human immunodeficiency virus type 1 isolates to growth in transformed t cell lines correlates with alterations in the responses of their envelope glycoproteins to soluble cd4. AIDS Research and Human Retroviruses 9:529-539.

262. Li, M., F. Gao, J. R. Mascola, L. Stamatatos, V. R. Polonis, M. Koutsoukos, G. Voss, P. Goepfert, P. Gilbert, K. M. Greene, M. Bilska, D. L. Kothe, J. F. Salazar-Gonzalez, X. Wei, J. M. Decker, B. H. Hahn, and D. C. Montefiori. 2005. Human immunodeficiency virus type 1 env clones from acute and early subtype b infections for standardized assessments of vaccine-elicited neutralizing antibodies. J. Virol. 79:10108-10125.

263. Julien, J.-P., A. Cupo, D. Sok, R. L. Stanfield, D. Lyumkis, M. C. Deller, P.-J. Klasse, D. R. Burton, R. W. Sanders, J. P. Moore, A. B. Ward, and I. A. Wilson. 2013. Crystal structure of a soluble cleaved hiv-1 envelope trimer. Science 342:1477-1483.

264. Liu, J., A. Bartesaghi, M. J. Borgnia, G. Sapiro, and S. Subramaniam. 2008. Molecular architecture of native hiv-1 gp 120 trimers. Nature 455:109-113.

265. Hraber, P., B. T. Korber, A. S. Lapedes, R. T. Bailer, M. S. Seaman, H. Gao, K. M. Greene, F. McCutchan, C. Williamson, J. H. Kim, S. Tovanabutra, B. H. Hahn, R. Swanstrom, M. M. Thomson, F. Gao, L. Harris, E. Giorgi, N. Hengartner, T. Bhattacharya, J. R. Mascola, and D. C. Montefiori. 2014. Impact of clade, geography, and age of the epidemic on hiv-1 neutralization by antibodies. J. Virol. 88:12623-12643.

266. Rusert, P., A. Krarup, C. Magnus, O. F. Brandenberg, J. Weber, A.-K. Ehlert, R. R. Regoes, H. F. Gnthard, and A. Trkola. 2011. Interaction of the gp120 v1v2 loop with a neighboring gp120 unit shields the hiv envelope trimer against cross-neutralizing antibodies. The Journal of Experimental Medicine 208:1419-1433.

267. Pinter, A., W. J. Honnen, Y. He, M. K. Gorny, S. Zolla-Pazner, and S. C. Kayman. 2004. The v1/v2 domain of gp120 is a global regulator of the sensitivity of primary human immunodeficiency virus type 1 isolates to neutralization by antibodies commonly induced upon infection. J. Virol. 78:5205-5215.

268. Cavrois, M., J. Neidleman, M. L. Santiago, C. A. Derdeyn, E. Hunter, and W. C. Greene. 2014. Enhanced fusion and virion incorporation for hiv-1 subtype c envelope glycoproteins with compact v1/v2 domains. J. Virol. 88:2083-2094.

269. Leaman, D. P., and M. B. Zwick. 2013. Increased functional stability and homogeneity of viral envelope spikes through directed evolution. PLoS pathogens 9:e1003184.

270. Kassa, A., A. Finzi, M. Pancera, J. R. Courter, A. B. Smith, and J. Sodroski. 2009. Identification of a human immunodeficiency virus type 1 envelope glycoprotein variant resistant to cold inactivation. J. Virol. 83:4476-4488.

271. Haim, H., B. Strack, A. Kassa, N. Madani, L. Wang, J. R. Courter, A. Princiotto, K. McGee, B. Pacheco, M. S. Seaman, A. B. Smith, III, and J. Sodroski. 2011. Contribution of intrinsic reactivity of the hiv-1 envelope glycoproteins to cd4-independent infection and global inhibitor sensitivity. PLoS Pathog 7:e1002101.

272. Medjahed, H., B. Pacheco, A. Dsormeaux, J. Sodroski, and A. Finzi. 2013. The hiv-1 gp120 major variable regions modulate cold inactivation. J. Virol. 87:4103-4111.

273. Blaak, H., A. B. van't Wout, M. Brouwer, B. Hooibrink, E. Hovenkamp, and H. Schuitemaker. 2000. In vivo hiv-1 infection of cd45ra(+)cd4(+) t cells is established primarily by syncytium-inducing variants and correlates with the rate of cd4(+) t cell decline. Proceedings of the National Academy of Sciences of the United States of America 97:1269-1274.

274. Riddick, N. E., E. A. Hermann, L. M. Loftin, S. T. Elliott, W. C. Wey, B. Cervasi, J. Taaffe, J. C. Engram, B. Li, J. G. Else, Y. Li, B. H. Hahn, C. A. Derdeyn, D. L. Sodora, C. Apetrei, M. Paiardini, G. Silvestri, and R. G. Collman. 2010. A novel ccr5 mutation common in sooty mangabeys reveals sivsmm infection of ccr5-null natural hosts and efficient alternative coreceptor use in vivo. PLoS pathogens 6:e1001064.

275. Ghaffari, G., D. L. Tuttle, D. Briggs, B. R. Burkhardt, D. Bhatt, W. A. Andiman, J. W. Sleasman, and M. M. Goodenow. 2005. Complex determinants in human immunodeficiency virus type 1 envelope gp120 mediate cxcr4-dependent infection of macrophages. J. Virol. 79:13250-13261.

276. Arrildt, K. T., C. C. LaBranche, S. B. Joseph, E. N. Dukhovlinova, W. D. Graham, L. H. Ping, G. Schnell, C. B. Sturdevant, L. P. Kincer, M. Mallewa, R. S. Heyderman, A. Van Rie, M. S. Cohen, S. Spudich, R. W. Price, D. C. Montefiori, and R. Swanstrom. 2015. Phenotypic correlates of hiv-1 macrophage tropism. J. Virol. 89:11294-11311.

277. Guo, D., X. Shi, K. C. Arledge, D. Song, L. Jiang, L. Fu, X. Gong, S. Zhang, X. Wang, and L. Zhang. 2012. A single residue within the v5 region of hiv-1 envelope facilitates viral escape from the broadly neutralizing monoclonal antibody vrc01. The Journal of Biological Chemistry 287:43170-43179.

278. Wang, W., B. Zirkle, J. Nie, J. Ma, K. Gao, X. S. Chen, W. Huang, W. Kong, and Y. Wang. 2015. N463 glycosylation site on v5 loop of a mutant gp120 regulates the sensitivity of hiv-1 to neutralizing monoclonal antibodies vrc01/03. Journal of Acquired Immune Deficiency Syndromes (1999) 69:270-277.

279. Pace, C. S., M. W. Fordyce, D. Franco, C.-Y. Kao, M. S. Seaman, and D. D. Ho. 2013. Anti-cd4 monoclonal antibody ibalizumab exhibits breadth and potency against hiv-1, with natural resistance mediated by the loss of a v5 glycan in envelope. Journal of Acquired Immune Deficiency Syndromes (1999) 62:1-9.

280. Mefford, M. E., K. Kunstman, S. M. Wolinsky, and D. Gabuzda. 2015. Bioinformatic analysis of neurotropic hiv envelope sequences identifies polymorphisms in the gp120

bridging sheet that increase macrophage-tropism through enhanced interactions with ccr5. Virology 481:210-222.

281. Klasse, P. J., R. S. Depetris, R. Pejchal, J.-P. Julien, R. Khayat, J. H. Lee, A. J. Marozsan, A. Cupo, N. Cocco, J. Korzun, A. Yasmeen, A. B. Ward, I. A. Wilson, R. W. Sanders, and J. P. Moore. 2013. Influences on trimerization and aggregation of soluble, cleaved hiv-1 sosip envelope glycoprotein. J. Virol. 87:9873-9885.

282. Lyumkis, D., J.-P. Julien, N. de Val, A. Cupo, C. S. Potter, P.-J. Klasse, D. R. Burton, R. W. Sanders, J. P. Moore, B. Carragher, I. A. Wilson, and A. B. Ward. 2013. Cryo-em structure of a fully glycosylated soluble cleaved hiv-1 envelope trimer. Science (New York, N.Y.) 342:1484-1490.

283. Pugach, P., G. Ozorowski, A. Cupo, R. Ringe, A. Yasmeen, N. de Val, R. Derking, H. J. Kim, J. Korzun, M. Golabek, K. de Los Reyes, T. J. Ketas, J.-P. Julien, D. R. Burton, I. A. Wilson, R. W. Sanders, P. J. Klasse, A. B. Ward, and J. P. Moore. 2015. A native-like sosip.664 trimer based on an hiv-1 subtype b env gene. J. Virol. 89:3380-3395.